Russian Original Vol. 32, No. 3, March, 1972

Translation published November, 1972

All articles and cutting should be extended see index

DOENO = ATOMNAYA ENERGIYA V. 32 #3

SOVIET ATOMIC ENERGY

АТОМНАЯ ЭНЕРГИЯ
(ATOMNAYA ÉNERGIYA)

TRANSLATED FROM RUSSIAN

CONSULTANTS BUREAU, NEW YORK

SOVIET ATOMIC ENERGY

Soviet Atomic Energy is a cover-to-cover translation of *Atomnaya Énergiya*, a publication of the Academy of Sciences of the USSR.

An arrangement with Mezhdunarodnaya Kniga, the Soviet book export agency, makes available both advance copies of the Russian journal and original glossy photographs and artwork. This serves to decrease the necessary time lag between publication of the original and publication of the translation and helps to improve the quality of the latter. The translation began with the first issue of the Russian journal.

Consultants Bureau journals appear about six months after the publication of the original Russian issue. For bibliographic accuracy, the English issue published by Consultants Bureau carries the same number and date as the original Russian from which it was translated. For example, a Russian issue published in December will appear in a Consultants Bureau English translation about the following June, but the translation issue will carry the December date. When ordering any volume or particular issue of a Consultants Bureau journal, please specify the date and, where applicable, the volume and issue numbers of the original Russian. The material you will receive will be a translation of that Russian volume or issue.

Subscription
$75.00 per volume (6 issues)
2 volumes per year
(Add $5 for orders outside the United States and Canada.)

Single Issue: $30
Single Article: $15

CONSULTANTS BUREAU, NEW YORK AND LONDON

c/b

227 West 17th Street
New York, New York 10011

Davis House
8 Scrubs Lane
Harlesden, NW10 6SE
England

Published monthly. Second-class postage paid at Jamaica, New York 11431.

Next 1 Page(s) In Document Denied

THE ROLE OF NUCLEAR POWER IN LONG-TERM FUEL – ENERGY BALANCE IN THE USSR

A. A. Makarov, A. S. Makarova,
A. G. Vigdorchik, A. N. Zeiliger,
G. B. Levental', and A. M. Belostotskii

UDC 621.039.003

The forecasted long-term program of extensive growth of nuclear power calls for comprehensive technological and economical research on the optimum scale and ways of this growth. These studies cannot be based (as they are now) on isolated comparison of the economical performance of nuclear and conventional power plants.

In fact, in the coming decades nuclear energy will undoubtedly affect the output of traditional energy resources (petroleum, natural gas, and coal) displacing the more expensive fuel sources and thus changing its own economical importance. Moreover, the growth of nuclear power will inevitably have a great impact on the structure of the electrical power systems. Thus, rational scales and ways of the growth of nuclear power cannot be determined without a study of the optimal structure of the long-term fuel–energy balance and of a unified electrical power system of the country.

One of the fundamental problems which must be solved in the study of the role of nuclear power is the length of the design period. On the one hand, this period should not be limited to the initial stage during which nuclear power techniques are mastered and put into practice and thus should be longer than five to 10 years; on the other hand the design period must not be excessively long in order to prevent the error in the initial information from growing into proportions which make the results of the study unreliable and unrealistic (this is particularly true of the effect of some cost indicators on the optimum structure of fuel–energy balance). As a result, at the first stage of this study the design period was limited to the time preceding the widespread use of fast reactors.

The choice of a sufficiently long design period turns the study of the prospects of nuclear power into the problem of predicting the gain it affords in the fuel–energy balance. A special method has been developed which is based on an analysis of the uncertainty zone in the optimal growth of the country's power resources [1]. The basis of the method is a mathematical model which simulates the power economy of the USSR.

On the one hand, this model describes in sufficient detail the conditions of simultaneous development of fuel production (including transportation of coal, gas, and fuel oil from one region to the other), of the Unified Electric Power System, and of the main classes of consumers. The model considers in particular detail the European Electric Power System block which describes the day-by-day and annual operating conditions of the existing and new power plants (of various types) and of the intersystem electrical transmission lines. Nuclear power is represented in the model by nuclear steam and heat electrical plants under various operating conditions, and by constraints on the total installed power of nuclear reactors. The overall dimensionality of the mathematical model includes 250 constraints and 700 variables.

On the other hand, the model makes it possible to obtain from the analysis or to generate independently a representative set of typical combinations of possible conditions of system development and to find in an acceptable time an optimal version of fuel–energy balance corresponding to each such combination. In the present study such versions were obtained for 100 different combinations of economical indicators of the basic objects and for 50 combinations of such decisive factors as the electrical power consumption

Translated from Atomnaya Énergiya, Vol. 32, No. 3, pp. 187-196, March, 1972. Original article submitted August 12, 1971.

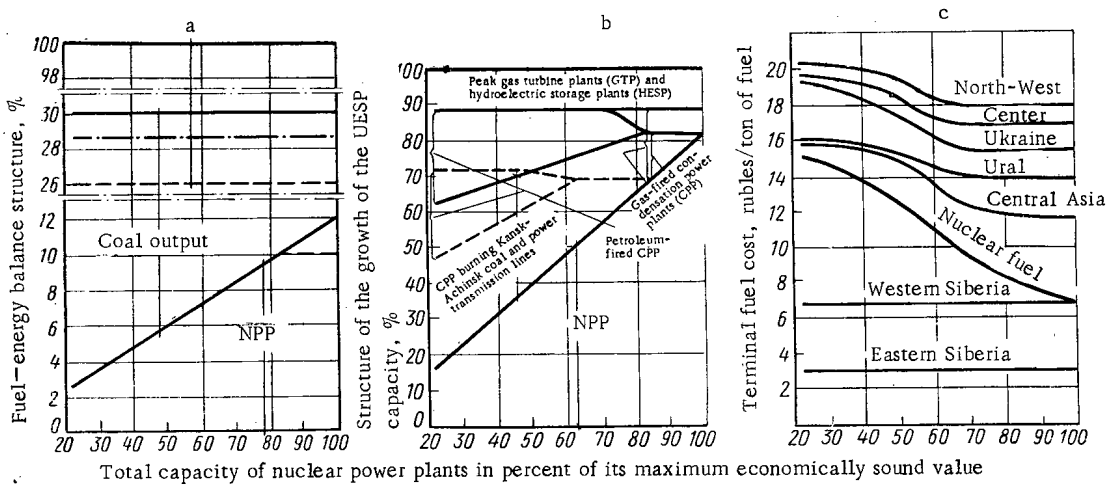

Fig. 1. Effect of the variation of total output of nuclear power plant (NPP) on: a) the fuel-energy balance structure; b) the growth structure of the Unified European Power System (UEPS); c) terminal fuel cost. Level of gas production: – – –) 1000 billion km^3; – · – · –) 960 billion km^3; ———) 880 billion km^3.

of the USSR, the potential volume of coal and petroleum production, the total capacity of nuclear electric plants and the operating characteristics of power plants.

An analysis of the resulting combinations of optimal versions of fuel–energy balance makes it possible to determine the energetic and economical factors that most significantly affect the optimal values of the growth parameters of nuclear power. In this study such parameters are: the total capacity of nuclear power plants, the proportion of nuclear steam and heat plants, the territorial distribution of the different types of plants, and the mode of utilization of nuclear steam plants.

The optimal values of these parameters are plotted graphically as functions of the basic economical and energetic factors. These functions are then analyzed for the presence of clearly defined "discontinuities" that separate the domains of the acceptable and unacceptable values of the investigated factors.

On this basis it is possible to formulate certain basic rules for the future growth of nuclear power which for the inspected energetic and economical factors (the cost of nuclear power plants, their regulation capabilities, distribution, etc.) are established as domains of their limiting values, and for all other factors as simplified but descriptive relations that reflect their effect on the investigated parameters of nuclear power.

Application of this method of prediction to the analysis of the future growth of nuclear power in the USSR led to the following results.

Effect of Nuclear Power on the Optimal Fuel–Energy Balance of the USSR. Multifactorial analysis of the optimum fuel–energy balance has been applied to a case in which the predicted level of consumption of electric power in the USSR will be four times as high and the output of all kind of energy resources twice as high as now; this includes an increase of natural gas production by a factor of 4-5 and of petroleum by a factor of 2-2.5. However, in spite of the rapid absolute growth of the production of high-quality fuels, the dynamical structure of the fuel–energy balance is expected by that time to undergo radical changes: the effect of the increasing contribution of petroleum and natural gas to fuel–energy balance, observed for the last 15 years and expected to continue in the coming decade, will be in the long-range much reduced or cease altogether. Taking into account the absolute growth of energy consumption this means the necessity of increasing the absolute capacity of coal and the use of nuclear energy.

The results of optimization of fuel–energy balance indicate that the maximum economically sound fraction of nuclear energy in the total energy output amounts at the considered stage to 10-12% (Fig. 1a). Such a growth in nuclear power production could afford a saving of 6-8 billion rubles annually in expenses and 3-4 billion rubles in capital investments.

The effect of nuclear power on the optimal growth of the main branches of the fuel industry is illustrated in Fig. 1a. The observed reduction in the use of organic fuels associated with the rise in the

capacity of nuclear power stations is due principally to a drop in coal production. The available petroleum and natural gas resources are fully utilized at all the considered levels of their production. Moreover, increased use of high-quality fuels even leads to a certain drop in the optimal capacity of nuclear power plants* as a result of competition of natural gas from the Eastern regions of the European USSR and because of region of variable load on the electric power consumption curve.

A detailed analysis indicates that future development of the main coal basins is almost entirely governed by the scale of growth of nuclear power – from total cessation of growth in case of high-capacity nuclear power stations to maximum growth in case of minimal use of nuclear power. The principal competitor of nuclear power in this case is coal from the Kansk-Achinsk and Kuznetsk Basins delivered to the European regions of the USSR by rail and partially in the form of direct current electricity transmitted by power lines (to distances of up to 2000-4000 km).

Changes in fuel supply conditions as a result of increased use of nuclear power affect most significantly the terminal consumers of fuel, i.e., the power plants of the European branch of the Unified European Power System. Figure 1b shows the changes taking place in the power generation structure of the Unified European Power System (with respect to the kind of fuel employed) as a function of the total capacity of nuclear power plants for minimum and maximum natural gas production. It is seen that, firstly, as their capacity increases nuclear power plants displace more and more conventional coal-burning plants (predominantly those using Donets Basin coal); with still higher capacity nuclear power plants begin to displace power plants using Kansk-Achinsk coal (in Ural and along the Volga) as well as the transmission of dc power to the Western regions of the USSR. Secondly, it it seen that over the entire range of variation of natural gas resources, most gas- and oil-fired power plants should be designed for peak load operation with possibly only a small fraction of them designed for load switching; most high-capacity base electric plants should be designed for solid fuel.

These results apply to average (expected) values of economical indicators. When these indicators vary within the limits of the assumed error (up to ±25-30%), the conclusions are correct only where nuclear energy can compete with natural gas from Northern deposits, i.e., when the economical indicators of its production and transportation are unfavorable.

The scale of development of nuclear power has a significant effect on the terminal expenditure on fuel, i.e., on the relative economical indicators that characterize the actual cost of production of additional quantities of fuel in the given region of the USSR.† Figure 1c shows the terminal expenditures on fuel in the principal regions of the USSR as a function of the total capacity of nuclear power plants (for minimum resources of high-quality fuel). It is seen that the terminal expenditures on fuel remain stable only in the Siberian regions (where they are governed mostly by the cost of mining and transportation of Kansk-Achinsk coal), and decrease by 3-4 rubles/ton of fuel with the growth of nuclear capacity in most regions of the USSR. This once more confirms the high economical efficiency of nuclear power. At the same time, one should consider that all measures of the current decade (1970-1980) for rationalizing the structure of the fuel–energy balance by increasing the share of petroleum and gas will provide a gain of only 2-3 rubles/ton of fuel.

Together with terminal expenditures on organic fuel, the analysis also gave an estimate of the maximum admissible expenditure on nuclear fuel (in it fuel equivalents), i.e., of the maximum cost of its production at which nuclear power plants still can compete with conventional plants (Fig. 1c).

Effect of Principal Economical Factors on Optimal Levels of Growth of Nuclear Power. In the preceding section we have discussed the effect of the pace of growth of nuclear power on the long-term structure of fuel-energy balance of the USSR and on the growth of other branches of our power economy. Another task of the analysis is to determine how the power economy, in turn, affects the optimal level of growth of nuclear power. For this purpose we have analyzed its dependence on the following economical factors:

1. In determining the limits of applicability of nuclear power it is of decisive importance to find the maximum possibilities of its territorial coverage. The mathematical model made it possible to consider the feasibility of constructing nuclear power plants in practically all regions of the country. The results of optimization obtained on this premise are illustrated in Fig. 2. The horizontal axis represents (in relative

* See the straight portion of the sloping line that represents the fuel equivalent of nuclear power in Fig. 1a.
† The economical sense and methods of calculation of the terminal expenditure on fuel have been discussed in detail in [2].

units) the required increase in electrical power capacity of the country for the last decade of the design period divided into 11 principal regions. The regions are arranged in the order of decreasing calculated cost of production of electric power by fossil-fuel steam power plants (SPP). These costs were calculated for base steam power plants for two limiting values of terminal expenditure on fuel corresponding to minimum and maximum gas production with no restrictions imposed on the growth of nuclear power. In this manner we have found the territorial variation of the cost of production of electricity by steam power plants that directly compete with nuclear power plants.

The results of this competition are illustrated in Fig. 2 which shows the calculated average and minimum costs of electricity produced by nuclear power plants. These costs are assumed to be the same in all regions of the USSR. As seen in the figure, in the European USSR (including Ural) in Central Asia, and in the far East the economical indicators of nuclear power are better than those of steam plants. In West Kazakhstan nuclear power is economically inferior to steam plants for average indicators and practically equal for minimum indicators. Only in the principal regions of Siberia is nuclear power uneconomical even under the most favorable conditions in comparison with electrical plants burning Kansk-Achinsk coal or with large hydroelectric power stations.

Thus, from the point of view of territorial coverage, the limits of applicability of nuclear power include all regions of the country except Siberia and East Kazakhstan. These regions should contribute more than two thirds of the total growth of electric power consumption of the USSR.

2. However, not all this growth can be satisfied by nuclear energy. This is due, first of all, to the lower relative economical advantage of nuclear power plants operating under variable loading conditions. A simple economical comparison indicates that nuclear plants are competitive with steam plants operating from 7000 to 4000 h/year in regions of high fuel costs (North-West) and from 5000 to 6000 h/year in regions of low-cost fuel (Ural), i.e., they cannot participate in meeting the demands of the peak and semipeak portions of the electrical load curve. This leads to an additional reduction of the limits of applicability of nuclear power (in addition to the limitations due to territorial considerations) but does not provide a basis of a quantitative evaluation of this restriction. In fact, by partially shifting the existing power plants into the variable-load portion of the load curve and by designing specialized peak-load and regulated plants it is possible to transfer a considerable portion of the anticipated electric load into that portion of the curve were nuclear plants can compete with conventional steam plants.

To study the effect of operating conditions on the maximum capacity of nuclear power plants, optimal structures of the Unified European Power System (as part of the fuel–energy balance) were computed for two extreme configurations of the possible composition and regulation capabilities of conventional power facilities. The second Unified European Power System structure corresponds to limited (as compared to the first) regulation capabilities.

The results were used to plot the maximum (from the point of view of operating conditions) capacity of nuclear steam power plants (NSPP) and the resultant gain in fuel–energy balance as a function of the regulation capability of nuclear and conventional plants (Fig. 3). It is evident that the capacity of nuclear plants decisively depends on the type and regulation capabilities of conventional power facilities. Thus, under constant-load operating conditions most favorable from the point of view of nuclear power generation (i.e., without nightly off-load operation for periods of 7000 h/year) the variation of structure and regulation of conventional power plants within the investigated limits leads to a reduction of the maximum capacity of nuclear plants by 15-18% and to an overexpenditure of about 700 million rubles in fuel–energy balance. This proves the great economical importance of improved regulation of electrical power equipment installed in the past period. These measures justify themselves by subsequent savings even if their initial costs amount to 10-15 rubles/kW in additional capital investments or to an increase of relative fuel consumption by 30-50 g/kWh.

The second important measure for increasing the capacity of nuclear power plants is to improve the regulation capabilities of nuclear facilities, i.e., to provide technical means for efficient operation under off-load conditions. Although this measure reduces the economical performance of the plants (in spite of high initial capital investment the advantage of low-cost electricity is lost), the measure is on the whole advantageous for the Unified European Power System and the fuel–energy balance as it compensates to a large extent the inadequate regulation capabilities of other facilities and provides great savings by increasing the total capacity of nuclear power plants (see Fig. 3).

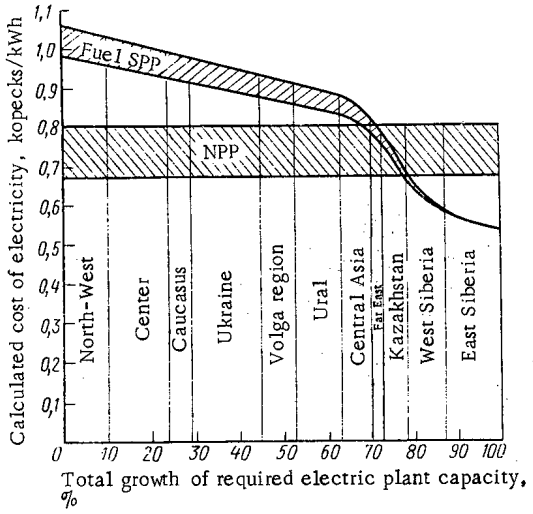

Fig. 2

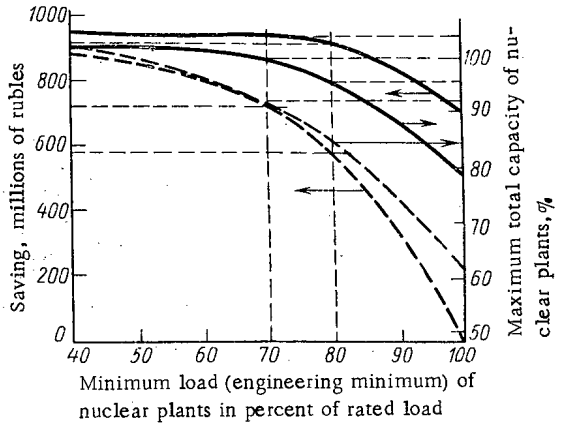

Fig. 3

Fig. 2. Competitive power of nuclear power plants and base steam power plants in the various territories of the USSR.

Fig. 3. Effect of load regulation capabilities of nuclear plants on maximum capacity and expenditure. Regulation of conventional plants: ———) high; – – –) low.

Obviously, even allowing for the provision of regulation capabilities (permitting daily shutdowns), it is impossible to attain unlimited off-load capabilities for the entire installed nuclear power capacity because of the existence of an approximately five-year transition period for nuclear power plants put into operation [3] and because of the start in the introduction of fast reactors. At the same time, the curves in Fig. 3 show that an increase of the minimum load (design minimum) of nuclear plants from 40 to 70-80% only slightly decreases their total capacity and efficiency, whereas any further increase of the minimum causes a sharp drop of these indicators. In other words, these relationships show a clearly defined "discontinuity": reducing the load on nuclear power plants to 80% of their capacity is economically acceptable. Moreover, such a load reduction is obviously realizable in practice. This would afford the following advantages:

with improved regulation of conventional steam plants it would be possible to increase the maximum nuclear plant capacity by 15-18% and obtain an additional saving of 150-200 million rubles;

with inadequate regulation of other power plants it would be possible to fully compensate the resulting drop in the maximum capacity of nuclear plants (to raise the latter by 20-23%) thus saving 500-600 million rubles.

Accordingly, the provision of nuclear plants with a regulation range of about 20% (i.e., with a minimum design load of 80%) is economically sound even if this requires an additional capital investment (on the average for all new nuclear plants) of up to 20 rubles/kW. The realization of this measure is thus fully justified.

Thus, the principal operative factors that govern the maximum capacity of nuclear power plants are the regulation capabilities of conventional and nuclear plants. Computations indicate that even in the most favorable circumstances these factors reduce by 35-38% the economically sound maximum capacity of nuclear power plants found taking into account territorial considerations (a relatively large increase of heating capacity of heat power plants).

3. The growth of nuclear power can also be advanced by building, in addition to steam plants, nuclear heat plants. This direction is attractive because it provides a potential opportunity of expanding (by a factor of nearly two) the acceptable field of application of nuclear power, and secondly because it provides a substitution for the least economical fuels (gas, fuel oil) with a high terminal cost. However, extensive realization of these advantages requires a comprehensive review of the very concept of the growth of heat power distribution and the development of special demands on the equipment and circuits of nuclear heat plants. Practical solutions of these problems and the energoeconomical efficiency of nuclear heat

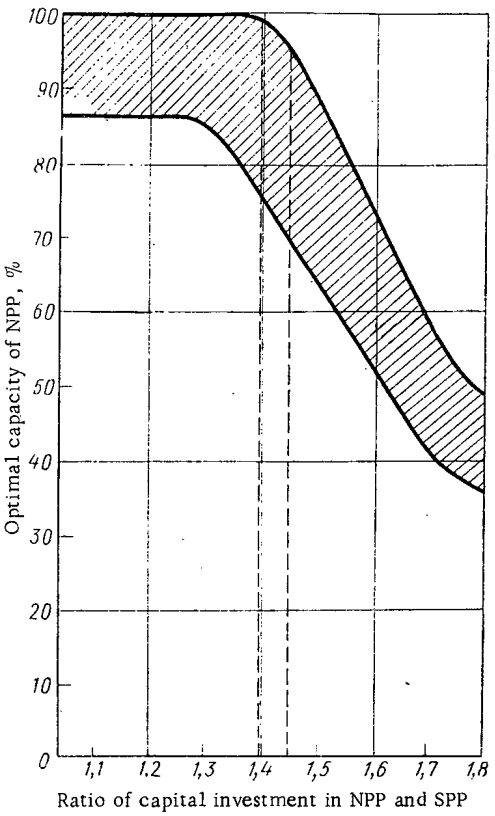

Fig. 4. Optimal capacity of nuclear plants as a function of the ratio of capital investments in nuclear and conventional plants at different levels of electricity consumption.

plants are at present unknown. Thus, in this study we have to deal with the least favorable conditions (assuming, in particular, reactors designed for steam plants). Under such premises, nuclear heat plants can be economically used in special heat-consuming centers with heat demands of at least 2.5 thousand Gcal/h. Under such unfavorable conditions the capacity of nuclear heat plants is relatively low and amounts to 8-10% of the total capacity of nuclear power plants (with respect to reactor power).

Taking into account the combined effect of territorial and load factors, the economically sound maximum capacity of nuclear steam and heat power plants at the end of the considered period turns out to be 30-33% of the total installed capacity of all power plants of the country, 42-47% of plant capacity of the European regions, 48-50% of the increase of total installed capacity in the last decade of the considered period, and about 70% of the increase in capacity of the European regions.

The growth of nuclear power within the limits of its maximum range can change substantially as a result of the following energo-economical factors.

4. The absolute economically sound capacity of nuclear plants is affected to a large extent by the resultant level of electricity consumption in the entire country. If the proportion of the European and Siberian regions remain unchanged, a one percent decrease in the demand in electricity results in a linear reduction in nuclear power capacity equal to about 2%. However, if the production of electricity decreases selectively at the expense of the Siberian or, on the contrary, the European regions, the maximum capacity of nuclear power remains the same in the first case, or drops by 3% for every percent of reduced production in the second case.

5. The optimal scale of incorporation of nuclear power plants into the power network depends also on organic fuel resources that can compete with nuclear power. As noted before, to such resources belong in the first place the Siberian and Kazakhstan coal deposits (provided they are used locally) which limit the territorial extent of nuclear power predominantly to the European regions of the USSR. But even here can nuclear power meet with competition from organic fuels such as natural gas and fuel oil.

As shown by several different versions of optimal fuel–energy balance, the variation of high-quality fuel resources within the actual limits does not affect the capacity of nuclear power plants, and only an increase in gas production leads to a reduction of maximum capacity by 15-20%. On the whole this factor can be neglected in this study.

6. Obviously, the optimal capacity of nuclear plants significantly depends on the resultant combinations of their own economical indicators and the indicators of competing power plants, as well as on the production and transportation of fuel. Consequently, the possible changes in optimal capacity of nuclear plants can be correctly evaluated only after a careful study of the region of uncertainty of the optimal fuel–energy balance due to the combined effects of the error in the economical indicators of all objects considered.

Figure 4 shows the results of such a study in the form of a dependence of the optimal capacity of nuclear plants on the factor $K = K_{NPP}/K_{SPP}$, i.e., on the ratio of the capital investments in nuclear and conventional plants. This statistical ratio is of primary importance for understanding the prospects of nuclear power.

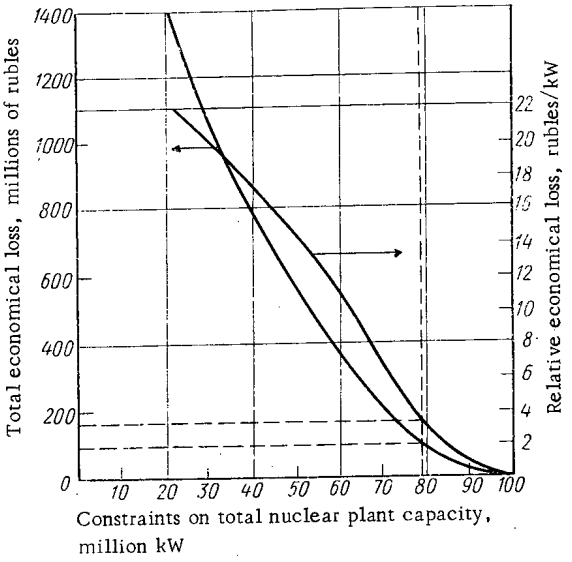

Fig. 5

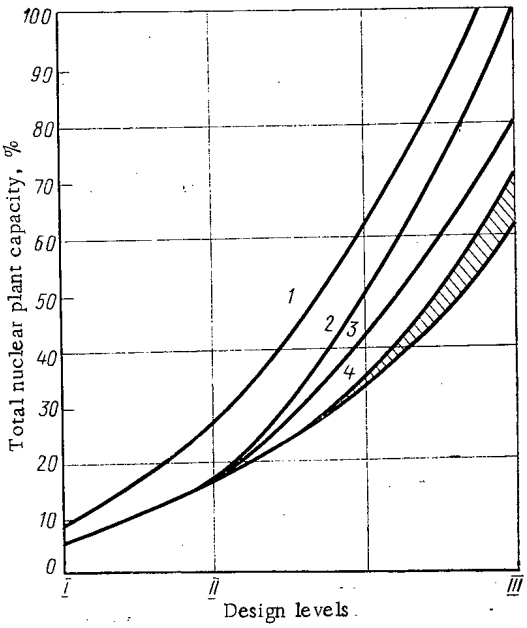

Fig. 6

Fig. 5. Economical consequences of constraints on the total capacity of nuclear power plants.

Fig. 6. Possible trends in the growth of nuclear power: 1) theoretical; 2) calculated; 3) rational; 4) probable.

In fact, the figure shows that as long as the relative capital investment in nuclear plants does not exceed the corresponding investment in steam plants by more than 40-50% ($K \leq 1.4$-1.5), the growth of nuclear power does not depend very much on the economical indicators of other energy resources and can be aimed for practically the maximum level (with only a 10-15% deviation from maximum capacity).

The optimal capacity drops sharply when the factor K exceeds 1.4-1.5 ("discontinuity" point). An increase of the capital investment ratio from 1.5 to 1.7 results in a 30-35% drop in optimal capacity. If the ratio increases still more (1.7-1.8), the rate of the decrease slows down as nuclear power is becoming less and less economical in regions of high-cost fuels. Nevertheless, for the maximum capital investment considered ($K = 1.8$), the economically sound capacity of nuclear power plants is only 40-50% of its maximum value.

Effect of Nonenergetic Factors on the Growth of Nuclear Power. Although the nuclear power growth levels discussed in the preceding section are optimal from the point of view of fuel–energy balance, they may prove unrealistic or unrealizable in practice for the national economy as a whole. This circumstance is now difficult to evaluate economically but its effect can be taken into account in the form of nonenergetic (national-economic) constraints on the growth of nuclear power, for example, on the total capacity of nuclear power plants. We have thus investigated not only the optimal scale of growth of nuclear power but also the energo-economical consequences of the reduction of nuclear plant capacity below optimum.

For this purpose, using average values of economical indicators, we have computed a large number of optimal fuel–energy balance versions in which the constraints on the total capacity of nuclear plants were varied for different levels of electricity consumption and different high-quality fuel resources. These computations made it possible to determine the economical loss to the power economy caused by different constraints on the total capacity of nuclear power plants. The magnitude of the loss was computed as the difference in the optimal total calculated power cost, i.e., of a functional of the fuel–energy balance model, when passing from unlimited (100%) nuclear plant capacity to increasingly "stringent" constraints on its total value.

The curves shown in Fig. 5 clearly illustrate the fact that as the total nuclear power capacity is reduced more and more the magnitude of the total and relative economical loss increases first very slowly and then, after reaching some critical value, very rapidly. This behavior has a quite obvious explanation. Forced reduction of the capacity of nuclear plants eliminates nuclear power first from the regions where

fuel is inexpensive and at the same time from the variable portion of the electrical load curve in regions of expensive fuel where nuclear power is attractive because of the excessive growth of relatively costly hydroelectric storage plants, the shift of existing plants to less favorable portions of the load curve, and other not very effective measures. In other words, in the presence of restrictions nuclear power plants are first forced out from regions where their economical performance is nearly equal to that of conventional plants so that the economical loss is relatively low. After all such possibilities are exhausted, further restrictions on capacity of nuclear plants affect their use as base load plants in regions of high-cost fuel resulting in a rapid increase of the relative and total economical loss.

The dashed lines in Fig. 5 show the approximate location of "discontinuities" in the dependence of the economic loss on the magnitude of constraints on nuclear capacity. An analysis of the position of these points in relation to optimal capacity proved that it remains nearly the same under different conditions of electricity consumption and gas resources, and is governed by the nuclear plant capacity equal to approximately 80% of the corresponding optimal capacity.

Thus, a drop in nuclear plant capacity by up to nearly 20% of optimal capacity is not associated with any significant losses to the power economy. In fact, the overall loss in the fuel–energy balance amounts in this case to only 20-100 million rubles (depending on the level of consumption and gas resources), i.e., about 7% of the maximum possible loss. The relative loss does not exceed 2-3 rubles/kW.

At the same time, such a 20% drop in nuclear plant capacity is, apparently, justified from the point of view of the national economy as a whole in view of the difficulties in the transfer of certain nonenergetic branches to nuclear power operation and as an insurance against the possible rise in cost of nuclear power plants.

The resulting values of total capacity of nuclear plants were additionally corrected in order to allow for dynamical factors. The meaning of this correction is illustrated in Fig. 6 which shows the different trends in the growth of nuclear plant capacity with time.

The first curve in this figure corresponds to the maximum (from the point of view of economical considerations) rates of growth of nuclear power that can be obtained theoretically in the case of total absence (starting with the present five-year period and on) of nonenergetic constraints on the capacity of nuclear power plants. The portion of this curve corresponding to the first and second time levels has been plotted from the results of optimization of fuel–energy balance assuming that nuclear plants are placed in the entire unoccupied portion of the base load growth in regions were such plants can be effectively used. The second portion of the curve was plotted from the results of the above-mentioned analysis. As seen in the figure, the average annual rate of growth of nuclear plant capacity is under these premises nearly 15%, i.e., leads by a factor of nearly two the rise in electricity consumption.

The second and third curves in Fig. 6 characterize the calculated optimal and acceptable (allowing for a 20% reduction) capacities of nuclear power plants. Both are based on the now accepted scale of development of nuclear power up to the second design level and proceed from the admittedly incorrect assumption that the conditions of development of nuclear power between the second and third levels are practically the same.

In reality however the effect of several factors that tend to restrain the growth of nuclear power will be felt during the first years of this period. The fourth curve of growth of nuclear power corresponds to the case when the effect of these factors would be felt only for two-three years. However, if the restraining factors act for a longer time, the growth of nuclear power is represented by the lowermost curve in Fig. 6.

Thus, the no longer optimal but rational (from the point of view of the national economy) probable capacity of nuclear plants in the last years of the design period amounts to 65-70% of the economically sound maximum capacity.

The above discussion leads to the following conclusions.

1. Together with Tyumen natural gas and Kansk-Achinsk and Kuznetsk coal, nuclear energy will become in the considered period one of the basic sources for satisfying the growing demand for electric energy in the USSR. The analysis indicates that it would be careless and economically expensive to strive for maximum development of any one specific resource at the expense of others; all four resources should be intelligently combined.

2. Such a moderate strategy of the development of the power economy corresponds to the incorporation of nuclear power plants with a capacity equal to 65-75% of the economically sound maximum capacity. The fraction of nuclear power in the overall output of all energy resources would then amount to 7-8% at the end of the considered period; the proportion of nuclear power plants in the structure of all generating plants will reach in the same period 20-23%, including 32-36% in the European regions (and about one half of the total output).

3. The indicated growth levels of nuclear power are economically sound even if their relative capital investment is 60-65% higher than the corresponding figures for conventional steam power plants. However, with still higher costs, the rational capacity of nuclear power plants should be decreased by 15% for every 10% increase of the investment ratio.

4. These growth levels require that nuclear power plants have an adequate regulation range that would allow off-load at least 20% below the average total installed capacity. If this condition is met, nuclear power plants will be efficiently employed not only for base load operation but also in the 17-18 h region of the 24 h load curve for annual loads of 5800-6000 h/year. If such a regulation range cannot be ensured the loss to the national economy will amount to 10-15 rubles/kW.

5. The following simple rule of the growth of nuclear energy corresponds to the set of the above "boundary" conditions: irrespective of the level of electricity consumption and other energo-economical factors, nuclear power plants should be used to provide for the growth of base (at the expense of heat plants using organic fuel) and some of the fluctuating (in accordance with the preceding paragraph) electric load in the North-West, Center, Ukraine, and Caucasus, without any special effort to extend their use to other regions of the USSR (with the exception of remote regions with specific climatic conditions) and without applying them to still more fluctuating portions of the load curve.

6. This work is only the first in a general study. Its aim is to give a deep understanding of the problems associated with the growth of nuclear power and the analysis of long-term development of the power economy including the role of fast reactors.

The study is a joint work of the staff of four organizations under the Scientific guidance of Academician L. A. Melent'ev. The work was done with the participation of G. V. Agafonov, I. M. Vol'kenau, E. A. Volkova, M. V. Sapozhnikov, G. E. Tkachenko, and L. D. Khabachev.

LITERATURE CITED

1. A. A. Makarov, A. S. Makarova, and A. N. Zeilinger, Ekonomika i Matem. Metody, No. 6, 424 (1970).
2. A. P. Andreev et al., Teploénergetika, No. 8, 68 (1967).
3. V. V. Batov and Yu. I. Koryakin, Economics of Nuclear Power [in Russian], Atomizdat, Moscow (1969), p. 41.

PHYSICAL AND TECHNOLOGICAL PRINCIPLES OF THE CONSTRUCTION OF ATOMIC POWER STATIONS WITH GAS-COOLED FAST REACTORS AND USING A DISSOCIATING COOLANT, NITROGEN TETROXIDE*

A. K. Krasin, V. B. Nesterenko, N. M. Sinev, V. P. Slizov, V. I. Khorev, B. I. Lomashev, V. P. Bubnov, B. E. Tverkovkin, and V. A. Naumov

UDC 621.311.2:621.039

One of the ways to obtain effective characteristics for gas-cooled fast reactors may be to use the dissociating compound nitrogen tetroxide (N_2O_4) as the coolant and working fluid in single-loop schemes of atomic power stations [1-7].

There exists a large class of inorganic polyatomic gases in which there are thermally reversible chemical reactions of dissociation and association taking place with thermal effects and changes in the number of moles. The most interesting of these is a dissociative system that has been studied in considerable detail:

$$N_2O_4 \rightleftarrows 2NO_2 - 149 \text{ kcal/kg} \rightleftarrows 2NO + O_2 - 294 \text{ kcal/kg}$$

The temperature range of the first stage of the reaction is 21-170°C, and the range of the second stage is 140-850°C. The most important physicochemical properties of N_2O_4 are given in [1].

Both the first and the second stages of the reaction are accompanied by large thermal effects, and this has an important influence on the thermophysical properties of the dissociating gases.

At the Nuclear Power Institute of the Academy of Sciences of the Belorussian SSR (IYaÉ AN BSSR) we conducted a comprehensive study of the thermophysical properties of N_2O_4 over a wide range of temperatures and pressures, including a study of: viscosity at 30-500°C and 1-150 abs. atm; p-v-t properties at 50-525°C and 8-125 abs. atm; enthalpy at 20-150°C and 100-170 abs. atm; the composition of the gas at 200-600°C and 1-7.5 abs. atm [1]. We conducted extensive investigations of the heat exchange taking place during boiling and condensation, as well as the convective heat transfer taking place during cooling.

The investigations showed that the effective thermal capacity and thermal conductivity of N_2O_4 are 3-9 times as high as the usual thermal capacity and molecular thermal conductivity of nondissociating gases. This means that there is a sharp increase in the heat-exchange coefficients (for example, the maximum values of the effective thermal capacity of N_2O_4 at 1 abs. atm and 80-100°C are as high as 2.4 kcal/kg · deg.

In the nonisothermal flow of a gas taking part in a chemical reaction, there is, in addition to the heat exchange through thermal conductivity, a substantial amount of heat exchanged in the form of chemical enthalpy through concentration diffusion. Chemical enthalpy may constitute a very large part of the total heat-transfer balance. In the experimental investigations conducted at the IYaÉ AN BSSR, with turbulent flow of N_2O_4 in a heated pipe at supercritical pressures of 115-160 abs. atm and temperatures of 250-530°C,

*Fourth International Conference on the Peaceful Uses of Atomic Energy (Geneva, September, 1971). Report No. 431.

Translated from Atomnaya Énergiya, Vol. 32, No. 3, pp. 197-203, March, 1972.

heat-flux densities of $(1-7)\cdot 10^5$ kcal/$m^2\cdot h$, and Reynolds numbers of $(1-2.5)\cdot 10^5$, we found that the heat-exchange coefficients were 18,000-42,000 kcal/$m^2\cdot h\cdot$deg, or 3-9 times the values obtained for inert gases under comparable conditions.

Because of the high thermophysical properties of N_2O_4, its use as a coolant results in effective heat removal from the active zone of a fast reactor with a thermal power of 2500-3000 MW at an average power density of 500-600 kW/liter in the active zone, a maximum temperature of 700-720°C in the fuel-element jackets (taking account of local overheating factors), a gas temperature of 520-540°C at the reactor outlet, a pressure of 140-170 abs. atm, and gas heating values of 230-270°C.

The most distinctive and advantageous features of an N_2O_4 dissociative system is the possibility of using the molecular weight, which varies with the temperature (and therefore with the gas constant R), for bringing about a considerable increase in the effective efficiency and specific power of a gas-turbine cycle. Gas cycles using helium and CO_2 have some well-known drawbacks; in such cycles, the coefficient of useful work of a cycle at 500-650°C is very low ($\varphi = (L_t - L_c)/L_t = 0.2-0.35$). In the case of N_2O_4, since the reactions are reversible and the chemical composition changes from $N_2O_4 \rightleftharpoons 2NO_2$ at 25-30°C with a gas "constant" of 9.2 to $NO + O_2$ at 650-850°C with a gas "constant" of 27.6, it is possible to have the thermodynamic gas cycle take place with different gas "constant" values in the turbine and in the compressor. The gas "constant" in the compressor is lower than the value in the turbine, and therefore it is possible to reduce the fraction of the power used up in the compression and circulation of the gas, to 30-45%, while in the case of helium the fraction is 70-80% at temperatures of 500-650°C. As a result, an N_2O_4 heat cycle has a much higher coefficient of useful work and a greater effective efficiency than inert-gas cycles [4-6] (Fig. 1).

A comparison of the gaseous coolants (He, CO_2, and N_2O_4) used in fast reactors with respect to the pump-through parameter (the specific power used up in circulating the gas, per unit of transmitted thermal power) at 100-120 abs. atm and 300-600°C showed that the specific power consumption for N_2O_4 is less (by a factor of 7-8) than for CO_2 and for He.

In the system $N_2O_4 \rightleftharpoons 2NO_2 \rightleftharpoons 2NO + O_2$ the parameters of the line of saturation are such that it can be used for gas–liquid cycles with the low parameters of 1.3-1.7 abs. atm and 27-32°C condensation temperature [1].

Nitrogen tetroxide has a low heat of vaporization (5.5 times the value for water). This makes it possible to simplify the heat regeneration scheme in the gas–liquid cycle, since the heat of the gases leaving the turbine is quite sufficient not only for heating the liquid to vaporization but also for superheating the gas in the regenerator by 100-200°C. In the regenerator, the chemical reactions of dissociation take place on the high-pressure side with a lower heat of chemical reaction (149 kcal/kg) than on the low-pressure side in the process of recombination (294 kcal/kg), and as a result, in gas–liquid cycles using N_2O_4 it is possible to achieve a higher degree of heat regeneration than in cycles using water or CO_2, and consequently to obtain better values for the thermodynamic indicators. Thus, if N_2O_4 is used, it is possible to construct an atomic power station with a gas-cooled reactor, as well as to use a thermal scheme involving a gas–liquid cycle with regeneration.

Our study of the mechanism of the chemical reactions and kinetic constants of N_2O_4 showed that in the gas-dynamics calculations of turbines and heat exchangers, as well as in calculations of heat-exchange coefficients, we had to take account of the time characteristics of the dissociation and recombination. Our estimates of the time of chemical relaxation indicated that the first stage of the reaction ($N_2O \rightleftharpoons 2NO_2$) takes place under equilibrium conditions in 10^{-6}-10^{-8} sec, and in the second stage of the reaction ($2NO_2 \rightleftharpoons 2NO + O_2$) the relaxation times may vary between 10^{-3} and 10^{-1} sec, depending on the thermodynamic parameters.

The investigations showed that among the many possible schemes for atomic power stations, the scheme with high efficiency is one with intermediate heat regeneration between the high- and low-pressure turbines. At intermediate regeneration pressures of 15-25 abs. atm, we obtain full regeneration effectiveness and practically eliminate the influence of the kinetics of the chemical reactions. In gas cycles using N_2O_4, in order to make sure of achieving high thermodynamic efficiency, the lower pressure of the cycle should be chosen in the 8-10 abs. atm range, which provides a sufficient approximation to equilibrium processes. Thus, gas turbines using N_2O_4 do not require a vacuum.

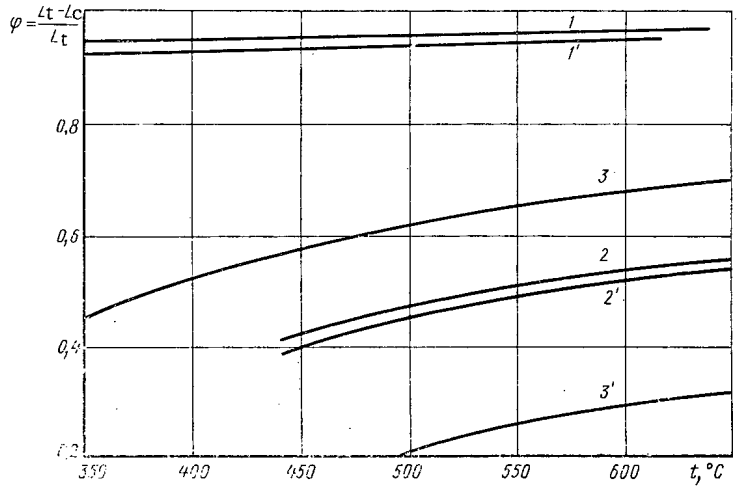

Fig. 1. Comparison of the coefficients of useful work of the thermodynamic cycles of atomic power stations using gas-cooled fast reactors. Gas–liquid cycle: 1) N_2O_4, p = 240 abs. atm; 1') N_2O_4, p = 150 abs. atm; 2) CO_2, p = 240 abs. atm; 2') CO_2, p = 170 abs. atm. Gas cycle: 3) N_2O_4, p = 150 abs. atm; 3') He.

For this reason, the use of N_2O_4 as the working fluid of turbines has a number of advantages over the use of other working fluids (for example, steam). At a pressure of 1.3-1.7 abs. atm downstream from the turbine, the specific volume of N_2O_4 is between 1/34 and 1/40 of the specific volume for steam at a condenser pressure of 0.035 abs. atm. This makes possible a considerable increase in the power of the gas turbine for one exhaust, bringing the value up to 1000 MW [1] (for last-stage dimensions analogous to those of steam turbine).

In addition, the use of N_2O_4 makes it possible to construct the flow-through part with a small number of stages, since the isentropic drops for N_2O_4 are 2.5 times the values for steam.

Design studies on a 1000 MW gas turbine using N_2O_4 yielded the following basic characteristics: gas-flow rate 2930 kg/sec; gas pressure and temperature before the turbine: 130 abs. atm and 565°C; pressure and temperature before the low-pressure turbine: 15 abs. atm and 91°C; pressure downstream from the turbine, 1.5 abs. atm; speed 3000 rpm. The high-pressure turbine has six stages, with a constant rotor root diameter of 1000 mm for the case of first-stage guide vanes 430 mm high. The low-pressure turbine has two stages. The average diameter of the last stage is 1660 mm, the height of the guide vanes is 560 mm, the velocity at the outlet of the rotor is 122 m/sec. In order to reduce the load on the thrust bearing and the dimensions of the guide vanes, the turbine is constructed with twin exhaust. The weight of the turbine is 390 tons. Our design calculations indicated that it is possible to construct an N_2O_4 turbine with a metal volume that is less by a factor of 4-4.5 than the volume for a steam turbine, with better aerodynamic indicators (there is no moisture in the flow-through part of the turbine) and considerably smaller dimensions. It is quite realistic to envisage the construction of a single-shaft two-stream turbine with a power of 2000-3000 MW in a single unit [1].

The results of the experimental investigation in the 25-550°C range indicate that N_2O_4 has sufficient thermal and radiation stability for practical use in atomic power generation. We made an experimental study of the radiation stability of N_2O_4 and calculated the radiolysis of this coolant in the $n-\gamma$ radiation field of a fast reactor. In the dissociative system of the coolant ($N_2O_4 \rightleftharpoons 2NO_2 = 2NO + O_2$), as a result of the specific properties of fast reactors, radiochemical effects are caused by the action of $n-\gamma$ radiation at a high dose rate (approximately 10^{19} eV/cm^3 · sec) at contact times of $\sim 10^{-2}$ sec in the active zone, gas temperatures of 200-550°C, and pressures of 130-170 abs. atm. The products of the radiolysis of NO_2 are N_2O, N_2, and O_2. The fraction represented by the decomposing coolant in a fast reactor is approximately 10^{-6}.

A large number of structural steels and alloys were studied experimentally in an N_2O_4 medium at temperatures of 25-700°C and pressures of 1-150 atm, and the results showed a high degree of corrosion resistance (0.001-0.005 mm/g) [8]; the materials included Kh18N10T, ÉI-847, ÉI-629, ÉI-654, 3KhV, ÉI-432,

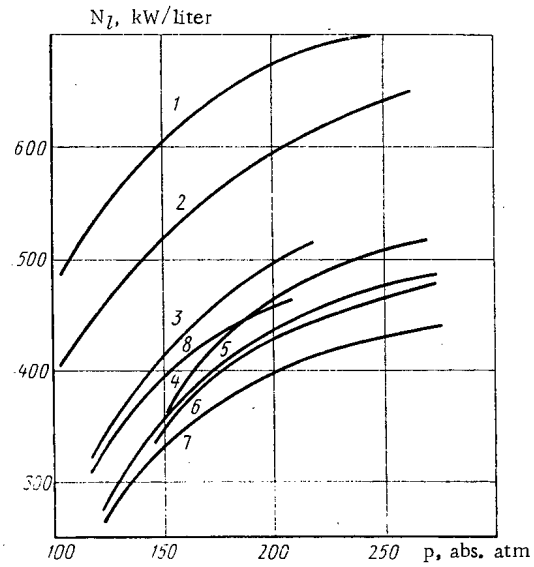

Fig. 2

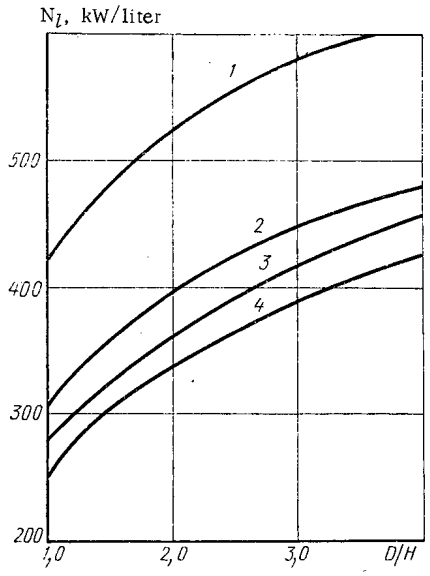

Fig. 3

Fig. 2. Specific thermal power density of gas-cooled fast reactors using N_2O_4, He, and CO_2, as a function of the pressure at the reactor outlet, for D/H = 2 and maximum jacket temperature ≤ 720°C: 1, 2) N_2O_4 ($d_{fuel\ element}$ = 6.4 mm, t_{gas} = 350 and 540°C, reactor pressure drop 12 and 10 abs. atm, respectively); 3, 5, 7, 8) He (t_{gas} = 670°C, 0.9, 0.95, 0.95, 0.9; $d_{fuel\ element}$ = 6.0, 6.0, 6.4, 6.4 mm, respectively); 4, 6) CO_2 (t_{gas} = 570°C; Δp = 16 abs. atm; $d_{fuel\ element}$ = 6.0 and 6.4 mm, respectively.

Fig. 3. Specific thermal power density of gas-cooled fast reactors as a function of the relative flattening of the active zone for p_{gas} = 150 abs. atm and maximum jacket temperature ≤ 720°C: 1) N_2O_4 (t_{gas} = 540°C; Δp = 10 abs. atm; $d_{fuel\ element}$ = 6.4 mm); 2) He (t_{gas} = 670°C; Δp = 16 abs. atm; $d_{fuel\ element}$ = 6 mm); 3) CO_2 (t_{gas} = 570°C; Δp = 16 abs. atm; $d_{fuel\ element}$ = 6 mm); 4) He (t_{gas} = 670°C; Δp = 8 abs. atm; $d_{fuel\ element}$ = 6 mm).

Kh25, and 3Kh3, as well as aluminum and titanium alloys, high-chrome cast iron, AG-1500 graphite, siliconized graphite, Teflon, and other materials in the operating range of temperatures. For the fuel-element jacket materials Kh18N10T and EI-847, a high corrosion resistance was found at temperatures of up to 800°C in tests lasting 10,000-12,500 h. The introduction of 0.7-1% NO into the coolant considerably reduces the corrosion of metals (to 0.02-0.05 mm/g) in the phase-transformation zone in the coolant.

Experimental studies in coolant technology are now being conducted at the Institute. A number of thermophysical test stands with N_2O_4 pressures of up to 150 abs. atm and gas temperatures of up to 550°C have been set up. These test stands were used for studying the thermophysical, gas-dynamics and corrosion characteristics of N_2O_4, for practical tests of techniques for the cleaning, repairing, filling, and emptying of loops in experimental heat-power units with ratings of up to 1000 kW. Some of the test stands have been in operation since 1965. An experimental power unit with a two-stage gas turbine having a useful power of 100 kW at gas temperatures of 500-520°C and pressures up to 6 abs. atm before the turbine, a gas flow rate of 1 kg/sec, and a test-stand thermal power of 1000 kW was tested in 1968. The first tests on this stand were conducted in order to study the stability of the parameters of the gas–liquid cycle with a maximum temperature of 504°C and a pressure of 5 abs. atm, with a circulation of 360 kg of N_2O_4 in the loop and a test-stand power of 1070 kW. The tests were continued for 372 h. During 170 h of continuous testing there were more than 1000 cycles of reversal of the dissociating coolant. The experiments showed a high stability for the parameters, and there were no indications of irreversibility in the coolant.

Complete reversibility of the gas–liquid cycle was also achieved in 1966-1967 in experiments conducted on a closed-circulation stand for 600 h using 80 kg of N_2O_4 at temperatures of 30-550°C and pressures of 10-60 abs. atm. Altogether, the stand was used under operating conditions for more than 1500 h, including 1000 h with no replacement of the N_2O_4. Chemical analysis of samples failed to indicate any appreciable change in the quality of the coolant (the impurities amounted to less than 0.8%).

TABLE 1. Physical Characteristics of Unprofiled Fast Plutonium Reactors with Power Ratings of 1000 MW (Electrical)

Parameter	Coolant					
	Na			N_2O_4		
Flattening, D/H	1	1,69	2,5	1	1,69	2,5
Critical charge of Pu^{239}, tons	1,91	1,93	2,00	1,89	1,91	1,96
Critical enrichment of Pu^{239}, %	9,00	9,10	9,36	8,88	8,99	9,25
Conversion ratio of active zone	1,242	1,226	1,183	1,256	1,237	1,194
Conversion ratio of side blanket	0,299	0,226	0,182	0,341	0,263	0,209
Total conversion ratio	1,657	1,661	1,677	1,727	1,731	1,752
Fuel resistance time in active zone, yr	1,120	1,126	1,181	1,160	1,164	1,211
Fuel resistance time in side blanket, yr	3,56	4,43	5,42	3,21	3,93	4,84
Doubling time, yr	7,67	7,60	7,58	7,14	7,09	6,93

At the IYaÉAN BSSR, tests were conducted for 500 h during 1969 and 1970 on a closed stand with a gas–liquid cycle in order to study the characteristics of heat exchange at gas parameters of 80-160 abs. atm pressure and 250-540°C temperature. These tests also indicated complete reversibility of the condensation cycle. From all of the above-mentioned experiments, it was possible to conclude that the gas–liquid cycle is completely reversible and N_2O_4 is usable in practice as a working fluid for power plants.

In order to determine the prospects for the use of He, CO_2, and N_2O_4 as gaseous coolants at atomic power stations with gas-cooled fast reactors, the efficiency and the coefficient of useful work of single-loop gas cycles and condensation cycles were compared under conditions of maximum thermal power density and using identical surface heat exchangers in each case. The thermophysical characteristics were studied by using fuel elements with metal jackets and a fuel composition of UO_2 + 30% Cr and Ni (PuO_2 + 30% Cr, Ni) [11]. The maximum temperature of the ceramic fuel was 1300-1400°C, and the power density was 450-500 kW/liter, i.e., equal to the accepted value for the active zone of the BN-1000 sodium-cooled fast reactor [7].

Current experience in the development of metal vessels lined on the inside with stainless steel has shown that it is possible to construct vessels that can be transported (by railroad) for fast reactors with thermal power ratings of 2600-3000 MW. At operating pressures of up to 170 abs. atm, such vessels should have a maximum diameter of 4.2-4.3 m and a height of 10-12 m. They can house an active zone with a diameter of 2.2-2.4 m, with a thermal power density of 500-600 kW/liter.

Figure 2 shows the variation of the thermal power density of gas-cooled fast reactors of single-loop atomic power stations using He, CO_2, and N_2O_4 at various pressures.

For the He and N_2O_4 gas cycles the maximum gas temperature varied between 500 and 670°C, while for the CO_2 and N_2O_4 gas–liquid cycles the range was 350-650°C. The investigations made it possible to identify the preferable range of gas parameters if a thermal power density of 450-500 kW/liter was to be attained: a temperature of 670°C and pressures of 200-240 abs. atm for He; 550-570°C and 190-220 abs. atm for CO_2; 520-540°C and 120-140 abs. atm for N_2O_4. With N_2O_4 at a temperature of 350°C, the same thermal power density values are also attained at pressures of 80-120 abs. atm, and a thermal power density of 650 kW/liter at 180 abs. atm.

In designs for gas-cooled fast reactors using N_2O_4, it is desirable to use a pressure of 150-170 abs. atm, a reactor outlet temperature of 520-540°C, and a specific thermal power density of 550-600 kW/liter. A further increase of the specific thermal power density can be achieved by flattening the active zone to a D/H value of 3.5-4.0. Increasing the active zone flattening D/H from 2.0 to 4.0 at 170 abs. atm makes it possible to increase the specific thermal power density: with CO_2 it is increased from 420 to 530 kW/liter, with He from 450 to 540 kW/liter, and with N_2O_4 from 550 to 650 kW/liter at 540°C and from 640 to 700-720 kW/liter at 350°C (Fig. 3). However, for such flattening values it is necessary to construct and test reactor vessels of prestressed reinforced concrete for pressure levels of 160-180 abs. atm.

We compared the physical characteristics of a number of plutonium reactors, all with cylindrical geometry, a power rating of 1000 MW (electrical), and identical active-zone composition but different values of flattening. As a result of our calculations, we obtained the fundamental physical characteristics for unprofiled reactors (Table 1).

TABLE 2. Physical and Thermophysical Characteristics of a Fast Plutonium Reactor with a Power Rating of 1000 MW (Electrical)

Characteristics	N_2O_4	Na
Average thermal power density, kW/liter	525	400
Flattening	1.25	3
Percentage of the volume that is represented by:		
fuel	33	50
coolant	32	33
steel	35	17
Diameter of fuel element (thickness of jacket), mm	6.2/0.30	7.8/0.30
Diameter and height of active zone, m	2.0/1.6	
Thickness of breeding blanket, mm	400	400
Matrix fuel	$PuO_2 + UO_2 + 30\%$	$CrPuO_2 + UO_2$
Relative dimension of inner zone	0.52	0.53
Critical charge, tons	1.800	2.4
Enrichment, %	9.6/12.8	10.1/13.5
Total conversion factor	1.51	1.50
Average conversion factor in active zone	1.00	0.95
Depth of burnup, %	10	10
Doubling time, yr	7.5	8
Coolant pressure, abs. atm	164/154	~1-7
Coolant temperature, °C	240/540	400/580
Maximum temperature of fuel element (taking account of overheating factors), °C	730	700/720
Maximum temperature of fuel core (taking account of overheating factors), °C	1280	2400

In the calculation of the doubling time is is assumed that the time required for reprocessing the packs in the active zones and blankets is one year, the average power density is 500 kW/liter, and the maximum degree of burnup is 10%. The calculations were carried out for a two-dimensional 18 group program (MIFI 18-4 RZ 15-B) [9]. The group constants used in this program were obtained on the basis of the BNAB system of constants [6].

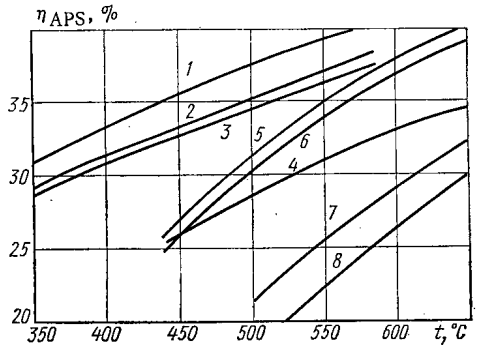

Fig. 4. Comparison of the thermodynamic efficiency of single-loop atomic power stations using gas-cooled fast reactors. Gas–liquid cycle: 1) N_2O_4, p = 240 abs. atm; 2) p = 170 abs. atm; 3) N_2O_4, p = 150 abs. atm; 5) CO_2, p = 240 abs. atm; 6) CO_2, p = 170 abs. atm. Gas cycle: 4) N_2O_4, p = 150 abs. atm; 7) He, p = 240 abs. atm; 8) He, p = 170 abs. atm.

An analysis of the calculation results shows that because of the harder spectrum and the higher leakage of neutrons from the active zone of the reactor in the case of the dissociating gas, the conversion factor can be increased by 3% over the value for sodium, the doubling time can be reduced by about 0.6 years, and the characteristics can be made more favorable from the point of view of plant safety (the effect of coolant removal is only one-half to one-third as great).

Calculations were carried out for gas reactors with carbide and matrix fuel compositions. Using carbide fuel reduces the doubling time by one year, which will make it possible in the future to obtain a doubling time of less than six years. The physical characteristics of a reactor using N_2O_4 with a matrix fuel composition are no worse than those for a sodium coolant. Table 2 shows the comparative characteristics of reactors using N_2O_4 and Na; it can be seen from this that the reactor using N_2O_4 has the preferable physical characteristics.

In determining the effectiveness of single-loop schemes for power stations using gas-cooled fast reactors, the hydraulic resistances of the main units were chosen on the assumption that for each coolant the maximum thermal power

density was achieved in the reactor, and the minimum surface areas were assumed for the heat exchangers.

Figure 1 shows a comparison of the coefficient of useful work of gas cycles using He and N_2O_4 with gas–liquid cycles using CO_2 and N_2O_4 In the gas-turbine cycle the coefficient of useful work of the atomic power station using N_2O_4 at a maximum temperature of 500-670°C reaches a value of 0.6-0.7, which is two or three times the value for atomic power stations using helium, and the efficiency of an atomic power station using N_2O_4 may be 28-35% (Fig. 4), whereas in a reactor using helium, for a regenerating scheme in which cooling takes place twice, the efficiency under comparable conditions is 20-31%. The coefficient of useful work of the cycle using N_2O_4 at a temperature of 50-550°C is 0.94-0.96, which is 1.9-2.3 times the value found for CO_2 under analogous conditions (see Fig. 1). The thermodynamic efficiency of the condensation cycles at maximum temperatures is 33-37% for the case of N_2O_4, whereas it lies between 26 and 35% in the case of CO_2.

In single-loop schemes of atomic power stations using a dissociating gas, it is possible to accept large values of pressure drop, attain relatively high values of specific thermal power density and have smaller dimensions for the heat-exchange devices. In single-loop schemes for atomic power stations using CO_2, even when the cooling-water temperature at the inlet is 15°C, the heat-exchangers weigh 2.2 times as much as do analogous heat exchangers in an N_2O_4 reactor with a temperature of 20-22°C.

In 1968-1970 the staff of the IYaÉAN BSSR carried out design studies for atomic power stations using N_2O_4 gas-cooled fast reactors with a single-loop scheme for the station and a gas–liquid cycle with intermediate regeneration. The design studies showed that it was possible to construct a gas-cooled fast reactor with a thermal power density of 500-600 kW/liter, a doubling time of less than seven years, and a single-shaft gas turbine with a power of 1000 MW whose metal volume was less by a factor of 4.5 than in the case of steam. The cycle used was a gas–liquid cycle with intermediate regeneration at 20-23 abs. atm, with a maximum cycle pressure of 150 abs. atm and a gas temperature of 520-540°C. On the basis of the design studies made at the Institute, engineering and economic indicators were calculated for an atomic power station with an electrical rated power of 2000 MW. These calculations show that it is possible to achieve an electrical rated power of 2000 MW in single-loop atomic power stations, with two gas-cooled fast reactors rated at 1000 MW each, using N_2O_4 and having fairly high engineering and economic indicators.

LITERATURE CITED

1. A. K. Krasin, Dissociating Gases as Coolants and Working Fluids in Power Plants, Proceedings of the All-Union Conference [in Russian], Nauka i Tekhnika, Minsk (1970), p. 6; V. B. Nesterenko, ibid., p. 11.
2. A. K. Krasin, V. B. Nesterenko, and N. M. Sinev, Proceedings of the Symposium "Mathematical simulation of thermal processes in power engineering" [in Russian], Nauka i Tekhnika, Minsk (1970), p. 95.
3. A. K. Krasin and V. B. Nesterenko, Thermodynamic and Transport Properties of Chemically Reacting Gaseous Systems [in Russian], Nauka i Tekhnika, Minsk (1967).
4. P. M. Kovtun, A. N. Naumov, and S. A. Kosmatov, Byul. Izobr. i Tov. Zn., No. 21, 62 (1964).
5. V. B. Nesterenko, V. P. Bubnov, and A. M. Matyunin, Izv. Akad. Nauk BSSR. Ser. Fiz.-Tekh. Nauk, No. 1, 57 (1966).
6. M. A. Bazhin, V. P. Bubnov, V. B. Nesterenko, and N. M. Shiryaeva, Optimization of the Parameters of Power Plants Using Dissociating Working Fluids [in Russian], Nauka i Tekhnika, Minsk (1970).
7. A. K. Krasin, V. B. Nesterenko, et al., Proceedings of the SÉV Symposium on Atomic Power Stations Using Fast Reactors [in Russian], Vol. 1, Obninsk (1967).
8. A. M. Sukhotin, N. Ya. Lantratova, and V. A. Gerasimova, Izv. Akad. Nauk BSSR, Ser. Fiz.-Énerget. Nauk, No. 2, 56 (1968).
9. V. V. Khromov and A. M. Kuz'min, in: Physics of Fast Reactors [in Russian], Atomizdat, Moscow (1968), p. 92.
10. L. Lais et al., Atomnaya Tekhnika za Rubezhom, No. 1, 7 (1970).
11. Advanced and High-Temperature Gas Cooled Reactors, SM-111/12, IAEA, Vienna (1968).

MEASUREMENT OF REACTIVITY EFFECTS IN THE REACTORS OF THE BELOYARSK ATOMIC POWER STATION

B. G. Dubovskii, A. Ya. Evseev,
I. M. Kisil', V. V. Korolev,
V. F. Lyubchenko, Yu. I. Mityaev,
and É. I. Snitko

UDC 621.039.519

The reactivity of a reactor is usually calculated on the basis of information relating to the manner in which the neutron flux varies with time. In recent years, special rapid and highly-sensitive analog computers (reactimeters) have been developed [1-8] to accelerate the determination of the steady-state reactivity and analyze its transient and instantaneous values.

Reactimeters may be divided into two types: open-cycle and closed-cycle, the latter incorporating a model of the reactor kinetics in the feedback circuit of the servo system. Reactimeters of the second type are used in the reactors of the Beloyarsk atomic power station.

A spatially-independent, single-point, monoenergetic model of the reactor kinetics is realized (without allowing for the temperature coefficient of reactivity) by combining a multiplier, an operational amplifier, and RC circuits designed to simulate the delayed neutrons.

The monoenergetic model of the reactor is constructed with due allowance for the following reactor kinetic equations:

$$\frac{dn}{dt} \approx \frac{\rho n}{\tau_0} - \sum_{i=1}^{6} \frac{dc_i}{dt} + S;$$

$$\frac{dc_i}{dt} = \frac{a_i n}{\tau_0} - \lambda_i c_i,$$

in which we have employed the generally-accepted notation of reactor theory.

Data relating to the a_i and λ_i of U^{235} subjected to fission by thermal neutrons are incorporated in the model of the reactor kinetics.

The power-measuring system of the reactimeter is made in the form of a multiple-decade electrometric operational amplifier, enabling ionization-chamber currents in the range 10^{-12}-10^{-4} A to be measured. The reactimeter has 14 scales, and measures positive reactivities in the range 10^{-5}-$5 \cdot 10^{-1}$ β_{eff} and negative reactivities in the range 10^{-5}-10 β_{eff}.

The dynamic range of the reactimeter corresponds to approximately one decade of reactor power; the rapidity of action is ~1 sec, and it is mainly determined by the inertia of the noise- and interference-smoothing system and the inertia of the reading and recording device, which is an EPP-09 electronic potentiometer. An example of the recordings of the reactimeter is presented in Fig. 1.

Figure 1 clearly demonstrates the high sensitivity of the instrument, even slight reactivity "noise" being readily perceptible. In power measurements it is easy to see the feedback associated with the negative temperature and power coefficients of reactivity (see Fig. 1b). The rate of change of reactivity due to these effects is $\sim 1.5 \cdot 10^{-7}$ K_{eff}/sec.

Translated from Atomnaya Énergiya, Vol. 32, No. 3, pp. 205-209, March, 1972. Original article submitted June 19, 1970.

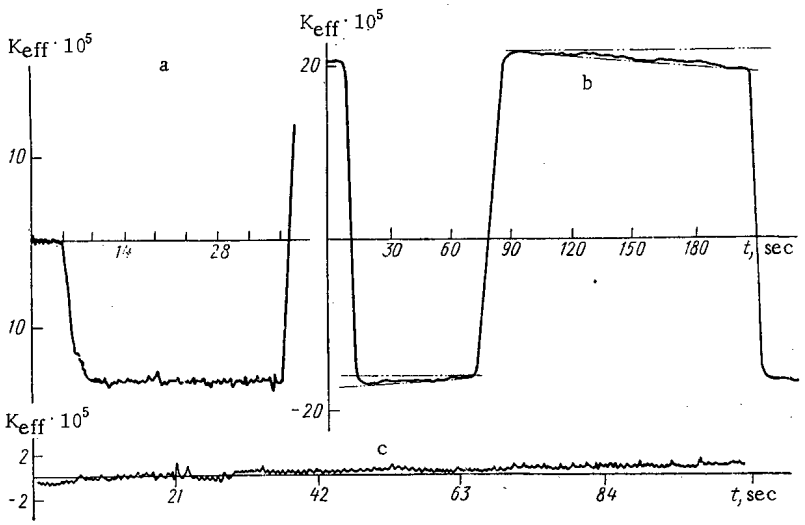

Fig. 1. Change in the reactivity of the first reactor of the Beloyarsk atomic power station on displacing the automatic control rods through distances equivalent to 0.05% (a) and 10% (b) of the nominal power; c) effect due to reactivity "noise."

The reactimeter was calibrated by comparing the results of measurements made by different methods for the same reactivity effects. The scatter in the resultant readings was no greater than ±5% of the measured quantity on all scales of the reactimeter.

Figure 2 illustrates a recording of reactivity taken during the removal of water from the steam-superheater channels, from which we readily see that the reactimeter records changes taking place in the reactivity outside the range of sensitivity of the automatic regulators.

Study of Reactivity Effects in the Reactors of the Beloyarsk Atomic Power Station

In starting the reactors of the Beloyarsk atomic power station, great attention was paid to an analysis of the reactivity effects. The reactivities of the fuel channels, the control-rod channels, and the water in these were measured at various points of the active zone for full loads in the critical assemblies; the compensating capacity and calibration curves of the control rods were measured, to estimate the reserve of reactivity, and the manner in which this varied with the amount of water in the fuel channels, to obtain relationships for the efficiencies of various absorbers, and also to plot the neutron distributions over the active zone of the reactor (by reference to the effectiveness of identical sections of the absorbing rods) and to correct calculated (design) data.

The results of some of the measurements are presented in Tables 1 and 2.

The results of the measurements carried out on the fuel-channel reactivity effects were used in connection with the recharging of the reactors in the Beloyarsk atomic power station.

Using the reactimeter, we estimated the reactivity effect associated with the filling of the gaps in the graphite stack of the first reactor with water. For this purpose we used special fuel channels enclosed in thin-walled sheaths, which were filled with water. The reactivity effects were measured at various distances from the center of the reactor and then extended to the whole active zone. We found that the total reactivity effect due to filling the gaps in the cells of all the IK-1.5 with water was equal to zero, while for the cells of all the IK-2 it equalled 0.94% K_{eff}.

The reserve of reactivity in the reactors of the Beloyarsk atomic power station was determined from the sum of the efficiencies of the compensating rods, measured by means of the reactimeter as each rod was extracted in turn. In these measurements, the compensating rods were arranged uniformly in the active zone with gaps of 60-70 cm. The neutron distribution corresponding to this arrangement will subsequently be called the "uniform" distribution.

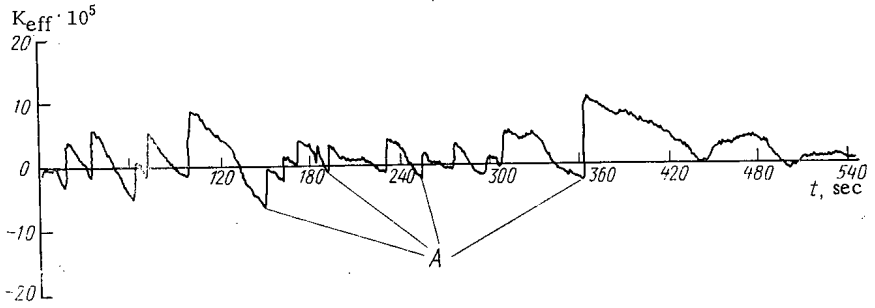

Fig. 2. Reactivity recording during the removal of water from the steam-superheater channels (A = instant at which the automatic regulator operates).

TABLE 1. Reactivity Effects during the Charging of One Evaporating Channel with 2% (IK-2) and 1.5% (IK-1.5) Uranium Enrichment in the Reactor of the First Unit (10^{-5} K_{eff})

Distance from center of reactor, cm	10	30	70	150	190	230	270	310	350
IK-2 with water	15,0	16,0	17,0	12,5	12,5	14,0	9,00	3,0	3,0
IK-1.5 with water	−7,5	−7,5	−1,2	−3,5	−2,5	−2,0	−1,0	−3,0	0

Further experiments showed that, for the uniform neutron distribution, the interference coefficient between a particular compensating rod and all the other rods (K_{int}) averaged over the reactor was almost equal to unity. The coefficient K_l allowing for the influence of a change in the neutron leakage from the reactor on the total efficiency of the rods was also close to unity. The relative increase taking place in the neutron flux in the cell of the extracted rod exerted the greatest influence. Direct measurements of the neutron distribution over the cell of the rod showed that this effect made the measured reserve of reactivity 6% higher than the true value. Thus the error in determining the reserve of reactivity from the sum of the efficiencies was ±10%.

The reactivity effect associated with introducing perturbations into the reactor may be measured by reference to the corresponding change in the reserve of reactivity or to the kinetic characteristics of the changes in the neutron flux passing through the reactor. If the perturbation introduces no serious changes into the diffusion characteristics of the active zone or the leakage of neutrons from the latter, the reactivities determined by the two methods should coincide; otherwise substantial differences may occur.

Let ρ_1 be the reactivity measured by reference to the change in the reserve of reactivity, ρ_2 that measured by reference to the period of the change in reactor power (or by means of the reactivity meter), and ρ_3 that associated with the change in the diffusion characteristics of the zone and the leakage of neutrons.

Let us give some examples relating to the measurement of reactivity effects in the reactors of the Beloyarsk atomic power station.

The Critical Assembly. In the critical assembly with 212 fuel channels of the reactor in the first unit, but without any water (one IK-2 to two IK-1.5), the efficiency of the IK-2 in one particular cell differed by roughly a factor of three for different positions of the compensating rods, this being mainly due to the great sensitivity of K_{eff} to a change in the leakage of neutrons from the reactor (which is small in the radial direction) and to the interference of the rods.

The Designed Charge. For the designed charge and a uniform neutron distribution, the sum of the efficiencies of the compensating rods $\Sigma_i \rho_i = 5.3 \pm 0.5\%$ K_{eff}, while for a severely-deformed distribution, quite independently of which part of the distribution (central or peripheral) is protruding, $-\Sigma_i \rho_i = 3.5 \pm 0.4\%$ K_{eff}.

For severe deformations of the radial field of the neutrons there is a considerable change in the neutron leakage, and K_{int} differs substantially from unity. In this case the reserve of reactivity is not equal to the sum of the efficiencies of the compensating rods, as confirmed by the foregoing data.

Expelling Water. On expelling water from the fuel units of the reactor in the first section of the power station, the reactivity effect was $\rho_2 = -0.65\%$ K_{eff}, while the reserve of reactivity changed by only +(0.1-0.2)% K_{eff}, corresponding to the calculated value. On expelling the water, in fact, the number of compensating rods introduced into the reactor fell by 12% (from 54 to 48), while their efficiency rose by 16%; the

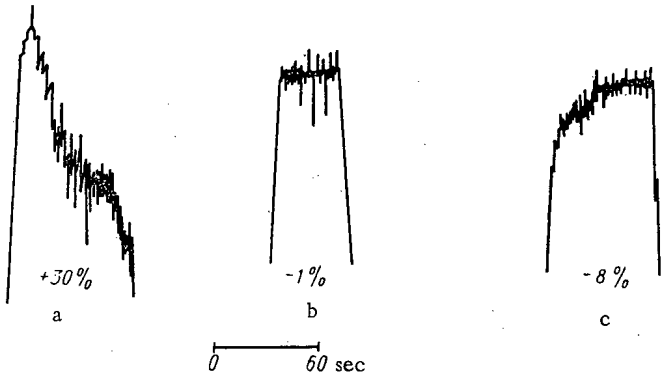

Fig. 3. Effect of the spatial redistribution of the neutrons on the initial readings of the reactimeter in relation to the distance r between the sensor of the reactimeter and the displaced rod: a) r = 1.1 m; b) r = 2.9 m; c) r = 4.9 m.

TABLE 2. Reactivity Effects in Various Fuel Channels of the Second Unit [9] in the Central and Peripheral Cells of the Active Zone (10^{-5} K_{eff})

Effect measured	In the center (cell 18-17)	On the periphery (cell 19-34)
Arrangement of IK-2 without water	2.6	−0.9
Pouring water into the IK-2	3.2	1.5
Arrangement of IK-2 with water	5.9	0.7
Arrangement of IK-3 without water	31.8	8.3
Pouring water into the IK-3	13.0	4.7
Arrangement of IK-3 with water	44.8	13.0
Arrangement of steam-superheating channel without water	29.0	7.5 7.5
Pouring water into the steam-superheating channel	8.8	2.2
Arrangement of steam-superheating channel with water	37.7	9.8

neutron distribution in both cases was almost uniform, and it was considered that K_{int} remained constant. The negative value of the reactivity effect was due to the increase in the efficiency of the compensating rods arising from the increase in the diffusion length in the water-free system.

The Reactor of the Second Unit. In the reactor of the second unit, with absorbing rods in the steam-superheating channels, the pouring of water into the fuel channels caused hardly any difference in the reserve of reactivity; the reactivity effects were:

on pouring water into all the evaporator channels +1.3% K_{eff};

on pouring water into the steam-superheating channels containing absorbing rods +0.45% K_{eff};

on pouring water into the steam-superheating channels without absorbing rods +0.6% K_{eff}.

The mean efficiency of the IK-1.5 for the reactor of the first unit equalled $-(1.5\text{-}2.0)\cdot 10^{-3}$% K_{eff}. However, on placing the IK-1.5 into a cell adjacent to an immersed compensating rod, the effect equalled $+12.10^{-3}$% K_{eff}, this being due to the reduction in the absorption of neutrons in the rod as a result of screening by the IK-1.5 channel.

Spatial and Power Effects in Reactimeter Measurements. The single-point representation of reactor kinetics is satisfied the less closely, the greater the dimensions of the reactor, and the closer to the reactor surface the reactimeter detector is placed.

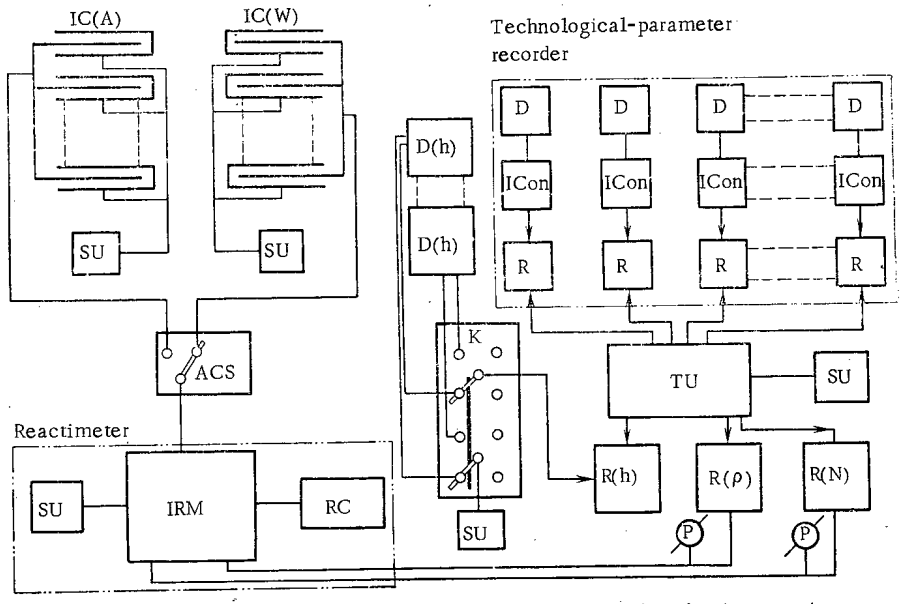

Fig. 4. Block diagram of the set of reactor-monitoring instruments: IC(A)) actuating ionization chamber; IC(W)) working ionization chamber; SU) supply unit; ACS) automatic chamber switch; IRM) instantaneous reactivity meter; RC) RC circuits of the monoenergetic model of the reactor kinetics; D(h)) detector (sensor) for the position of the automatic control rods; K) switch (key); D) detector (sensor) of technological parameters; ICon) information converter (converting the information into a form suitable for recording); R) recorder; TU) timing unit (generator of timing pulses); R(h)) recording unit for the position of the automatic control rods; R(ρ)) reactivity recorder; R(N)) power recorder; P) parallel instruments on the control desk.

The spatial distribution assumed by the neutrons in the reactor on introducing a perturbation of reactivity is described by a superposition of ground and higher harmonics, which add up in such a way that in the zone of perturbation the sign of the deformation in neutron flux follows the sign of the perturbation in reactivity, while in the diametrally opposite zone the signs of the deformation and perturbation oppose one another.

For a reactimeter incorporating a single-point model of the reactor kinetics, a change in the neutron density will be perceived as an instantaneous distortion of the initial conditions. Hence there may be an error in the determination of the instantaneous values of the reactivity: if the sensor of the reactimeter is situated close to the zone of perturbation, then in the initial period the readings of the reactimeter will be too high; if the sensor is situated on the opposite side of the reactor from the perturbation, then the readings will be too low (Fig. 3).

In order to eliminate these errors, a time delay is required (after the perturbation), during which the neutrons may be redistributed and the higher harmonics attenuated, while the RC circuits in the reactor-kinetics simulator may be recharged.

Hence when making measurements with the reactimeter it is essential to create conditions conducive to a single-point representation of the reactor, for example, by connecting several sensors (distributed around the active zone) in parallel to the reactimeter, or by arranging the sensor a fair distance from the active zone.

For measurements in the power mode, the reactimeter will measure the total change in reactivity, i.e., that due to the effect being studied (for example, the displacement of a rod) plus that due to the associated power, temperature, or other reactivity effects. The desired effect may be separated out from the others by making additional measurements, for example, by subtracting the reactivity effect associated with the motion of the compensating rods, which may be obtained from the calibration curve or from preliminary measurements of the effect under consideration at zero power.

It is also possible to design a circuit enabling the reactivity introduced by the rods to be evaluated automatically, and separating the fast and slow reactivity components [7].

Set of Reactor-Monitoring Instruments

Experience in starting the reactors of the Beloyarsk atomic power station showed that, in order to monitor the operation of these, it was desirable to use a set of monitoring instruments enabling the changes taking place in the reactivity, the power of the reactor, and the position of the automatic control rods to be measured and recorded all at the same time. The recording of these parameters together, with those of the temperature and flow of the coolant, the temperature of the fuel elements, and other technological parameters (Fig. 4) may be used in order to study the transient modes and dynamic characteristics of the reactor, to monitor the absence of nuclear hazard, to verify the operative control of the technological process and the operation of the regulating mechanisms, and to analyze possible emergency situations.

The reactimeter constitutes a fundamental part of the set of reactor-monitoring instruments. The reactimeter is used to measure changes in reactivity lying outside the range of sensitivity of the automatic control system. The reactimeter may also be used for measuring the effects of temperature and power level on the reactivity.

The set of instruments is particularly useful for those reactors which are not furnished with information and computing facilities capable of executing continuous measurements or calculations and recording the parameters in question. This set of instruments was used in bringing the second unit of the Beloyarsk power station up to full power, and a similar set has been incorporated in the standard equipment of the reactors in the Bilibinsk and Shevchenko atomic power stations.

LITERATURE CITED

1. G. Stubbs, IRE Trans. NS-4, No. 1, 14 (1957).
2. C. Sastre, Nucl. Sci. Engng., 8, No. 5, 37 (1960).
3. P. Bonnaure, L'onde Electrique, No. 377-8 (1958).
4. P. Shea, IRE, Intern. Convent., Rec., 9, No. 4, 53 (1962).
5. E. Suzuki and T. Tsunoda, J. Nucl. Sci. Techn., 1, No. 6, 210 (1964).
6. R. Shomo, S. Hamilton, and R. Leamer, Trans. ANS, 9, No. 1 (1966).
7. I. I. Sidorova, Analog Simulation in Nuclear Power [in Russian], Atomizdat, Moscow (1969).
8. B. G. Dubovskii et al., "Measurement of reactivity in the reactor of the Beloyarsk atomic power station," Contribution to the Symposium on the Physics and Technology of Thermal-Neutron Reactors [in Russian], London (June 27-29, 1967).
9. I. S. Akimov et al., At. Énerg., 28, 321 (1970).

DETERMINATION OF CONTENT AND SPATIAL DISTRIBUTION OF URANIUM IN FLUORITES FROM TRACKS OF FISSION FRAGMENTS OF URANIUM

I. G. Berzina, I. V. Mel'nikov, and D. P. Popenko

UDC 549.755.35

Fluorites are common minerals occurring in deposits of various types. They contain impurity elements, one of which is uranium.

The uranium content in fluorite crystals has been determined earlier [1-4] by chemical and luminescence methods which have a low lower sensitivity limit and permit only a determination of the gross content of uranium in the sample without elucidating its spatial distribution characteristics.

In the present article we present the results of determination of concentrations and spatial distribution of uranium in fluorite crystals by the method of f-radiography [5]. This method enables one to determine the amount of uranium in the form of isomorphic impurity and the nature of its distribution in fluorite crystals and the enclosing rock. The possibility of using this information as a prospecting criterion for discovery of ores, which contain uranium is demonstrated.

Crystals and slices of natural fluorite and enclosing rocks of fluorite, tin ore, and uranium–molybdenum deposits were investigated.

The sensitivity of the method used is 10^{-12} g/g and the accuracy of the determination is 10-15% [6]. The method is based on the possibility of detecting tracks of fission fragments of uranium nuclei in the minerals capable of spontaneous fission or fission under the action of neutrons [5].

A crystal, in which the fission of uranium nuclei has occurred, or a detector that has recorded multiply charged ions from the surface of the crystal, retains a "memory" of the fission of uranium nuclei and shows the location of these nuclei. The tracks of the fission fragments are revealed with the use of selective chemical etching of the investigated surface.

It is well known [7-9] that a large number of dislocations are revealed on the surface of fluorite crystals on chemical etching; the density of these dislocations is 10^3-10^6 cm^{-2}. The etch figures on the dislocations and the tracks of the fission tracks on the shear plane of fluorites are difficult to distinguish: in both cases they have the shape of pyramids with bases that vary depending on the type of etching. However, when the density of the dislocations does not exceed $5 \cdot 10^4$ cm^{-2}, tracks of the fission fragments of uranium can also show up along with the dislocations. To verify this multiple etching of the mineral was done, as a result of which it was possible to distinguish between the etch figures on the dislocations and the tracks of fission fragments [10].

The most significant difference between the tracks and the dislocations is that a track can end at any point of the crystal and its length is determined only by the specific energy losses of the fission fragment in the crystal lattice. A dislocation can not terminate inside the crystal. It must come out either on the free surface or on the surface of an extended defect, or close on itself. In the process of prolonged etching the etch figure, forming on a dislocation, will become deeper and wider, retaining the shape of a pyramid. With the etching of a defective region the etch figure on a track becomes plane-bottomed and takes the shape of a truncated pyramid. Thus a track can be distinguished from a dislocation with double etching in the appropriate regime. The scheme of etching and the microphotograph of one of the samples, subjected to etching, are shown in Figs. 1 and 2 by way of example.

Translated from Atomnaya Énergiya, Vol. 32, No. 3, pp. 211-215, March, 1972. Original article submitted April 19, 1971.

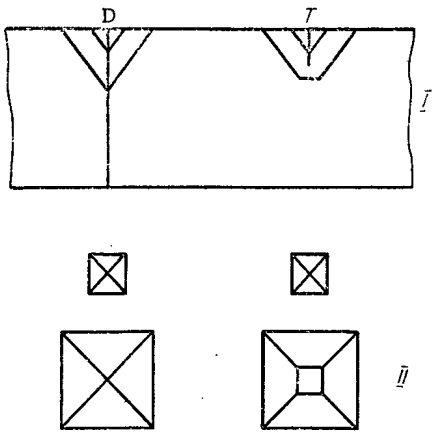

Fig. 1

Fig. 2

Fig. 1. Scheme of formation of etching holes on dislocation (D) and track (T). I and II) Shape of the etch figures in the body and at the surface of the sample respectively.

Fig. 2. Etch figures on tracks and dislocations at the shear surface of a natural fluorite. Etching in 3 N HCl at 20°C for 40 min.

The experiments on the identifications of etch figures on tracks and dislocations enabled us to detect tracks of spontaneous fission of uranium in natural fluorite crystals. This in turn facilitated discrimination of uranium which entered the crystal lattice of the fluorite during its formation and uranium penetrating into the crystal along fissures in a subsequent process, if any. For the latter case a nonuniform distribution of uranium from the periphery to the center is typical.

Colorless, green, and violet fluorites were investigated. The density of tracks of fragments of spontaneous fission of uranium did not exceed $n \cdot 10^4$ cm^{-2} (n = 1, 2, 3) and was uniform in uniformly tinted fluorites. The last fact indicates that in these crystals uranium entered into the fluorite lattice during its crystallization and the uranium content in the fluorite is extremely low ($C \approx 10^{-6}$-10^{-7} wt. %).

It should be mentioned that in fluorites from uranium–molybdenum deposits a nonuniform distribution of uranium is observed along the zones of growth of the crystal, accompanied by a sharp increase in the density of dislocations in the parts adjacent to these zones (Fig. 3).

The increase in the density of dislocations in these parts does not permit determination of the distribution of uranium directly in the crystal itself. In order to reveal the characteristics of the spatial distribution of uranium and to determine its concentration in these cases one should use the records of tracks of forced fission of uranium by external detectors. For this purpose a detector is annexed to the investigated surface of the crystal; the detector records fission fragments escaping from the crystal during its bombardment by neutrons in a nuclear reactor. After irradiation the detector is subjected to chemical etching, as a result of which the tracks of the fission fragments can be seen under an optical microscope; they are observed in the form of black points and dashes on a clear background.

The concentration of uranium C is computed on the basis of the following reasoning. The density of tracks ρ, recorded by the detector, is proportional to the concentration of uranium in the crystal and to the integral flux of neutrons. The neutron flux is determined with the use of especially prepared standard targets having mass m_i. The thickness of the target is such that fission fragments escaping from it reach the detector placed in contact with the target during its irradiation [5].

The concentration of uranium in the material is computed from the formula [6]

$$C = \frac{2}{7} 10^4 \frac{\rho}{\sqrt{\bar{A}}} \cdot \frac{m_i}{\rho_i},$$

where $\bar{A}$ is the average atomic weight of the subject material (for fluorite $\bar{A}$ = 26.8 amu); ρ_i is the density of tracks in the detector adjoining the target.

In order to compute ρ curves of statistical distribution of the density of tracks over the sample are constructed. The form of these curves serves as the basis for the determination of the forms of occurrence

Fig. 3

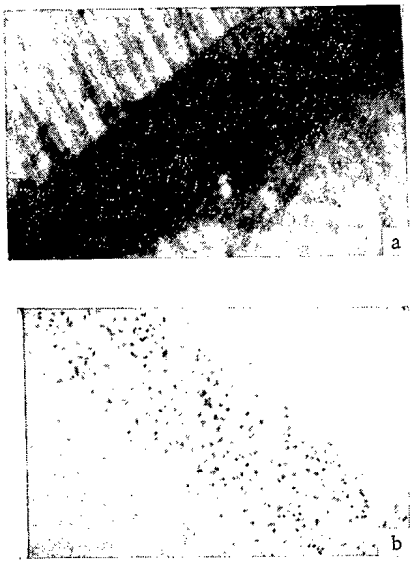

Fig. 4

Fig. 3. Dislocation bands along the zones of growth of the crystal, containing increased amount of impurities.

Fig. 4. Microphotograph of a thin section of fluorite with uraninite deposited along the faces of growth of fluorite (a), and of the detector (b) recording the tracks of fragments of forced fission of uranium. Detector: Lavsan film with thickness of 12 μ; etching regime: 40% KOH, τ = 20 min, t = 60°C.

TABLE 1. Uranium Concentration ($\cdot 10^{-5}$ wt. %) in Fluorites from Different Segments of the Vein* of Fluorite Deposit

Color of fluorite	Number of section				
	1	2	3	4	5
Porcelain type	1,2	—	1,2	—	—
Colorless	0,4	0,2	0,3	0,3	0,2
Light green	0,6	0,3	0,3	0,4	0,4
					0,3
Green	—	0,9	—	—	0,9
Violet	—	0,2	—	0,3	0,3
					0,4

*Uranium concentration in enclosing rocks is equal to $13.6 \cdot 10^{-5}$ wt. %

of uranium in the crystal. Revealed in this process are uranium distributed uniformly along the crystal, uranium deposited along the growth faces, and uranium timed with microinclusions of the rock or minerals [11].

The concentration and spatial distribution of uranium in fluorites from deposits of different types were determined. Since small crystals (~1 cm^2) were used, it was necessary to determine the stability of the distribution along the course and depth of the fluorite vein. For this purpose crystals from five segments of the fluorite vein with overall distance of ~190 m from the first to the last segment were used. The results of the analysis showed that the uranium concentrations in fluorites of the same color depend practically on their location (Table 1).

The stability of the uranium content in fluorites of a given color made it possible to reduce the number of analyzed crystals considerably.

The uranium content in fluorites taken from different deposits vary within an order of magnitude (Table 2), but the nature of the distribution of uranium is different. Thus, for example, in crystals from fluorite and tin-ore deposits the distribution of uranium is uniform, just as in porcelain type (white) fluorite from a fluorite deposit, which is distinguished from the remaining fluorites of this deposit by large uranium content.

As mentioned above, in the case of a nonuniform distribution of the content of uranium deposited along the growth zones of fluorites an increased density of dislocations is observed, which makes it difficult to reveal the tracks of fission fragments directly on the crystal.

In such segments of the crystals an increased concentration of uranium (~10^{-3} wt. %) in zones with thickness of a few tens of microns could be detected with the use of an external detector (Fig. 4). The deposition of uranium along the growth zones of fluorite crystals in the form of extremely thin crusts of independent uranium minerals is apparently accompanied by recrystallization; as a result stresses develop in closed volumes, since the growth of the crystals does not stop after the deposit of the uranium minerals.

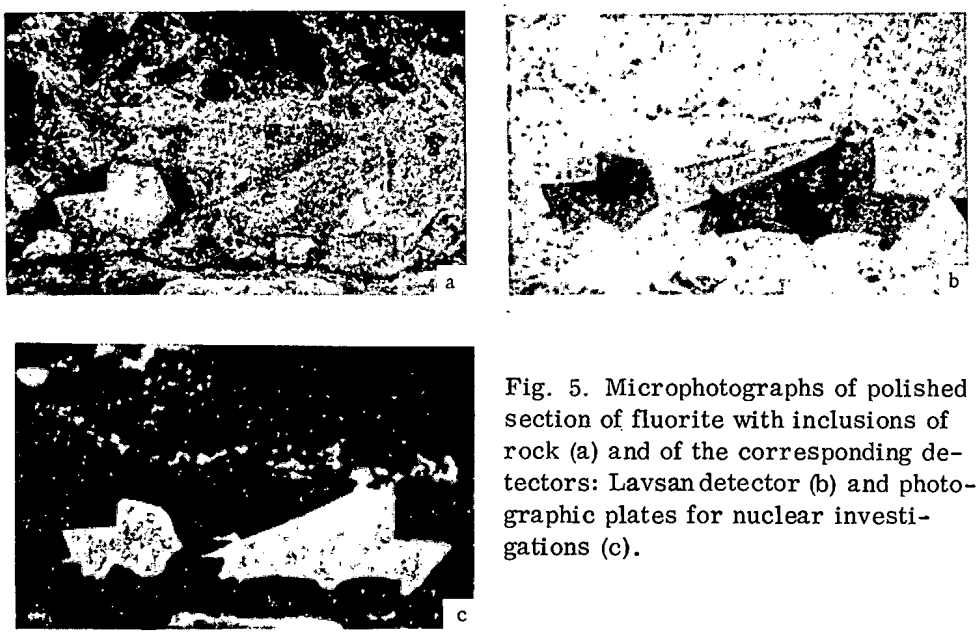

Fig. 5. Microphotographs of polished section of fluorite with inclusions of rock (a) and of the corresponding detectors: Lavsan detector (b) and photographic plates for nuclear investigations (c).

TABLE 2. Uranium Concentration ($\cdot 10^{-5}$ wt. %) in Crystals of Fluorites and in Enclosing Rocks from Different Deposits

Characteristic of sample	Type of deposit		
	fluorite	tin-ore	uranium–molybdenum
Violet fluorite	0.3	0.8	1.4-3.6
Green fluorite	0.9	1.5	1.5
Light green fluorite	0.4	0.2	0.8-3.3
Colorless fluorite	0.3	–	3.8
Enclosing rock	13.6	4.3	103.5

As a rule, 20-100 μ wide violet bands are observed on both sides of the zone along which the crust formation occurs; the intensity of their tint for single-age fluorites depends on the amount of deposited uranium. In this case the violet color of fluorite can be explained by the effect of the natural radioactivity of uranium, causing the formation of definite tint centers. This is indicated by the fact that the tint of the fluorite at these points disappears on heating.

In fluorites taken from uranium–molybdenum deposits an increased uranium content was noticed in the entire violet zone of the irradiated crystals. Due to the small width of the zone uranium cannot be separated from the mineral in its sampling in the corresponding analysis. Therefore, in gross uranium analysis an increased value of the concentration of uranium can be obtained in polycrystalline fluorite.

Apparently an increased uranium content in fluorite is often obtained due to the presence of minute inclusions of the rock (Fig. 5). It should be noted that the blackening of the plate for nuclear investigations occurs only in contact with the fluorite, whereas the parts of the plate, that adjoin the chips of the rock, remain unilluminated, even though the uranium content in the rock is higher by an order of magnitude. Thus the blackening of the photographic plates cannot be an unambiguous indicator of radioactivity of violet fluorites as assumed earlier [3].

We observed nonuniform distribution of uranium only in crystals taken from veins of uranium–molybdenum deposits. It was found from mineragraphic investigations that the growth zones of fluorite crystals are enriched by a uraninite (Fig. 6); the uranium content of the fluorite in this case is $\sim 10^{-3}$ wt. %. Minute depositions of uranium occur also in the enclosing rock. The maximum concentration of uniformly distributed uranium in such fluorite crystals (see Table 2) is 10^{-5} wt. %.

The increased uranium content in the growth zones of fluorite crystals can be explained in the following way. Fluorite veins with increased uranium content, coming out to the surface of the earth above

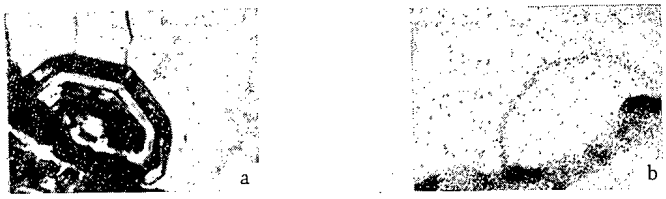

Fig. 6. Microphotographs of a section containing fluorite (a) and of Lavsan detector (b) recording uranium pressed back into the peripheral zones of the fluorite crystal (uraninite band is observed at the base of the crystal).

hidden ores, could be formed from hydrothermal solutions washing in their path the ore materials which would enrich the solutions with uranium. Since the solubility of uranium in fluorite is finite, the surplus uranium in the solution must be deposited along the growth zones of the crystals and around fully grown crystals in the form of minute bands of uraninite.

The nature of distribution of uranium and its concentration in rocks enclosing fluorite veins are also different. Tin-ore and fluorite deposits are characterized by low uranium content. In these cases the uranium is timed to definite accessory minerals, characteristic for the given rock, and no redistribution of uranium occurs.

A different pattern is noticed near uranium–molybdenum ore materials, where the uranium content is two-three times higher in the enclosing rocks than in fluorite crystals. This is apparently explained by the deposit of uranium from solutions enriched by this element. Besides, in the rocks uranium is distributed nonuniformly: a large number of fine grains of uranium minerals and formations, which appear on the surface of the detector in the form of star-shaped segregations and cannot be diagnosticated, are observed. Thus the proximity of the ore material, through which the hydrothermal solutions pass, affects the forms in which uranium appears in the rocks enclosing the fluorite veins.

The following conclusions can be made on the basis of these investigations. As a rule, in the lattice of fluorite crystals uranium is distributed uniformly in the form of impurity. The content of this uranium does not exceed $n \cdot 10^{-5}$ wt. %. During the growth of the crystals the uranium "surplus" is deposited along the growth zones or is pushed back to the peripheral parts of the crystals in the form of independent uranium minerals. A nonuniform distribution is characteristic of rocks enclosing fluorites in the case of uranium surplus. The presence of surplus uranium, deposited along the growth zones of fluorite, and an increased uranium content in the crystal lattice can be used as a prospecting criterion for the detection of ores with high uranium content.

LITERATURE CITED

1. N. N. Vasil'kova and S. G. Solomkina, Typomorphic Characteristics of Fluorite and Quartz [in Russian], Nedra, Moscow (1965).
2. F. Daniels, Ch. Boyd, and D. Saunders, Uspekhi Fiz. Nauk, 51, 271 (1953).
3. K. Pshibram, Tint and Luminescence of Minerals [Russian translation], IL, Moscow (1959).
4. H. Haberlandt, in: Rare Elements in Volcanic Mountain Rocks and Minerals [Russian translation], IL, Moscow (1952), pp. 17–40.
5. I. G. Berzina et al., At. Énerg., 23, 520 (1967).
6. I. G. Berzina et al., Izv. Akad. Nauk SSSR, Ser. Geol., 8, 70 (1969).
7. I. G. Guseva and A. A. Urusovskaya, Kristallografiya, 9, 432 (1964).
8. W. Kleber, M. Hahnert, and L. Ludke, Kristall und Technik, 1, 585 (1966).
9. A. Patel and C. Desai, Z. Kristallogr., 123, No. 1, 51 (1966).
10. I. G. Berzina and I. B. Berman, Dokl. Akad. Nauk SSSR, 174, 3, 553 (1967).
11. I. G. Berzina, B. G. Lutts, and A. P. Akimov, Izv. Akad. Nauk SSSR, Ser. Geol., 1, 14 (1967).

THE PENETRATION OF BEAMS OF HIGH-ENERGY PARTICLES THROUGH THICK LAYERS OF MATERIAL

V. S. Barashenkov, N. M. Sobolevskii, and V. D. Toneev

UDC 539.12.17

A procedure for calculating a nucleon–meson cascade in a slab of material was described in [1] and the distributions of particle fluxes inside and outside slabs of various compositions and thickness initiated by high-energy primary radiation were investigated also. Using the same procedure we study more detailed characteristics of secondary particle fluxes beyond a thick shield. Calculations simulating the fate of each particle in the material are performed by the Monte Carlo method. Each inelastic interaction of a particle with a nucleus is treated by the Monte Carlo method using the cascade-evaporation model [2-4]. The behavior of neutrons with energies $E < 10.5$ MeV is simulated on the basis of reactor constants [5].

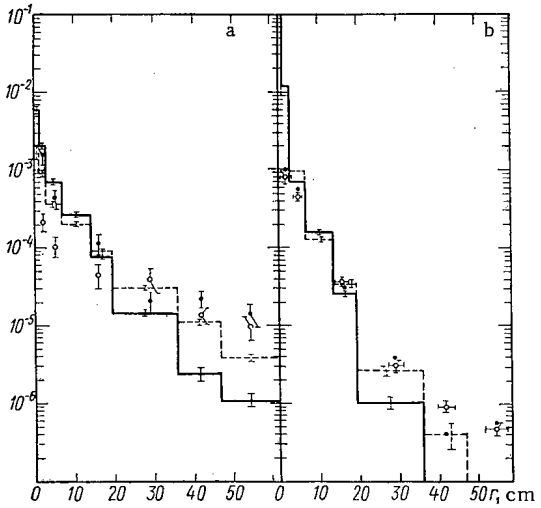

Fig. 1. Spatial distribution of a) neutron fluxes and b) proton fluxes beyond an aluminum shield of thickness z bombarded with 660 MeV protons. Histograms are calculated; experimental points are taken from [7, 8]; ——— (•), $z = 75$ g/cm^2; – – – (○), $z = 150$ g/cm^2; r is the distance from the axis of the beam.

For comparison we used the results of measurements performed on the OIYaI synchrocyclotron for energies $T = 340$ and 660 MeV [6-8].* In the calculations the geometry of the experiments was reproduced exactly: aluminum slabs having thicknesses z of 75 and 150 g/cm^2 were bombarded with a collimated beam of protons approximately 1 cm in radius. Since the exact shape of the beam was simulated by using a matrix determined experimentally, it was not necessary to introduce any geometric corrections.

The calculated results, plotted in Fig. 1, show that the neutron and proton fluxes fall off almost exponentially with the distance from the axis of the beam. The calculation gives

*Some preliminary results obtained within the framework of a simplified model were reported at a conference on dosimetry and shielding physics at Dubna in 1969 [9].

TABLE 1. Fluxes of Secondary Particles Beyond an Aluminum Shield of Thickness z Bombarded by 660 MeV Protons

Particles, energy	$z = 75$ g/cm^2		$z = 150$ g/cm^2	
	experiment	theory	experiment	theory
Neutrons, $\mathcal{T} > 50$ MeV	0,50±0,15	0,34±0,01	0,29±0,11	0,33±0,02
Neutrons, $\mathcal{T} < 30$ MeV	1,05±0,32	0,65±0,05	0,76±0,22	1,14±0,13
All protons	0,82±0,15	0,69±0,01	0,40±0,07	0,39±0,01

Translated from Atomnaya Énergiya, Vol. 32, No. 3, pp. 217-221, March, 1972. Original article submitted June 24, 1971.

TABLE 2. Energy Spectra of Protons (%) beyond a Shield of Thickness 75 g/cm^2 at a Distance r from the Axis of a 660 MeV Primary Beam

E, MeV	r = 2 cm		r = 16 cm		r = 29 cm	
	experiment	theory	experiment	theory	experiment	theory
0—50	1,0	1,7	6,0	7,2	19,2	15,6
50—100	1,3	2,7	9,1	13,4	20,4	28,1
100—150	0,7	2,4	12,1	24,1	16,8	28,1
150—200	4,6	2,1	22,0	17,0	19,7	15,6
200—250	2,3	1,6	6,1	12,5	7,1	9,5
250—300	5,1	1,2	6,1	15,1	7,3	3,1
300—350	5,2	1,5	6,8	6,2	2,9	—
350—400	4,9	1,1	5,3	3,6	1,5	—
> 400	74,9	85,7	26,5	0,9	5,1	—
Total number of events	307	2 664	132	206	137	32

TABLE 3. Energy Spectra of Protons (%) beyond a Shield of Thickness 150 g/cm^2 at a Distance r from the Axis of a 660 MeV Primary Beam

E, MeV	r = 2 cm		r = 16 cm		r = 29 cm	
	experiment	theory	experiment	theory	experiment	theory
0—50	1,0	0,7 (0,7)	8,8	8,7	4,3	9,1
50—100	1,4	1,2 (1,2)	10,0	17,5	12,8	27,4
100—150	1,6	1,3 (1,3)	16,5	24,5	28,2	32,8
150—200	9,7	1,7 (1,7)	16,5	18,0	21,3	25,5
200—250	12,3	2,2 (2,2)	8,4	21,8	5,8	5,3
250—300	21,4	12,0 (3,0)	11,5	6,8	7,4	—
300—350	23,6	72,0 (89,7)	11,5	1,6	6,4	—
350—400	13,6	8,7 (0,1)	8,0	0,6	3,7	—
> 400	15,4	0,2 (0,1)	8,8	0,5	10,1	—
Total number of events	281	1 215	272	183	188	55

Note: The values in parentheses are calculated by neglecting multiple scattering and the energy spread of the primary beam.

TABLE 4. Energy Spectra of Protons (%) beyond a Shield of Thickness 75 g/cm^2 at a Distance r from the Axis of a 340 MeV Primary Beam

E, MeV	r = 2 cm		r = 16 cm		r = 29 cm	
	experiment	theory	experiment	theory	experiment	theory
0—50	20,7	12,2 (6,3)	65,8	37,5	32,5	17
50—100	56,0	64,3 (93,2)	24,4	25,0	27,5	17
100—150	18,1	20,8 (0,2)	7,8	12,5	27,5	49
150—200	4,8	2,5 (0,2)	1,0	25,0	2,5	17
200—250	0	0,2 (0,1)	1,0	—	2,5	—
250—300	0,4	0 (0)	—	—	7,5	—
Total number of events	229	3 786	193	8	40	6

Note: The values in parentheses are calculated by neglecting multiple scattering and the energy spread of the primary beam.

the correct character of the spatial distribution of radiation beyond the shield and is in satisfactory quantitative agreement with experiment. This agreement is somewhat less satisfactory for fluxes close to the axis of the primary beam ($r \approx 2$ cm).

It should be noted that the agreement between the calculated and measured proton fluxes results not only from the exact account of the beam geometry but also from the multiple scattering correction for those protons which passed clear through the slab without a nuclear interaction. Such "uncollided" protons make up the main part of the particle beam close to its axis but Coulomb scattering effectively increases its size. Thus, for example, in spite of the fact that the radius of the beam is only 1 cm almost 30% of the protons emerging from a target of thickness $z = 150$ g/cm^2 at a distance of 5 cm from the axis of the primary beam

TABLE 5. Spectra of Protons (%) with Energies E > 10 MeV in a Given Range of Polar Angle beyond a Shield of Thickness 75 g/cm^2 for 660 MeV Primary Protons

E, MeV	0–30°		30–60°		60–90°		0–90°	
	experiment	theory	experiment	theory	experiment	theory	experiment	theory
0–50	0,4	0,9	25,2	10,3	60,0	26,5	2,4	2,0
50–100	2,0	1,5	33,3	15,2	20,3	42,9	3,1	3,3
100–150	1,6	1,5	20,2	18,3	15,6	12,2	1,8	3,3
150–200	4,9	1,5	9,8	15,9	3,1	14,3	5,3	3,1
200–250	2,3	1,3	3,7	15,7	0,4	4,1	2,4	2,8
250–300	5,2	1,7	3,2	12,2	0,5	—	5,3	2,7
300–350	5,3	2,6	1,6	7,9	0,1	—	5,0	3,1
350–400	5,8	2,3	0,5	4,5	—	—	4,7	2,5
> 400	72,5	86,7	2,5	—	—	—	70,0	77,2
Total number of events	—	7 437	—	732	—	77	—	8 246

TABLE 6. Spectra of Protons (%) with Energies E > 10 MeV in a Given Range of Polar Angle beyond a Shield of Thickness 150 g/cm^2 for 660 MeV Primary Protons

E, MeV	0–30°		30–60°		60–90°		0–90°	
	experiment	theory	experiment	theory	experiment	theory	experiment	theory
0–50	0,9	0,6 (0,6)	28,8	14,7	74,0	38,5	7,7	2,2
50–100	2,7	2,2 (2,2)	26,7	20,5	18,1	38,5	9,3	4,2
100–150	4,8	3,0 (3,0)	29,5	26,3	5,3	19,2	15,3	5,3
150–200	12,3	4,4 (4,4)	10,5	20,0	1,2	3,8	15,6	5,9
200–250	11,9	5,4 (5,4)	1,8	14,0	0,5	—	8,8	6,2
250–300	19,7	12,8 (6,3)	0,8	3,8	0,9	—	12,6	11,9
300–350	21,3	65,2 (77,9)	0,8	0,4	—	—	12,7	58,6
350–400	12,4	6,1 (0,1)	1,1	0	—	—	8,3	5,5
> 400	14,0	0,2 (0,1)	—	0,3	—	—	9,7	0,2
Total number of events	—	2766	—	293	—	26	—	3085

Note: Values in parentheses were calculated by neglecting multiple scattering and the energy spread of the primary beam.

for T = 660 MeV are particles which have passed through the slab without nuclear collisions. At a distance of 2 cm the fraction of such protons increases to 50%.

The calculated values of the total radiation fluxes beyond the shield are shown in Table 1.

The importance of the contribution of uncollided particles for small values of r can be clearly traced in the energy spectra (Tables 2–4). Even a small uncertainty in reproducing the experimental conditions has an appreciable effect on the calculated results. Thus if it is assumed that the primary beam is monochromatic a sharp maximum appears in the calculated spectrum (cf. numbers in parentheses in Tables 3 and 4). If it is assumed that the incident protons have a certain energy spread, e.g., 10 MeV for T = 660 MeV and 25 MeV for T = 340 MeV, the tables show that the maximum is spread out and the spectral shapes approach the experimental. In this case the energy spread taken into account is not that of the whole primary beam but only of those protons which have penetrated the whole slab without a nuclear interaction. It is clear that better agreement with experiment can be achieved by varying the dispersion and taking account of the spread for the whole beam. Thus in the present cases (z = 75 g/cm^2, T = 340 MeV, and z = 150 g/cm^2, T = 660 MeV) the experimental conditions are known almost exactly. On the other hand for z = 75 g/cm^2 and T = 660 MeV the energy loss in the slab is small and the effect of the energy spread of the primary beam is beyond the limits of measurement of the spectrum. In this case the calculated spectra are in good agreement with the experimental (Table 2).

All the above continues to hold in the analysis of the correlations between the angle of emergence and the energy of the secondary particles (Tables 5-7). Even here where the effect of the energy spread in the primary beam on the shape of the measured spectra is unimportant, agreement with experiment is adequate (Table 5). Both the correlations between the angle of emission and the energy of the particles and the spatial-angular distribution of charged particles beyond the shield are correctly given (Table 8).

TABLE 7. Spectra of Protons (%) with Energies E > 10 MeV in a Given Range of Polar Angle beyond a Shield of Thickness 75 g/cm^2 for 340 MeV Primary Protons

E, MeV	0—30°		30—60°		60—90°		0—90°	
	experiment	theory	experiment	theory	experiment	theory	experiment	theory
0—50	16,5	11,7	62	66,3	50,5	82	20,4	12,5
50—100	46,2	67,3	36	23,6	48,5	0	46,0	66,6
100—150	30,9	18,7	1,2	4,5	1,0	18	27,5	18,5
150—200	5,3	2,28	0,8	5,6	—	—	4,7	2,32
200—250	0,6	0,02	—	—	—	—	1,0	0,06
250—300	0,5	—	—	—	—	—	0,4	0,02
Total number of events	—	6935	—	79	—	11	—	7025

TABLE 8. Angular Distribution of Protons (%) Emerging from a Shield of Thickness 75 g/cm^2 at Various Distances from the Axis of a 660 MeV Primary Beam

Angle, deg	r = 2 cm		r = 16 cm		r = 29 cm		Total value (over all r)	
	experiment	theory	experiment	theory	experiment	theory	experiment	theory
0—15	84,6	87,0	9,1	0	8,8	0	76,9	77,7
15—30	10,6	7,1	49,2	17,8	27,0	15,4	12,2	12,3
30—45	3,3	3,0	22,7	58,0	35,7	53,9	6,3	6,3
45—60	0,7	2,0	12,1	18,7	21,9	23,0	2,9	2,8
60—75	0,6	0,8	6,1	5,5	5,1	7,7	1,3	0,7
75—90	0,2	0,1	0,8	0	1,5	0	0,4	0,2
Total number of events	—	2664	—	206	—	32	—	8246

Thus our method of calculating the penetration of high-energy particles through a slab of material by simulating pion– and nucleon–nuclear interactions with the Monte Carlo method can be used successfully to calculate integral characteristics such as the total particle flux, and to obtain detailed information on the spatial structure of radiation beyond the shield, various spectral–angular characteristics, their correlations, etc. A comparison of the calculated and experimental results shows that at the present time the accuracy of the calculations depends mainly on a sufficiently complete knowledge of the experimental conditions. Some uncertainty in the values of individual parameters of the model is not very important.

LITERATURE CITED

1. V. S. Barashenkov, N. M. Sobolevskii, and V. D. Toneev, Atomnaya Énergiya, 32, 123 (1972).
2. V. S. Barashenkov, K. K. Gudima, and V. D. Toneev, OIYaI P2-4065, P2-4066, Dubna (1968).
3. V. S. Barashenkov, A. S. Il'inov, and V. D. Toneev, OIYaI P2-5282, Dubna (1970).
4. V. S. Barashenkov et al., OIYaI P2-5507, P2-5549, Dubna (1970).
5. L. P. Abagyan et al., Group Constants for Nuclear Reactor Calculations [in Russian], Atomizdat, Moscow (1964).
6. V. E. Dudkin et al., Atomnaya Énergiya, 22, 491 (1967).
7. V. E. Dudkin et al., Atomnaya Énergiya, 23, 241 (1967).
8. A. I. Vikhrov et al., in: Dosimetry and Radiation Shielding Problems [in Russian], Vol. 11, Atomizdat, Moscow (1970), p. 70.
9. V. E. Dudkin et al., in: Dosimetry and Shielding Physics for Accelerators [in Russian], OIYaI 16-4888, Dubna (1970), p. 75.

NEUTRON SPECTRA IN NOVO-VORONEZH ATOMIC POWER STATION REACTORS

S. S. Lomakin, G. G. Panfilov,
V. I. Petrov, L. I. Golubev,
V. P. Kruglov, and V. A. Vikin

UDC 621.039.524:621.039.51

During the start-up of the second reactor of the Novo-Voronezh atomic power plant the spectral parameters, the thermal neutron flux density distribution, and the absolute values of the neutron flux density over the height of the reactor core were measured with activation detectors.

The experiments were performed at various coolant temperatures and reactor powers in instrument channels passing into fuel assemblies with 1.5 and 2% enrichment in U^{235}.

The spectral indices A were measured with 3 mm diameter detectors made of lutecium and europium metal on an aluminum base. Copper foils 50 μ thick were used as 1/v detectors. Absolute thermal neutron flux densities were determined with gold foils 0.1 μ thick. Copper detectors 50 μ thick and gold foils 10 μ thick, all 2 mm in diameter, were irradiated in 0.5 mm thick cadmium covers to separate the thermal and epithermal components of the neutron spectrum.

The average values of R_{Cd}, A, and T_n measured in the instrument channels are listed in Table 1.

Analysis of the data obtained in these experiments and those on the first reactor [1] shows that the variations of such parameters as the spectral indices and the cadmium ratios over the height of the reactor core are of much the same nature for all measurements.

The ratio of thermal to resonance neutrons in the central part of a fuel assembly (region 30-200 cm) is constant. The reflector causes an increase in the cadmium ratios at the edges of an assembly. The spectral index for lutecium over an assembly increases somewhat toward the top of the core.

The neutron spectra for the first and second Novo-Voronezh atomic power plant reactors vary considerably over the assemblies.

TABLE 1. Spectral Characteristics of Neutrons in Second Novo-Voronezh Atomic Power Station Reactor Channels

Temperature of coolant, °C	Uranium enrichment, % U^{235}	R_{Cd}^{Au}	R_{Cd}^{Cu}	A_{Cu}^{Lu}	T_n, °K	$n_T\bar{v}$*, neutrons/cm^2·sec
30	1,5	1,75±0,05	6,50±0,19	1,00±0,03	375±19	(9,85±0,98)·10^{10}
	2	1,57±0,05	5,33±0,16	1,01±0,03	396±20	(8,03±0,80)·10^{10}
108	1,5	1,69±0,05	6,10±0,18	1,15±0,03	462±23	(7,18±0,72)·10^{10}
218	1,5	1,65±0,05	5,70±0,17	1,37±0,04	607±30	(7,32±0,73)·10^{11}
260	1,5	1,54±0,05	5,14±0,15	1,37±0,04	642±32	(2,88±0,29)·10^{13}
	2	1,51±0,05	4,31±0,13	1,42±0,04	713±35	(2,36±0,24)·10^{13}

*The absolute values of the thermal neutron flux density were measured at 129 cm from the bottom of the reactor core.

Translated from Atomnaya Énergiya, Vol. 32, No. 3, p. 223, March, 1972. Original article submitted April 13, 1971; abstract submitted October 29, 1971.

LITERATURE CITED

1. S. S. Lomakin et al., Atomnaya Énergiya, 30, 301 (1971).

VARIATIONS IN COMPOSITION IN RADIOISOTOPE X-RAY FLUORESCENCE ANALYSIS OF POLYMETALLIC ORES

Yu. P. Betin and I. A. Krampit

UDC 543.09

Methods for coping with the effect of changes in the chemical composition of samples on the results of radioisotope x-ray fluorescence analysis of complex ores are discussed.

The formulas for the intensities of the characteristic x-radiation of the element to be determined, and the backscattered radiation, in forms convenient for numerical calculations, are derived. Formulas are derived for the case of a semiinfinite flat surface. Absorption of both primary and secondary radiations on the forward and backward path is also taken into cognizance in the derivation of the formulas, in addition to geometrical factors.

The computational results made it possible to evaluate the effect of changes in the contents of accompanying elements on the intensity of x-ray fluorescence emission from the element to be determined in the analysis. The example of x-ray fluorescence analysis of lead in complex ores (lead–zinc and lead–barium ores) is invoked to demonstrate that the relative error in lead determinations due to redistribution of the accompanying elements may attain the level of several tenths of a percent (when secondary emission is excited with the aid of a Cd^{109} radioisotope source, and the L-emission from lead is recorded). The feasibility of recording the ratio of intensities of L-fluorescence in lead and singly scattered radiation of energy ≈20 keV, i.e., the ratio $r_{Pb} = N_{PbL}/N_S$, in order to minimize the dependence of the results of analysis of lead-containing samples on changes in the content of accompanying elements (barium, zinc, iron), is demonstrated on the basis of computational data. The computational results are in close agreement with experimental data obtained in measurements taken on artificial mixtures simulating lead–zinc ores in chemical composition.

The possibility of minimizing systematic errors due to changes in the composition of samples to be analyzed, on the basis of records taken of the above ratio, was again confirmed in x-ray fluorescence analysis of lead in lead–barium ores. Three distinct methods of dealing with the effect of changes in lead content on the results of a zinc determination were pointed out in x-ray fluorescence analysis of zinc in lead–zinc ores: 1) using one of the calibration graphs (corresponding to a specified lead content) in a family of $\eta_{Zn} = N_{ZnK}/N_S = f(C_{Zn})$ graphs as an aid in interpreting the analysis data; 2) determining zinc content from a calibration graph in the family of $N_{ZnK} = \varphi(C_{Zn})$ graphs; 3) using the "compensation" technique. The first of these methods is preferred in this application.

Translated from Atomnaya Énergiya, Vol. 32, No. 3, p. 224, March, 1972; abstract submitted April 9, 1971.

THE SPECTRUM OF SECONDARY ELECTRONS IN MATTER IRRADIATED WITH γ-RAYS

A. M. Kol'chuzhkin, V. V. Uchaikin, and V. I. Bespalov

UDC 539.124.16:535.33

The secondary electrons accompanying the propagation of γ-rays through matter produce ionization, radiation damage, and other effects. The electron energy spectrum is related to the differential γ-flux by the expression

$$\Phi_e(\boldsymbol{r}, E)=\int d\Omega \int dV' \int d\Omega' \int dE' G_e(\boldsymbol{r}, \Omega, E; \boldsymbol{r}', \Omega', E') \int d\Omega'' \int dE'' \Sigma_{e\gamma}(\Omega', E'; \Omega'', E'') \Phi_\gamma(\boldsymbol{r}', \Omega'', E''),$$

where $\Sigma_{e\gamma}$ is the differential cross section and G_e is the Green's function for the electron transport equation. For photon energies below 10 MeV the variation of the γ-flux over a distance of the order of a mean free path of the secondary electrons is negligible and therefore neglecting the variation of the γ-flux in the integrand we obtain

$$\Phi_e(\boldsymbol{r}, E)=\int dE' G_e(E; E') \int dE'' \Sigma_{e\gamma}(E'; E'') \Phi_\gamma(\boldsymbol{r}; E''),$$

where $G_e(E; E')$ is the equilibrium electron spectrum.

The equilibrium electron spectrum is calculated by the Monte Carlo method using the catastrophic collision model. A lexicographical scheme is used to construct and process the branching electron trajectories, and the flux is determined from the mean free path, since this method is more efficient than an estimate from the collision density. The program uses a new method of sampling the electron energy from a Möller distribution.

An analysis of the catastrophic collisions model shows that the results of the calculations are practically independent of the magnitude of the threshold energy separating the catastrophic collisions from continuous energy losses, and the calculation time decreases significantly with an increase in threshold.

Calculation of the secondary electron spectrum in lead for $E_0 = 1$ MeV shows that scattered γ-radiation can make a significant contribution to $\Phi_e(r, E)$, and the contributions of the photoelectric effect and Compton scattering can be equally important for unscattered radiation. The conclusion drawn in [1, 2] that unscattered γ-radiation and Compton scattering are predominant is valid only for thin absorbers of low Z materials and high enough γ-energies.

LITERATURE CITED

1. O. Oen and D. Holmes, J. Appl. Phys., 30, 1289 (1959).
2. J. Cahn, ibid., p. 1310.

Translated from Atomnaya Énergiya, Vol. 32, No. 3, p. 224, March, 1972. Original article submitted May 27, 1971; abstract submitted November 23, 1971.

FEW-GROUP COMPUTATIONAL MODEL OF SLOWING-DOWN FOR WATER – ALUMINUM CORES

E. A. Garusov and Yu. V. Petrov

UDC 621.039.51

A program of constantly updated reactor calculations is greatly aided by the availability of a simple, but at the same time reasonably exact, theoretical model of slowing-down of neutrons. The simplest such model is the few-group diffusion model [1]. But the possibility of utilizing this model in the design of cores containing ordinary water is not at all obvious because the conditions for validity of the diffusion approximation are violated. As a consequence of the steep decline in the scattering cross section of hydrogen with increasing neutron energy, and the small number of collisions needed to produce the slowing-down, the contribution made by as-the-crow-flies neutrons to the total migration area is relatively large. The net result is that, while sources are concentrated in the first group, slowing-down in pure light-water reactors with (or without) a light-water reflector is described best of all by the one-group diffusion model [2]. An increase in the number of energy groups entertained in the model calls for a switch to a nondiffusion approximation. Including aluminum in the composition of the core actually contributes to diffusion entrainment of neutrons.

Consider the simplest unreflected reactor. The probability of nonleakage $P(B^2\tau)$ can be represented as a series expansion in powers of $B^2\tau$ [3]:

$$P(B^2\tau) = \sum_{m=0}^{\infty} (-1)^m C_{2m} (B^2\tau)^m;$$
$$C_{2m} \equiv \frac{\langle r^{2m} \rangle}{(2m+1)!\,\tau^m}, \quad C_0 = C_2 = 1. \tag{1}$$

Here $\langle r^n \rangle$ is the n-th spatial moment of the slowing-down kernel.

$B^2\tau \ll 1$ in the case of large reactors, and the neutron age τ is virtually the unique parameter useful for determining $P(B^2\tau)$ independently on the slowing-down model. In the case of small cores, the contribution to leakage is made by high m terms, and the coefficients C_{2m} are dependent upon the specific slowing-down model selected. By comparing C_{2m} values calculated on the basis of the various available computational models, and C_{2m} values arrived at empirically in experiments or on the basis of more exact theoretical methods, we decide upon the selection of a given computational model. The number of terms retained in the power series (1) is determined both by the value of the product $B^2\tau$ and by the accuracy to which τ and C_{2m} are known. The formulas for $P^{(N)}(B^2\tau)$, $C_{2m}^{(N)}$, $C_4^{(N)}$ are tabulated for the simplest slowing-down models (N is the index of the model).

Utilizing an explicit expression for $P^{(1)}(B^2\tau)$ and an integral representation, we obtain, for $C_{2m}^{(1)}$, after some indicated transformations, the formulas (here $q \equiv B^2\tau$):

$$C_{2m}^{(1)} = \frac{(-1)^m}{m!} \cdot \frac{d^m P^{(1)}(q)}{dq^m}\Big|_{q=0} = \frac{1}{m!} \sum_{k=1}^{n} \chi_k \underbrace{\int_0^{\infty} \dots \int_0^{\infty}}_{n-k+1} e^{-\sum_{i=k}^{n} y_i} \left(\sum_{i=k}^{n} \alpha_i y_i\right)^m \prod_{i=k}^{n} dy_i = \sum_{k=1}^{n} \chi_k \sum_{i_1=k}^{n} \alpha_{i_m} \sum_{i_2=i_1}^{n} \alpha_{i_2} \dots \sum_{i_m=i_{m-1}}^{n} \alpha_{i_m}. \tag{2}$$

If the second spatial moment, averaged over the sources, is never in excess of the total moment during the slowing-down process,

Translated from Atomnaya Énergiya, Vol. 32, No. 3, pp. 225-227, March, 1972. Original article submitted March 26, 1971; revision submitted July 9, 1971.

TABLE 1

N	Slowing-down model	$P^{(N)}(B^2\tau)$	$C_{2m}^{(N)}$	$C_4^{(N)}$	Remark
1	n-Group diffusion	$\sum_{k=1}^{n} \chi_k \prod_{i=k}^{n} (1+\alpha_i B^2\tau)^{-1}$	$\sum_{k=1}^{n} \chi_k \sum_{i_1=k}^{n} \alpha_{i_1} \cdots \sum_{i_m=i_{m-1}}^{n} \alpha_{i_m}$	$\frac{1}{2}\sum_{k=1}^{n} \chi_k \left[\sum_{i=k}^{n} \alpha_i^2 + \left(\sum_{i=k}^{n} \alpha_i \right)^2 \right]$	$\sum_{k=1}^{n} \chi_k = 1$ $\sum_{k=1}^{n} \chi_k \sum_{i=k}^{n} \alpha_i = 1$
2		$\prod_{i=1}^{n} (1+\alpha_i B^2\tau)^{-1}$	$\sum_{i_1=1}^{n} \alpha_{i_1} \sum_{i_2=i_1}^{n} \alpha_{i_2} \cdots \sum_{i_m=i_{m-1}}^{n} \alpha_{i_m}$	$\frac{1}{2}\left[\sum_{i=1}^{n} \alpha_i^2 + 1 \right]$	$\chi_i = \delta_{i_1}$ $\sum_{i=1}^{n} \alpha_i = 1$ $0 \leqslant \alpha_i \leqslant 1$
3		$\sum_{k=1}^{n} \chi_k (1+\alpha B^2\tau)^{k-n-1}$	$\frac{\sum_{k=1}^{n} \chi_k \frac{(n+m-k)!}{(n-k)!\, m!}}{\left[\sum_{k=1}^{n} \chi_k (n-k+1) \right]^m}$	$\frac{\sum_{k=1}^{n} \chi_k \frac{(n-k+2)(n-k+1)}{2}}{\left[\sum_{k=1}^{n} \chi_k (n-k+1) \right]^2}$	$\sum_{k=1}^{n} \chi_k = 1$ $\alpha_i^{-1} \equiv \alpha^{-1} =$ $= \sum_{k=1}^{n} \chi_k (n-k+1)$
4		$(1+\alpha B^2\tau)^{-n}$	$\frac{(n+m-1)!}{(n-1)!\, m!\, n^m}$	$\frac{n+1}{2n}$	$\chi_i = \delta_{i1}$ $\alpha_i \equiv \alpha = n^{-1}$
5	Two-group diffusion	$(1+\alpha_1 B^2\tau)^{-1} \times$ $\times (1+\alpha_2 B^2\tau)^{-1}$	$\frac{(1-\alpha_1)^{m+1} - \alpha_1^{m+1}}{1-2\alpha_1}$	$1-\alpha_1(1-\alpha_1)$	$\chi_1 = 1,\ \chi_2 = 0$ $\alpha_2 = 1-\alpha_1,\ \alpha_1 < 1$
6		$(1+0{,}5B^2\tau)^{-2}$	$2^{-m}(m+1)$	0,75	$\chi_1 = 1,\ \chi_2 = 0$ $\alpha_1 = \alpha_2 = ,5$
7	One-group	$(1+B^2\tau)^{-1}$	1	1	$\alpha \equiv 1$
8	Age	$e^{-B^2\tau}$	$(m!)^{-1}$	0,5	$\alpha_i \equiv \alpha = n^{-1}$ $n \to \infty$
9	Crow's flight	$\frac{\operatorname{arctg}(3B^2\tau)^{1/2}}{(3B^2\tau)^{1/2}}$	$3^m(2m+1)^{-1}$	9/5	Nondiffusion model

Remark. χ_k is the fraction of the total number of source neutrons becoming part of the k-th energy group; α_k is the ratio of the square of the slowing-down length within the k-th group to the total square of the slowing-down length. All of the models, except for the last one, are particular cases of the first model.

$$\sum_{k=1}^{e} \chi_k \sum_{i=k}^{e} \alpha_i \leqslant \sum_{k=1}^{e} \chi_k, \quad e = 1, 2 \ldots n, \tag{3}$$

then the last expression for $C_{2m}^{(1)}$ in Eq. (2) can be used to show that the inequality $C_{2(m+1)}^{(1)} \ll C_{2m}^{(1)}$ holds. And since $C_0^{(N)} = C_2^{(N)} = 1$ by definition, we then infer than $C_{2m}^{(N)} \leq 1$ for all of the diffusion models figuring in Table 1. When m is fixed, the minimum value of $C_{2m}^{(N)}$ is attained in the neutron-age model, and is found to be $C_{2m}^{(8)} = (m!)^{-1}$. If we take into account the fact that the source is nonmonoenergetic, we find that this value must be increased. Actually, when the number of equal groups $\bar{n}$ is finite, the Hölder inequality [4] can be invoked to show that the inequality

$$C_{2m}^{(3)} \geqslant C_{2m}^{(4)}, \tag{4}$$

holds here, and is retained in the limit as $\bar{n} \to \infty$.

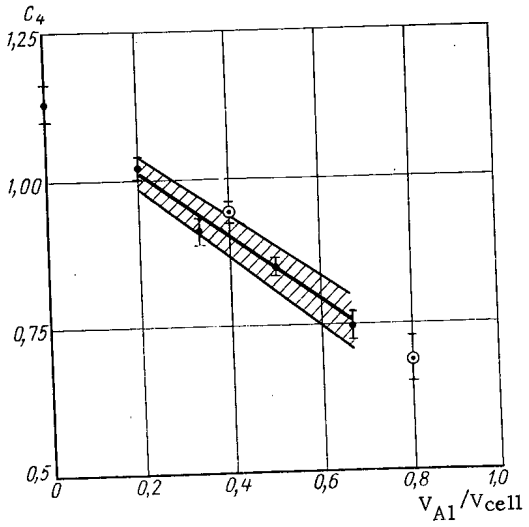

Fig. 1. Dependence of coefficient C_4 on aluminum fraction in reactor core cell (V_{Al}/V_{cell}). Less reliable data points, shown encircled with error bars, were not used in plotting the straight line.

The values of the coefficients C_{2m} depend on the volume fraction of the aluminum in the reactor cell V_{Al}/V_{cell}. In order to find the values of C_4 and C_6, we make use of the values of the experimentally determined moments $\langle r^2 \rangle$, $\langle r^4 \rangle$, $\langle r^6 \rangle$, [5-7], and the values computed by the Monte Carlo method [8-10]. As was demonstrated in several papers [6, 9, 10], a certain disparity in the values reported for the moments in these papers can be accounted for to a partial extent by the anisotropy effect appearing in migration of neutrons through a medium consisting of parallel slabs in water.

In the range $0.2 \leq V_{Al}/V_{cell} \leq 0.66$, the dependence of C_4 on the ratio V_{Al}; V_{Al}/V_{cell} can be represented as a straight line drawn by the method of least squares through V_{Al}/V_{cell} points with the values 0.2, 0.33, 0.50, and 0.66 (see Fig. 1), with the rms values obtained by weighting with the square of the reciprocal error of the results reported in [5-9] taken as the values of C_4. The values of the moments $\langle r^{2m} \rangle$ obtained from the neutron distributions measured solely in the direction perpendicular to the parallel slabs are first reduced to homogeneous values with the aid of the anisotropy coefficients borrowed from [6, 9, 10]. The calculated moments of the slowing-down density are then reduced to the flux moments according to [9, 11]. All of the values of the moments were taken for zero slab thickness. The region of total errors in the C_4 values is shown shaded in the diagram.

When we compare the straight line in Fig. 1 and the C_4 values in Table 1, we see clearly that we can rely on the two-group model in the range $0.3 \leq V_{Al}/V_{cell} \leq 0.66$. When $V_{Al}/V_{cell} \geq 0.67$, the diffusion model must feature a larger number of groups. When the aluminum fraction is increased, the C_4 value tends to a value given by the neutron-age theory [which, according to inequality (4), must be larger than 0.5 in any case]. When the aluminum content is low, either conditions (3) are not met or the diffusion models are not applicable at all.

The two-group diffusion slowing-down model (5th row in Table 1) was used in design calculations of type VVR-M water–aluminum cores with an ordinary water reflector. The total age τ is arrived at in such a way as to keep calculations and experimental data in close agreement for one of the critical masses [12]. The τ value so determined depends, of course, on what procedure is followed in the calculations, and is not more accurate, in and of itself, than the result obtained directly in the experiment. But it is to be hoped that this τ value will lead to closer agreement with experiment, in calculations of other values of critical masses. The α_2 value determined from the straight line C_4 in Fig. 1 for the concrete ratio $V_{Al}/V_{cell} = 0.458 \pm 0.033$ and a concrete plate thickness, makes it possible to select the upper boundary of the epithermal group. The α_2 value obtained from the data for C_6 in the interval $0.3 \leq V_{Al}/V_{cell} \leq 0.66$ lies in the range of errors for α_2 obtained from C_4.

This type of two-group slowing-down model has been used in calculating the critical masses of annular cores of different dimensions. The calculated values were in agreement with experimental values to within several tenths of a percent as the masses themselves varied by a factor of 2.5. The adjusted value of τ then agrees with the experimental value to within 1.5% [12].

Of course, we can also resort to other many-group diffusion models. It is worthwhile verifying, however, the extent to which the C_4 coefficient calculated from the formulas in Table 1 actually agrees with the experimental values plotted in Fig. 1.

LITERATURE CITED

1. G. I. Marchuk, Nuclear Reactor Design Methods [in Russian], Atomizdat, Moscow (1960).
2. E. A. Garusov and Yu. V. Petrov, At. Energ., 17, 375 (1964).
3. A. Weinberg and E. Wigner, Physical Theory of Nuclear Reactors [Russian translation], IL, Moscow (1961).

4. E. Beckenbach and R. Bellmann, Inequalities [Russian translation], Mir, Moscow (1965).
5. R. Paschall, Nucl. Sci. and Engng., 26, 73 (1966).
6. P. Palmedo, Nucl. Sci. and Engng., 32, 302 (1968).
7. J. Spencer and T. Williamson, Nucl. Sci. and Engng., 27, 568 (1967).
8. H. Alter, NAA-Memo-11239, Atomics International (1965).
9. P. Palmedo, Nucl. Sci. and Engng., 32, 313 (1968).
10. P. Palmedo, Trans. Amer. Nucl. Soc., 10, 240 (1967).
11. H. Alter, Nucl. Sci. and Technology, A/B, 20, 37 (1966).
12. T. B. Ashrapov et al., Preprint No. 152, FTI [in Russian], Leningrad (1968).

DESIGN OF REACTOR CONTROL SYSTEMS BASED ON OPTIMAL CONTROL THEORY

G. N. Aleksakov, V. I. Belousov, and A. P. Kryukov

UDC 621.3.078

The purpose of the work described here was to study ways and options of improving control and protection systems of nuclear power facilities on the basis of optimizing control theory.

The problem of nuclear reactor control optimized with respect to speed of response is structured as follows.

Given:

1) the mathematical model of the controlled plant, describing the kinetics of the nuclear reactor (1) and the dynamics of the control servomechanism:

$$\frac{dn(t)}{dt}=\frac{k(t)(1-\beta^*)-1}{l}n(t)+\sum_{i=1}^{6}\lambda_i C_i(t); \tag{1a}$$

$$\frac{dC_i(t)}{dt}=\frac{k(t)\beta_i^*}{l}n(t)-\lambda_i C_i(t),\quad i=1, 2, \ldots, 6; \tag{1b}$$

$$\frac{dk(t)}{dt}=\beta^* u(t), \tag{1c}$$

where n(t) is the neutron flux density; $C_i(t)$ is the concentration of delayed-neutron sources of the i-th group; k(t) is the effective neutron multiplication ratio; l is the average lifetime of the prompt neutrons; β_i^* is the effective fraction of delayed neutrons belonging to the i-th group; β^* is the total delayed-neutron fraction; λ_i is the decay constant of the i-th group of delayed neutrons; u(t) is the control response;

2) limitations on the relative rate of change of neutron flux

$$\left|\frac{1}{n(t)}\cdot\frac{dn(t)}{dt}\right|=\left|\frac{1}{T}\right|\leqslant\frac{1}{T_{\min}}, \tag{2}$$

where T_{min} is the minimum allowable period for the reactor to ride up from a low power level;

3) the functional giving an estimate of the performance:

$$J=\int_0^t 1\cdot dt. \tag{3}$$

It is required to find: 1) limitations on the magnitude of the control response at which the functional is minimized; 2) the control law with feedback corresponding to the minimum of the functional.

In contrast to the familiar statements of a similar problem [2-5], the control limitations are included in the array of parameters to be determined, rather than in the set of prespecified conditions.

The optimum conversion of the reactor from one power level to another (optimized in terms of response time), with the limitations (2), can be achieved in a unique way:

Translated from Atomnaya Énergiya, Vol. 32, No. 3, pp. 228-229, March, 1972. Original article submitted April 28, 1971.

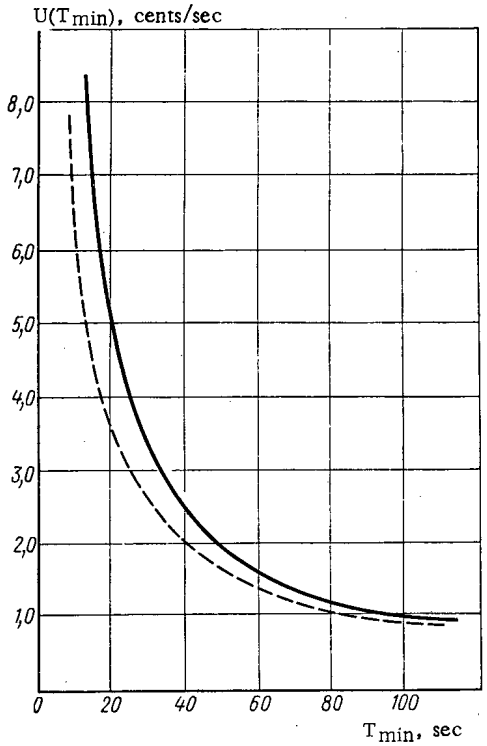

Fig. 1

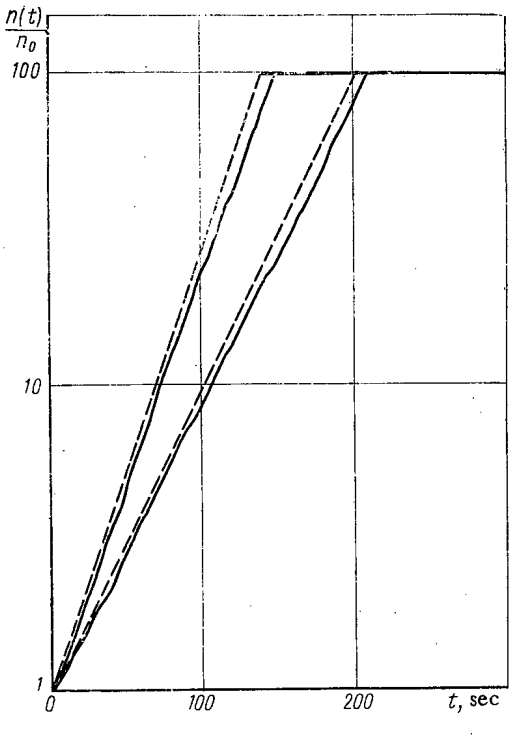

Fig. 2

Fig. 1. Dependence of control response on minimum allowable period for reactor riding up from low power level: ——) u↑; – – –) u↓.

Fig. 2. Theoretically predicted (– – –) and actual (——) pattern of variation in power level in optimizing control of the IRT-2000 reactor.

1) during the transient the limiting allowable rate of change in neutron flux must be maintained:

$$\frac{1}{n(t)}\cdot\frac{dn(t)}{dt}=\frac{1}{T_{\min}},\quad 0<t<t_0; \tag{4}$$

2) starting from the time the specified power level is attained, the neutron flux must remain constant:

$$\frac{dn(t)}{dt}=0,\ n(t)=n_0,\ t\geqslant t_0. \tag{5}$$

Analysis of conditions (4) enables us to find the control variation program

$$u(t)=\frac{1}{T_{\min}}\sum_{i=1}^{6}\beta_i^*/\beta^* e^{-\left(\frac{1}{T_{\min}}+\lambda_i\right)t}\quad (0<t<t_0) \tag{6}$$

and the limitation on the control response:

$$u_1=\frac{1}{T_{\min}}, \tag{7}$$

which can be enlisted to increase the neutron flux with a minimum allowable period. The analysis of conditions (5) yields the program variation control:

$$u(t)=-\sum_{i=1}^{6}\frac{\lambda_i\beta_i^*/\beta^*}{1+\lambda_i T_{\min}}\left[1-e^{-\left(\frac{1}{T_{\min}}+\lambda_i\right)t_0}\right]e^{-\lambda_i t},\quad t\geqslant t_0, \tag{8}$$

as well as the limiting value of the control response

$$u_\downarrow=\sum_{i=1}^{6}\frac{\lambda_i\beta_i^*/\beta^*}{1+\lambda_i T_{\min}}, \tag{9}$$

which will stabilize the power at the specified level without overshoots. The dependences $u\downarrow(T_{min})$ and $u\uparrow(T_{min})$ are plotted in Fig. 1.

The limitations on the control response (7) and (9) are independent of the neutron flux level. These restrictions determine the power of the actuating motor which moves the control rod:

$$P \geqslant \frac{u_{\uparrow}(T_{\min})\,G}{\eta\varkappa}, \tag{10}$$

where η is the efficiency of the actuating motor; $\varkappa$ is the worth of the control rod, cents/m; G is the weight of the control rod, N.

The period stabilization condition (4) and power stabilization condition (5) can be arrived at, on the average, in an on–off feedback type automatic control system if the power of the actuating motor in this system is selected to conform to formula (10).

The parameters of the motor, on the one hand, and the characteristics of the ionization chamber, on the other, along with the system accuracy, determine the requirements to be imposed on the technical characteristics of all of the system components. The engineering design procedure developed on that basis was checked in the synthesis of the automatic control system for the IRT-2000 reactor at MIFI [Moscow Engng. Physics Inst.]. The transients recorded by the panel-mounted instruments when the system was being tested are compared, in Fig. 2, to graphs plotted on the basis of theoretical data.

Analysis of the results obtained, and comparison between the theoretical inferences and experiment, led to the following conclusions:

1. The on–off control mode is the optimum one, with respect to speed of response, in the control of reactor power level.
2. The limiting values of the control response, dependent solely upon the allowable reactor warm-up period, make it possible to impose completely specific technical requirements on the servomechanism and on other components of the control system, and also make it possible to calculate the scram system parameters.
3. The limitations on reactivity control that were mentioned correspond to the total rate of change in reactivity. When a specific reactor control system is being designed, the contribution made by temperature effects to the rate of change in reactivity must be taken into consideration, as must the effect of poisoning, burn-up, etc. Analysis of an effect of that nature can be carried out with the aid of methods described by Murray et al. [6].
4. The proposed engineering design procedure is applicable to the design of control and protection systems for nuclear power facilities featuring any dynamic characteristics whatever. It proves most useful in the development of control systems for the power plants of moving vehicles.

LITERATURE CITED

1. G. R. Kipin, Physical Fundamentals of Nuclear Reactor Kinetics [Russian translation], Atomizdat, Moscow (1967).
2. V. G. Boltyanskii, Mathematical Methods of Optimizing Control Theory [in Russian], Nauka, Moscow (1969).
3. V. I. Plyutinski, V. I. Kazachkov, and V. I. Vishnyakov, in: Control of Nuclear Power Facilities [in Russian], No. 1, Atomizdat, Moscow (1966).
4. B. E. Chuprun, in: Control of Nuclear Power Facilities [in Russian], No. 2, Atomizdat, Moscow (1967).
5. G. N. Aleksakov and V. S. Popov, in: Control of Nuclear Power Facilities [in Russian], No. 4, Atomizdat, Moscow (1970).
6. R. Murray et al., Nucl. Sci. and Engng., 18, 481 (1964).

PERFORMANCE OF FISSION IONIZATION CHAMBERS FOR REACTOR CONTROL SYSTEMS

A. B. Dmitriev, E. K. Malyshev,
V. G. Belozerov, and O. I. Shchetinin

UDC 621.039.56

Power level control over a range of four to five decades in nuclear reactors can be achieved with the aid of pulsed ionization type fission chambers backed up by current type ionization chambers. Installation of two separate chambers is sometimes found to be undesirable, even impossible.

One way to expand the working range of ionization type fission chambers is to use them sequentially in the pulsed mode and in the current mode. This article discusses an investigation of two types of fission pulse chambers employed in nuclear reactor control and protection systems: the KNT-31 and KNT-5 chambers [1], with respective thermal sensitivities of $2.5 \cdot 10^{-5}$ and $5 \cdot 10^{-5}$ pulse/neutrons/cm^2.

When the fission chamber is operated in the current mode, its discrimination properties with respect to α-radiation are inferior to those in the pulsed mode. Background currents due to prompt γ-emission (in fission), to radiation from fission products, to natural α-activity of the radiator, to leakage through the insulators, and miscellaneous causes, are all recorded.

In the case of the KNT-31 and KNT-5 chambers, the background current due to the α-activity of the radiator is $5.8 \cdot 10^{-9}$ A and $2.0 \cdot 10^{-11}$ A, respectively. The sensitivity to γ-emission of the isotope Co^{60} is respectively $4.4 \cdot 10^{-11}$ and $1.5 \cdot 10^{-2}$ A/R/h. The sensitivity to thermal neutrons is $1.0 \cdot 10^{-13}$ and $2.6 \cdot 10^{-16}$ A/neutrons/cm^2 · sec in the current mode.

In order to avert a rise in noise level on account of a buildup of active fission products and activation of the structural elements, the KNT-31 starting chambers are usually removed from the high-flux region after the reactor has been brought up to rated power level. This operation is an undesirable one from the standpoint of efficient operation.

The KNT-31 chambers were subjected to protracted in-pile testing. The noise level was measured periodically. By the end of the tests, the collected integrated flux was 10^{18} neutrons/cm^2. The rise in the noise level was insignificant.

Pulses comparable in amplitude to pulses caused by neutrons can appear when pulse chambers are used in high γ-radiation fields, on account of the buildup of pulses due to the interaction of γ-quanta with the chamber materials. On the basis of the assumption [2] that these pulses are due to a superposition of m or more rectangular "elemental" pulses initiated by secondary electrons over an interval equal to the time constant T of the amplifier, a formula relating the count rate N of spurious pulses to the dose rate of γ-radiation P_γ was derived:

$$N = 8.89 \cdot 10^6 \sqrt{\frac{\eta S P_\gamma}{E_\gamma (\tau + \sigma)}} \exp\left[-\frac{7 \cdot 10^{-16} E_\gamma (\tau + \sigma)\, m^2}{\eta S P_\gamma T} \right],$$

where η is the quantum yield of the chamber wall materials; S is the wall area, cm^2; E_γ is the γ-photon energy, MeV; τ is the photoelectric absorption coefficient, cm^2/g; σ is the absorption coefficient of the energy of γ-photons in the Compton effect, cm^2/g.

When T = 0.1 μsec the dose rate P_γ bringing about a count rate of spurious pulses of 1 count/sec is respectively $6 \cdot 10^6$ R/h and $4 \cdot 10^9$ R/h in the case of the KNT-31 and KNT-5 chambers. A roughly 10-fold

Translated from Atomnaya Énergiya, Vol. 32, No. 3, pp. 230-231, March, 1972. Original article submitted January 21, 1971.

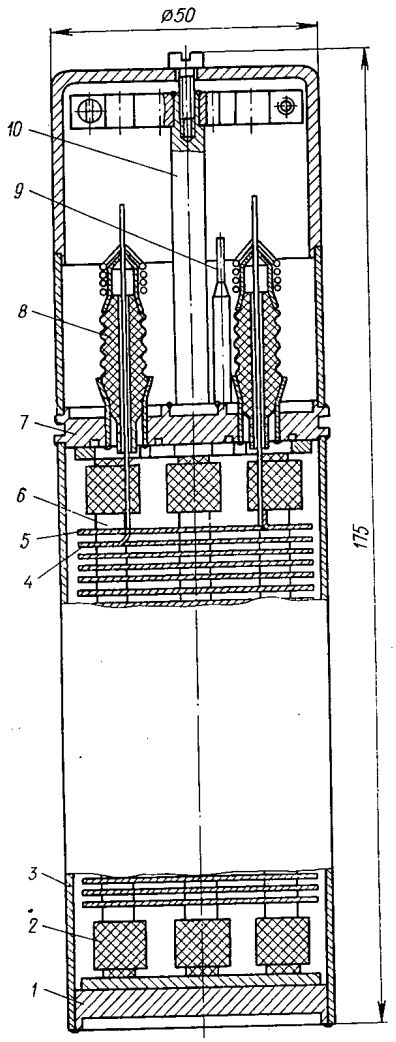

Fig. 1. Design of KNT-54-1 type ionization chamber: 1) flanges; 2) supporting insulator; 3) housing; 4, 5) electrodes; 6) support column; 7) flanges; 8) lead-out insulator; 9) evacuation tube; 10) mounting bracket.

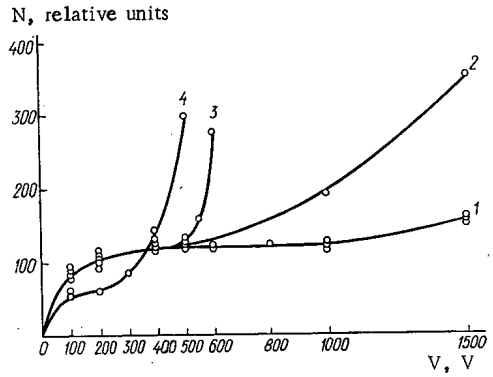

Fig. 2. Count characteristics of chamber at different temperatures: 1) 20-400°C; 2) 500°C; 3) 600°C; 4) 400°C (KNT-31).

decrease in T has the effect of increasing the allowable dose rate of the γ-emission by the same degree.

One disadvantage of the design of the KNT-31 and KNT-5 chambers is the absence of a guard electrode, which is particularly conspicuous at high temperature (above 300°C). The KNT-54-1 design of fission chamber with guard electrode included was developed. The chamber (Fig. 1) employs a plane-parallel array of electrodes; the interelectrode gap is 1.6 mm. The electrodes are coated electrolytically on two sides with a uranium coating $U_3^{235}O_8$ with a thickness 1 mg/cm^2. The total area plated is 1000 cm^2. The electrode array is mounted on six rack support columns resting on ceramic insulators. The role played by the guard electrode is to provide a grounded casing for the chamber. The metallic parts of the chamber are made of Kh18N9T stainless steel, while the insulators are made of type M-7 high-alumina ceramic [3].

Figure 2 shows the count characteristics of the chamber as a function of ambient temperature. The chambers were subjected to short-term (2 h) heating in an electrically heated furnace, during the tests. There is a plateau at temperatures of 600°C which allows reliable recording of neutron-derived pulses. For comparison, Fig. 2 also illustrates the count performance of a chamber with no guard electrode (the KNT-31 chamber) when the ambient temperature is 400°C (curve 4).

When the chamber capacitance is 300 pF and the load resistance is 1.2 kΩ, the average pulse amplitude is about 100 μV. The chamber sensitivity at a discrimination threshold of 70 μV is 0.59 counts/neutrons/cm^2 with respect to the undisturbed isotropic thermal flux.

The chamber sensitivities were $1.5 \cdot 10^{-13}$ A/neutrons/cm^2·sec when the chambers measured average current. The background current due to the α-activity is $6 \cdot 10^{-9}$ A. In order to join the end of the pulse mode range to the beginning of the current mode in a simple manner, current sufficient to compensate the background current must be introduced into the recording circuit. The maximum operating current of the chamber, 3 mA, is attained at 500 V supply voltage. The chamber sensitivity to γ-emission of the isotope Co^{60} is $1.3 \cdot 10^{-11}$ A/R/h In the region of intermediate reactor power levels, neutron recording becomes more difficult because of the presence of high γ-radiation background, the intensity of which varies out of proportion to the reactor output level. Reliance on the method of statistical discrimination of the γ-background [4] makes it possible to improve the accuracy of the measurements considerably when the chamber is operated under γ-radiation conditions in the current mode.

LITERATURE CITED

1. A. B. Dmitriev, E. K. Malyshev, and I. A. Reformatskaya, Pribory i Tekh. Éksperim., No. 4, 55 (1968).
2. A. B. Gillespie, Signal, Noise, and Resolution of Amplifiers [Russian translation], Atomizdat, Moscow (1964).
3. V. A. Presnov et al., Ceramics and Metal-Ceramic Joints in Engineering [in Russian], Atomizdat, Moscow (1969).
4. A. I. Mogil'ner and S. A. Morozov, At. Énerg., 24, 151 (1968).

A METHOD FOR STUDYING URANIUM DISTRIBUTION IN MAGNESIUM – BERYLLIUM FUEL-ELEMENT CLADDING

A. F. Gorenko, G. M. Shevchenko,
N. I. Bugaeva, A. S. Zadvornyi,
N. A. Skakun, and A. P. Klyucharev

UDC 621.039.546

Mutual diffusion is observed at sites of contact between fuel-element meat and fuel-element cladding, in the preparation and use of fuel elements. The diffusion interaction can bring about impairment of the cladding, and contamination of the coolant as a consequence. Serious restrictions are imposed on the selection of cladding material, as well as on temperature conditions and on the service life of fuel elements.

The uranium distribution in magnesium–beryllium cladding 500 to 600 μ thick was studied in a rod type fuel element with natural uranium meat. The cladding was removed from a 2.5 cm long specimen layer by layer, by using a solution (1 : 15) of nitric acid. A total of 15 layers, each ~40 μ thick, were removed from the specimen. This was followed by extraction of the uranium by a 20% solution of tributylphosphate in CCl_4. The uranium was back-extracted in 1 N HCl [1] from organic extracts, and the solution was transferred dropwise onto a metallic substrate from which it was evaporated.

The uranium extract, together with the substrate, was applied closely to a previously prepared mica plate [2], and was routed via pneumatic shuttle to exposure under a beam of γ-photons. The peak photon energy attained the level of 22.3 MeV.

In photofission, only the nuclei of the heavy elements exhibit appreciably large cross sections, and their fission fragments leave specific tracks on the mica. The source of error may be only a uranium impurity present in the chemical reagents, in the mica, in the metallic substrate, and in the magnesium –beryllium charge from which the cladding was made. It is also essential that the chemical operations of dissolution, solvent extraction, back-extraction, and precipitation be carried out with losses as small as possible, or at least with losses proportional to the uranium concentration in each specimen.

Preparations with uranium concentrations of 10^{-8}, $5 \cdot 10^{-8}$, and 10^{-7} g were prepared in order to monitor the chemical operations. The uranium was mixed with the magnesium–beryllium charge, and afterwards all of the operations were carried out in a manner similar to the handling of preparations from layers of cladding. The background uranium concentration in the mica and in the substrate was also monitored in terms of the number of tracks All of the preparations containing uranium and the control standards were irradiated simultaneously by a beam of γ-photons for 1.5 h. The electron current to the convertor was 5 μA. The change in the γ-ray flux density over the length of a stack of specimens was determined with the aid of Lavsan monitoring films, in terms of induced activity. The films were placed at the beginning and at the end of the film pack. After the irradiation was completed the mica plates were treated with hydrofluoric acid, and the tracks were counted under a microscope.

Figure 1 shows the dependence of the number of fission-fragment tracks on the uranium concentration in standard specimens. The linear relationship is an indication that the chemical operations are readily reproducible, while the losses, if any, are proportional to the uranium concentration.

Figure 2 shows results of a track count taken from uranium preparations made from different layers of cladding. The test specimen studied was an arbitrarily selected portion of a finned fuel element with the outer surface contaminated in its original state. The uranium distribution was traced through all the layers

Translated from Atomnaya Énergiya, Vol. 32, No. 3, pp. 231-232, March, 1972. Original article submitted April 28, 1971.

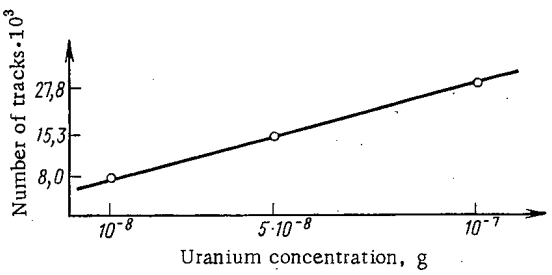

Fig. 1. Dependence of number of tracks on uranium concentration in standard specimens.

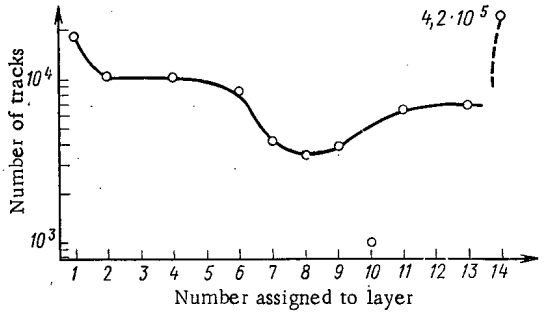

Fig. 2. Uranium distribution in magnesium–beryllium cladding.

all the way to the meat–cladding interfaces. The uranium concentration in the last layer rose sharply because of the onset of etching of the fuel meat itself.

This example provides an illustration of the possibilities inherent in the procedure we worked out, which features excellent sensitivity and reproducibility. It is applicable in principle to the investigation of fuel-element cladding made of any material, and can be modified to facilitate determinations of plutonium diffusion or diffusion of other fissionable materials.

LITERATURE CITED

1. V. K. Markov et al., Uranium and Methods for Determining Uranium [in Russian], Atomizdat, Moscow (1964), p. 250.
2. Ya. E. Geguzin, I. G. Berezina, and I. V. Vorob'eva, Izv. Akad. Nauk SSSR, Seriya Geol., No. 6, 21 (1966).

CALORIMETERS FOR CRITICAL ASSEMBLIES

O. A. Gerashchenko, V. B. Klimentov, and A. V. Nikonov

UDC 621.039.517.536.629

The determination of the magnitude and distribution of heat release in nuclear reactors and critical assemblies is one of the most important problems in reactor engineering. The indirect calculation methods now used often lead to inaccurate answers so that directly measured data are of considerable interest.

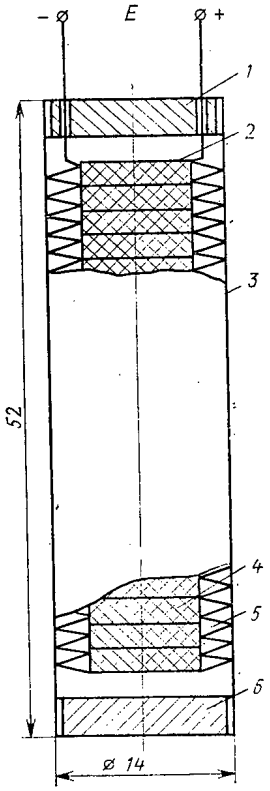

Fig. 1

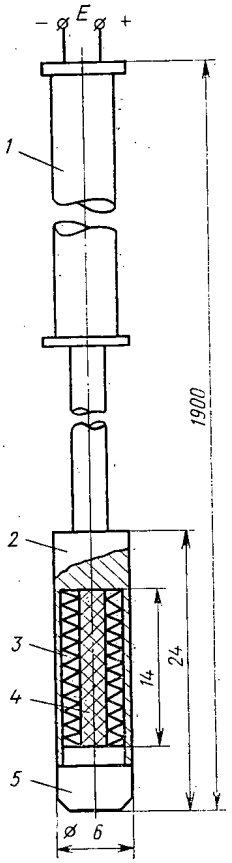

Fig. 2

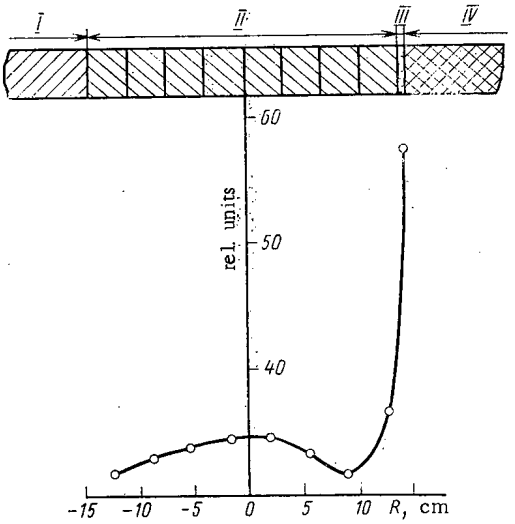

Fig. 3

Fig. 1. Calorimeter for measuring heat release: 1) top aluminum cover; 2) aluminum cup; 3) stainless steel calorimeter case; 4) uranium dioxide pellets; 5) laminar thermoelements; 6) bottom aluminum cover.

Fig. 2. Calorimeter for measuring relative heat release distribution: 1) holder; 2) plastic calorimeter case; 3) laminar thermoelements; 4) uranium dioxide; 5) plastic end cap.

Fig. 3. Radial relative heat release distribution in the core of the VVR-M critical assembly: I) beryllium reflector; II) fuel elements; III) water gap (10 cm thick); IV) graphite column.

Translated from Atomnaya Énergiya, Vol. 32, No. 3, pp. 232-234, March, 1972. Original article submitted April 12, 1971.

The measurement of heat release in reactors and critical assemblies is associated with certain experimental difficulties. Because of the insignificant amount of heat released in the investigated object the main difficulty in critical assemblies is due to the need of very high sensitivity. When results obtained in critical assemblies are applied to full-scale reactors, to the various corrections associated with simulation one must also add a correction for energy released in γ-radiation. No such simulation problem has been raised in this work.

Heat release in the VVR-M critical assembly [1] was measured directly by specially designed high-sensitivity calorimeters (Figs. 1 and 2) by means of which measurements can be taken in the course of operation. The calorimeters form closed thermometric capsules in which the samples to be tested are placed. The capsule is made up of laminar heat flux sensors [2].

The calorimeter shown in Fig. 1 is used to measure heat release in cylindrical samples of fissionable material 0.9 cm in diameter and up to 4 cm long. The samples were uranium dioxide pellets enriched to 90%. The second calorimeter (Fig. 2) was used to measure the relative heat release distribution along the critical assembly core. The calorimeter held a nickel cup 0.24 cm in diameter and 1.4 cm high filled with 90% enriched uranium dioxide. The calorimeter signals were measured with the aid of a potentiometric circuit including a P-306 dc potentiometer and an M-135 galvanometer as an indicating instrument.

The calorimeters were calibrated by plotting the output signal as a function of heat released inside the cavity. As the reference heat source we used an electric heater whose power was measured with the aid of a potentiometer and standard resistor using the four-conductor method. The resulting calibration curve is linear within the considered heat release range and has a slope of 20.4 ± 0.7 mV/W.

With a thermal neutron flux density $\Phi = (3.6 \pm 0.4) \cdot 10^7$ neutrons/cm$^2 \cdot$ sec, the relative heat release of the uranium sample (0.9 cm in diameter and 4 cm long) in the calorimeter was

$$q_V = (34.0 \pm 1.7) \cdot 10^{-4} \text{ W/cm}^3.$$

As a comparison we have performed the following activation experiments: 1) measurement of thermal neutron flux density on the surface of an uranium core by means of gold foils; 2) determination of the average fission density blocking factor by means of thin U^{235} foils; 3) determination of the average longitudinal fission density using paper indicators for collecting fission fragments; 4) determination of the cadmium ratio for U^{235} for estimating the epicadmium heat release. These measurements gave the relative heat release in the investigated sample as

$$q_V = (28 \pm 6) \cdot 10^{-4} \text{ W/cm}^3.$$

The results obtained by the two methods are seen to agree quite well considering the experimental error.

For the second calorimeter, whose diameter is sufficiently small to fit into the internal channel of VVR-M fuel elements, we have plotted the radial relative heat release distribution in the critical assembly core (Fig. 3).

The high effectiveness of these calorimeters in measuring heat release in critical assemblies has been proved experimentally. The miniature calorimeter allows rapid plotting of the axial and radial heat release distribution in the critical assembly core.

LITERATURE CITED

1. V. B. Klimentov et al., At. Énerg., 20, 63 (1966).
2. O. A. Gerashchenko and V. G. Fedorov, The Technique of Thermotechnical Experiments [in Russian], Naukova Dumka, Kiev (1964).

THE SOLUBILITY OF OXYGEN AND HYDROGEN IN A EUTECTIC ALLOY OF SODIUM AND POTASSIUM

M. N. Arnol'dov, M. N. Ivanovskii,
S. S. Pletenets, and A. D. Pleshivtsev

UDC 621.039.534.6

The use of an alloy of sodium and potassium as a coolant in nuclear reactors requires their profound purification from impurities, chief among which are oxygen and hydrogen. In view of this it is necessary to note the temperature dependences of the solubility of these impurities in the alloy. However, the published data either have been obtained for a narrow range of temperatures, or diverge substantially. Therefore, it seemed useful to conduct an experimental investigation of the solubility of oxygen and hydrogen in an alloy of sodium and potassium.

The experiments were conducted on a circulation circuit equipped with devices for the purification, introduction of measured amounts of impurities, a sample collector, as well as with a plate indicator of impurities.

The method of determination of the solubility consisted of the following. A measured amount of oxygen or hydrogen was introduced into the alloy, purified by means of a cold trap. After equalization of the concentration of the impurity through the volume of the circulating metal, the temperature of saturation of the alloy with the impurity was determined with the plug indicator [1]. Then another portion of the impurity was introduced, and the temperature of saturation of the alloy was determined again, etc.

The amount of hydrogen present in the alloy was monitored with an electrical indicator [2], while the amount of oxygen was monitored with a sample collector–distiller.

The results of the experiments, together with the published information, are cited in Fig. 1. The results of the determination of the solubility of oxygen, treated by the method of least squares, are described by the function

$$\lg C \cdot 10^4 = 6.08 - \frac{1970}{T} \quad (373 < T < 548^\circ \text{K}), \tag{1}$$

where C is the concentration of oxygen, % by weight; T is the temperature, °K. The calculated heat of solution of oxygen in the alloy was equal to 9000 ± 500 kcal/mole.

The confidence interval of the mean square deviation of the experimental points for the 0.95 probability level is ±10-18% of the averaged value cited in formula (1).

As can be seen from Fig. 1, the data on the solubility of oxygen in the alloy, obtained by different researchers, differ appreciably. The same figure cites the calculated dependence of oxygen in the alloy (curve A), obtained with the aid of the Wagner formula. This formula describes the solubility of the impurity in an alloy of two metals according to the known solubility of this impurity in the individual components of the alloy [7]:

$$\ln C_{all} = (1-N)\ln C_1 + N \ln C_2, \tag{2}$$

where C_{all}, C_1, and C_2 are the solubility of the impurity in the alloy and in its individual components, respectively; N is the concentration of the second component in the alloy. The formula is correct for components close in physicochemical properties. Data on the solubility of oxygen in sodium and potassium

Translated from Atomnaya Énergiya, Vol. 32, No. 3, pp. 234-235, March, 1972. Original article submitted April 28, 1971.

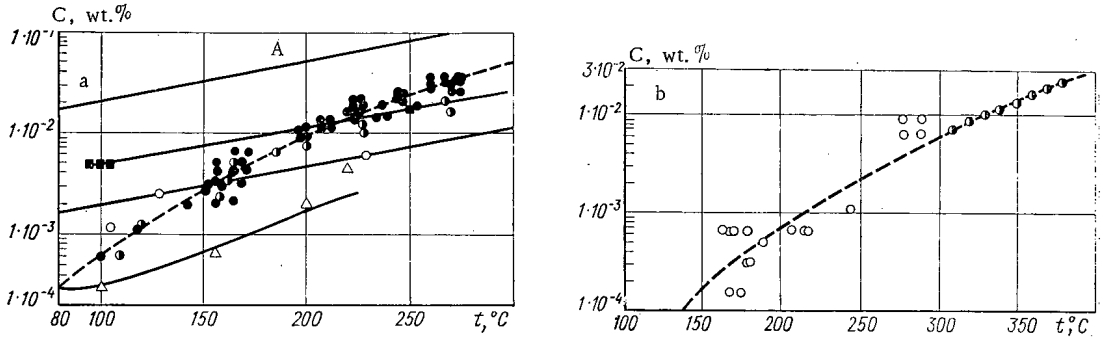

Fig. 1. Solubility of oxygen (a) and hydrogen (b) in an alloy of sodium and potassium: a) ●) our data, oxygen content determined according to the amount introduced; ◑) our data, oxygen content determined by chemical analysis; ○) data of [3]; △) data of [4]; ■) data of [5]; b) ○) our data; ◑) data of [6].

were used for the calculation [3]. It is evident that the discrepancy between the calculated curve, the position of which is greatly influenced by the solubility of oxygen in potassium, and the experimental data obtained on the whole is no poorer than in the studies of other researchers.

Figure 1 presents data on the solubility of hydrogen, together with the results obtained earlier by the hot volume method [6]; they are in sufficiently satisfactory agreement with one another. Treatment according to the method of least squares leads to the following temperature dependence of the solubility of hydrogen in the alloy:

$$\lg C \cdot 10^4 = 6.23 - \frac{2530}{T} \qquad (433 < T < 653^\circ \mathrm{K}), \tag{3}$$

where C is the hydrogen concentration, % by weight. The heat of solution of hydrogen in the alloy is equal to 11,600 ± 1500 kcal/mole.

The confidence interval of the mean square of the points (at the 0.95 probability level), equal to 20-50% of the value of the concentration given by formula (3), was determined by statistical treatment of the data obtained. Within this range, formula (3) and the formula proposed in [6], obtained as a result of the use of entirely different methods, coincide. This circumstance indicates the absence of any significant methodological errors, and in our opinion, increases the reliability of the data obtained on the solubility of oxygen.

LITERATURE CITED

1. F. A. Kozlov et al., in: Liquid Metals [in Russian], Atomizdat, Moscow (1967), p. 324.
2. M. N. Ivanovskii et al., At. Énerg., 24, 392 (1968).
3. D. Williams et al., J. Phys. Chem., 63, 68 (1959).
4. É. E. Konovalov et al., At. Énerg., 24, 478 (1968).
5. É. S. Bannykh and G. F. Fefelova, in: Transactions of Ural Scientific-Research Institute [in Russian], No. 5, 105 (1958).
6. M. N. Arnol'dov et al., At. Énerg., 28, 18 (1970).
7. K. Wagner, The Thermodynamics of Alloys [Russian translation], Metallurgizdat, Moscow (1957).

AN ISOTOPIC Be(α, n) SOURCE WITH A NEUTRON LINE SPECTRUM

N. D. Tyufyakov, A. S. Shtan',
L. A. Trykov, V. B. Pavlovich,
A. G. Kozlov, and S. G. Tsypin

UDC 539.12.03

We investigated the energy spectrum of neutrons from a source made from layers of Pu^{238} dioxide and metallic beryllium deposited on separate substrates in the form of stainless-steel disks (substrate thickness 0.5 mm, diameter 50 mm).

To obtain the required neutron yield over a solid angle of 4π, the source was composed of 14 pairs of layers in a stainless-steel capsule, tightly compressed and sealed. In each pair, the order of the α-emitter and target layers was the same. The diameter of the complete source was 56 mm, and its length 28 mm.

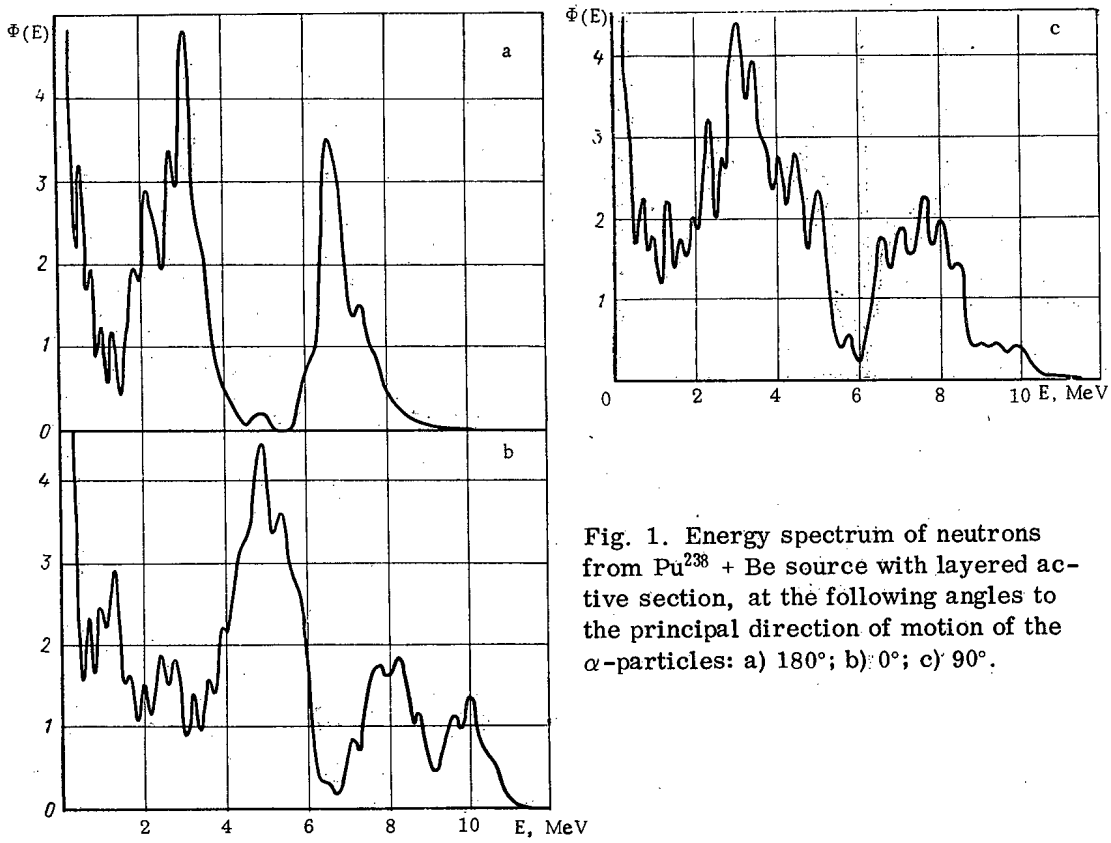

Fig. 1. Energy spectrum of neutrons from Pu^{238} + Be source with layered active section, at the following angles to the principal direction of motion of the α-particles: a) 180°; b) 0°; c) 90°.

Translated from Atomnaya Energiya, Vol. 32, No. 3, pp. 235-236, March, 1972. Original article submitted August 17, 1971.

The neutron energy spectra of this source and of a single pair of layers were measured at angles of 0, 90, and 180° to the principal direction of the α-particles. The measurements were made with a one-crystal scintillation fast-neutron spectrometer with discrimination of the γ-background based on pulse shape. In the spectrometer we used a stilbene crystal 30 mm in diameter and 10 mm long, together with an FÉU-93 photomultiplier. The instrumental pulse distribution was registered by a 512-channel analyzer. The results for 0, 90, and 180° are plotted in Fig. 1. From this figure we see that the spectrum of the neutrons emerging at 90° to the principal direction of motion of the α-particles is rather similar to the neutron spectrum from a Pu^{238} + Be source with a homogeneous active section.

The neutron spectrum of the one-layer source is the same as that of the 14-layer source. This agrees with the conclusion of Trykov [1] that the shape of the neutron spectrum of a Be(α, n) source depends only weakly on its dimensions.

From Fig. 1 we see that the energy spectrum of neutrons from a Be(α, n) source made by the above method is similar to a line spectrum and depends on the direction of measurement. The positions of the neutron intensity maxima agree with the theoretical values for the corresponding angles of incidence of α-particles on the target. If other isotopes capable of (α, n) reactions are used together with the beryllium to prepare the target, we can get additional maxima in the neutron spectra.

The source has been in use for over a year. It has proved very convenient for adjusting and calibrating neutron-spectrometric apparatus. In certain cases it has successfully replaced accelerators as a source of monoenergetic neutrons. Its main advantages are timewise stability, reliability of operation, and small size.

The specific neutron yield over a solid angle of 4π is about one-fifth of that for a source with a homogeneous active section.

LITERATURE CITED

1. L. A. Trykov and N. D. Tyufyakov, in: Radiation Technique [in Russian], No. 9, Atomizdat, Moscow (1971).

A HIGH-YIELD Cm^{244} + Be NEUTRON SOURCE

N. D. Tyufyakov, A. S. Shtan',
L. A. Trykov, Yu. V. Fadeev,
Yu. V. Chushkin, G. N. Strel'nikov,
Yu. N. Luzin, and V. I. Zinkovskii

UDC 539.12.03

One of the most promising isotopes among the transuranium elements that seem to be usable for preparing high-yield isotopic neutron sources (~10^9 neutrons/sec or more) with a sufficiently time-stable yield is Cm^{244} [1, 2].

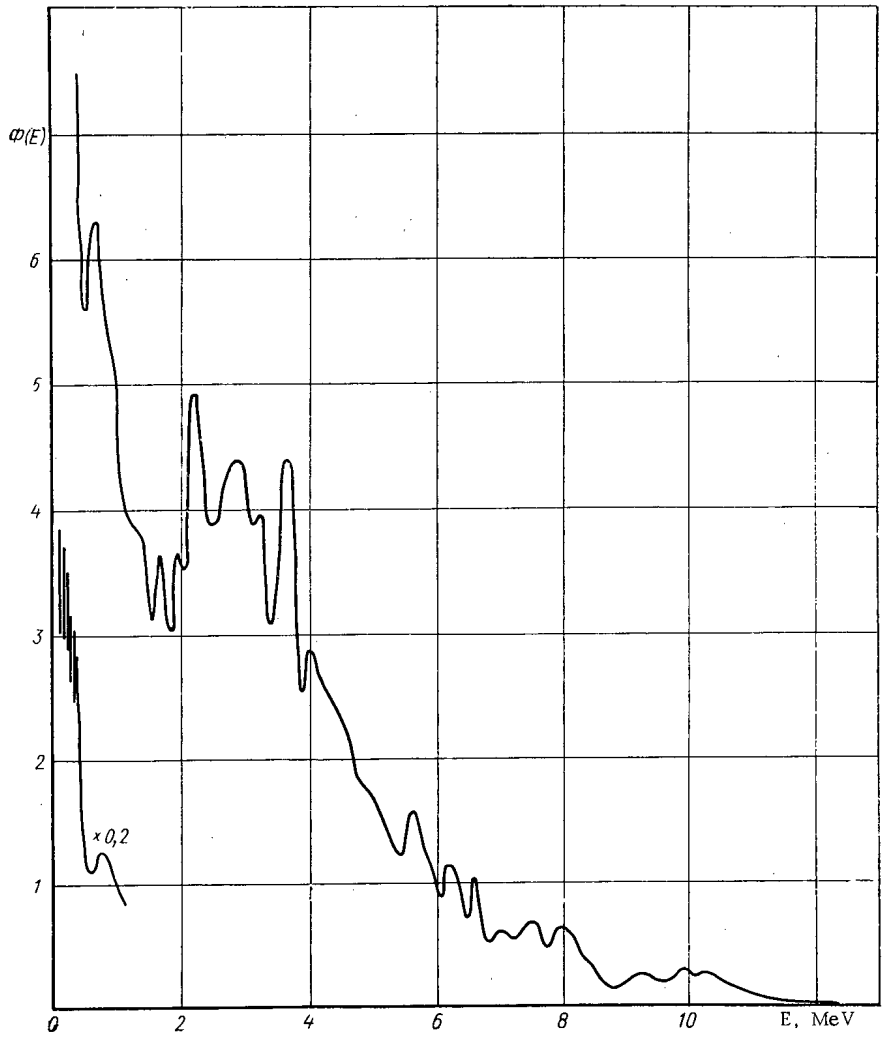

Fig. 1. Energy spectrum of neutrons from a Cm^{244} + Be source with a yield of $(1.8 \pm 0.1) \cdot 10^9$ neutrons/sec.

Translated from Atomnaya Énergiya, Vol. 32, No. 3, pp. 237-238, March, 1972. Original article submitted August 17, 1971.

Basic Characteristics of Cm^{244}

Half-life (α-decay) [3]	18.1 yr
Number of α-disintegrations	$3 \cdot 10^{12}$ dis/g·sec
Energy and yield of α-particles [3]	5806 keV (76.5%)
	5764 keV (23.5%)
Energy and yield of γ-radiation accompanying the α-disintegration [3]	42.8 keV (0.021%)
	100 keV ($1.4 \cdot 10^{-3}$%)
	150 keV ($1.4 \cdot 10^{-3}$%)
	590 keV ($2 \cdot 10^{-4}$%)
	825 keV ($6.5 \cdot 10^{-4}$%)
Half-life for spontaneous fission [3]	$1.346 \cdot 10^{7}$ yr
Number of spontaneous fissions	$3.9 \cdot 10^{6}$ fissions /g·sec
Yield of spontaneous-fission neutrons	$1.09 \cdot 10^{7}$ neutrons/g·sec
Number of prompt γ-quanta	$\sim 2.7 \cdot 10^{7}$ quanta/g·sec
Heat generation	~2.8 W/g

In order to solve the problems arising in the production and practical application of high-yield isotopic neutron sources, we prepared an experimental Cm^{244} + Be source with a neutron yield of $(1.8 \pm 0.1) \cdot 10^{9}$ neutrons/sec for an angle of 4π. The active part of the source was prepared in the form of a mixture of oxides of Cm^{244} with powdered metallic beryllium. This mixture was hermetically sealed in a double ampoule made of stainless steel. The outer ampoule was 35 mm in diameter and 60 mm high, and the active part was 25 mm in diameter and 25 mm high. In sealing the source, we took into account the possibility of pressure increases in the inner ampoule as a result of gas generation (mainly He) during the α-disintegration and spontaneous fission of Cm^{244} nuclei.

The energy spectrum of the neutrons of the source described above is shown in Fig. 1. The spectrum was measured by means of a single-crystal scintillation-type fast-neutron spectrometer with discrimination of the γ-background based on the shape of the pulse. The spectrometer was constructed with a stilbene crystal 10 mm high and 10 mm in diameter. The amplitude distributions were recorded on a 512 channel LP-4050 analyzer.

The average neutron energy, calculated on the basis of the measured spectrum, was 3.6 MeV. A comparison of the data of Fig. 1 with the corresponding spectra of (α, n) sources made with Po^{210}, Pu^{238}, Pu^{239}, Am^{241}, and other elements shows that for the Cm^{244} + Be source under study the neutron spectrum is much "softer" than for the above-mentioned sources or for a Cm^{244} + Be source with a yield of $6.5 \cdot 10^{6}$ neutrons/sec [1, 4]. The most important factors causing the reduction in the average neutron energy and the increase in the fraction of neutrons in the low-energy part of the spectrum are the dimensions of the source and the higher energy of the Cm^{244} α-particles in comparison with those of other isotopes generally used for making (α, n) sources.

LITERATURE CITED

1. N. D. Tyufyakov et al., in: Radiation Technology [in Russian], Atomizdat, Moscow (1970), p. 90.
2. D. Stewart et al., Nucl. Appl. Techn., 9, 875 (1970).
3. V. M. Gorbachev et al., Basic Characteristics of Isotopes of Heavy Elements [in Russian], Atomizdat, Moscow (1970).
4. N. D. Tyufyakov et al., in: Applied Nuclear Spectroscopy [in Russian], No. 1, Atomizdat, Moscow (1970), p. 16.

SCINTILLATION COUNTERS WITH ELONGATED CRYSTALS

G. F. Novikov, A. Ya. Sinitsyn,
Yu. O. Kozynda, and V. V. Vyshenkov

UDC 539.1.074.3

Scintillation counters having NaI(Tl) and CsI(Tl) crystals are widely used in prospecting, surveying, and exploitation of ore deposits. The present tendency toward reduction of bore and shot holes demands a reduction in the diameter of γ-logging instruments [1] including a reduction in the diameter of the scintillator. To maintain the necessary accuracy in the determination of the γ-spectrum from radioactive elements, the reduction in crystal diameter can be compensated by an increase in its length.

This paper presents instrumental γ-ray spectra from large masses of uranium and thorium for scintillators of varying lengths and gives calculated values for the statistical errors in the determination of uranium and thorium in ores and rocks at the point of occurrence, both of which demonstrate the advantage of elongated crystals in comparison with standard NaI(Tl) and CsI(Tl) crystals having a maximum ratio of length l to diameter d equal to 1.6 [2]. For the experiments we selected NaI(Tl) scintillators 30 mm in diameter and 20-70 mm long with a resolution of 10.2% and CsI(Tl) crystals 30 mm in diameter with lengths of 20, 40, 70, and 140 mm having resolutions of 11.8, 11.6, 12.0, and 13.5% respectively for Cs^{137}. Instrumental spectra of the γ-radiation from uranium and thorium ores were studied under conditions of 4π geometry and saturation for all crystals by means of an AI-100-1 pulse-height analyzer with a window width of 30 keV. The results obtained with the NaI(Tl) scintillators are shown in Fig. 1. The counting rate N was normalized to 0.01% uranium and thorium and to 1 cm^3 of scintillator. In the region of the Compton distribution [3], the N(E) curves for the different crystals practically coincide. In the region of clearly defined maximum photopeaks (E = 2.62 MeV for thorium and 2.19 MeV for uranium), the specific counting rate n_0 rises for elongated scintillators. Thus in a comparison of crystals 70 and 20 mm long, the ratio of the values of n_0 is 1.6; it is about 1.3 for crystals 70 and 40 mm long. This data is in good agreement with calculations of the absorbed fraction of γ-radiation incident on the lateral surface of a cylindrical scintillator at various angles.

Table 1 gives the counting rate per cm^3 of scintillator in the optimum energy window of the γ-spectrometer [4] for separating uranium, thorium, and potassium in the case of CsI(Tl) crystals having different resolutions.

According to this data, the specific counting rates remain practically constant for all crystals studied in spectral regions away from the photopeaks (see Table 1, window I, for uranium and thorium); in the photopeak region (window I for potassium, window II for uranium, and window III for thorium), the counting rate increases markedly as scintillator length increases. This regularity breaks down somewhat in the

TABLE 1. Specific Counting Rate n_0 for CsI(Tl) Scintillators of Various Lengths

Scintillator dimensions				Window I, 1.35-1.55 MeV			Window II, 1.65-1.85 MeV			Window III, 2.50-2.80 MeV			Resolution ω, %
d, mm	l, mm	l/d	volume V, cm^3	U	Th	K	U	Th	K	U	Th	K	
30	20	0,67	14,1	25,4	10,2	0,90	13,4	7,3	0,1	0,9	5,2	—	11,8
30	40	1,33	28,3	25,8	10,7	1,02	14,0	7,7	0,2	1,0	6,1	—	11,6
30	70	2,33	49,5	26,7	10,9	1,26	16,8	8,0	0,1	1,2	7,1	—	12,0
30	140	4,66	99,0	25,3	10,6	1,21	18,0	7,9	0,4	1,5	7,0	—	13,5

Translated from Atomnaya Énergiya, Vol. 32, No. 3, pp. 238-240, March, 1972. Original article submitted April 19, 1971.

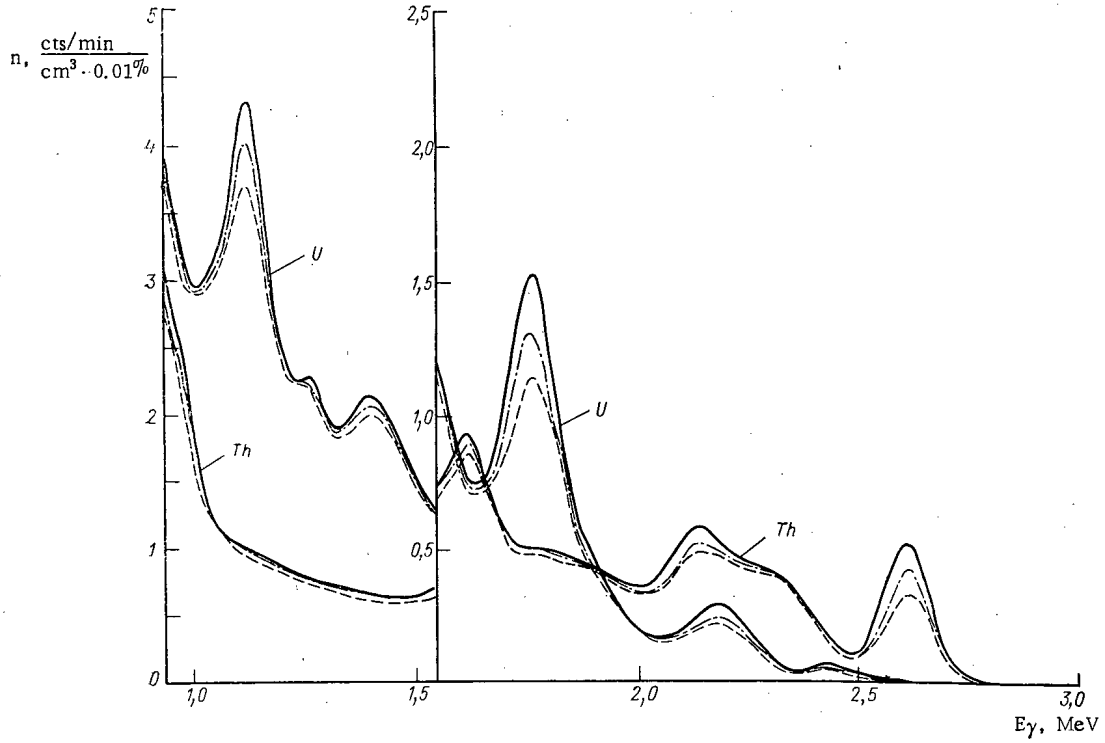

Fig. 1. Instrumental γ-ray spectra from uranium and thorium measured with NaI(Tl) scintillators having the dimensions: ——) 30 × 70 mm; – · – · –) 30 × 40 mm; – – –) 30 × 20 mm (first dimension is diameter). Window width, 30 keV.

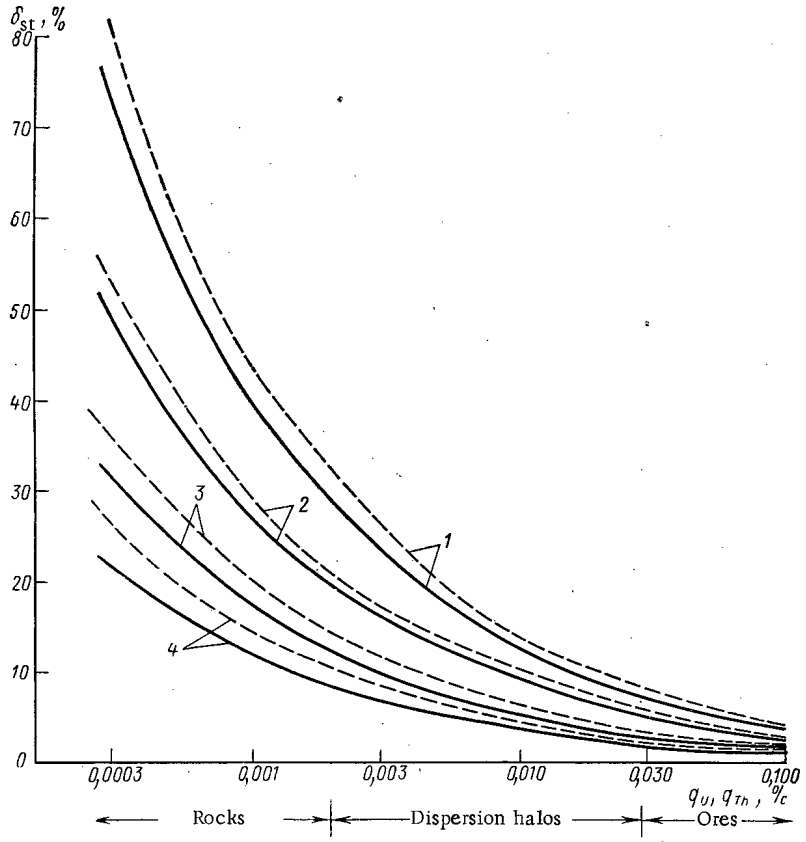

Fig. 2. Statistical error in γ-spectrum determination of uranium and thorium under drilling conditions. Counting time, 1 min. CsI(Tl) scintillators with dimensions: 1) 30 × 20 mm; 2) 30 × 40 mm; 3) 30 × 70 mm; 4) 30 × 140 mm; ——) uranium; – – –) thorium.

comparison of the scintillators 70 and 140 mm in length because of the poorer resolution of the latter crystal.

The specific counting rate n_0 was used for calculating the relative statistical error δ_{st} in the determination of uranium and thorium by the γ-spectrum method in rocks, dispersion halos, and dispersion flows, and in uranium–thorium ores in drilling situations. The scheme for calculating δ_{st} was similar to that used in [5].

The uranium and thorium content was identical in all cases, and the counting time was 1 min.

Values of δ_{st} are shown in Fig. 2. They vary from 1.2-4.4% for logging ore with 0.1% uranium and thorium content to 20-80% during studies of Clark concentrations of those elements. The use of elongated CsI(Tl) crystals 30 mm in diameter and 140 mm long made it possible to reduce the error in determination of uranium and thorium content by factors of 2.2-2.4 in comparison with nearly isometric crystals 30 mm in diameter and 40 mm long and by factors of 3.0-3.2 in comparison with crystals 30 mm in diameter and 20 mm long. In comparison with crystals 30 mm in diameter and 70 mm long, the error decreased by a factor of approximately 1.5.

The slight degradation in scintillator energy resolution resulting from the increase in length to 140 mm (see Table 1) has practically no effect on the accuracy of the determination of radioactive element content.

The experimental material material presented confirms the feasibility of using elongated scintillators with an $1/d$ ratio close to five. This permits more extensive use of γ-logging in small-diameter holes and increases its accuracy and efficiency.

LITERATURE CITED

1. R. M. Kogan, I. M. Nazarov, and Sh. D. Fridman, Fundamentals of Spectrometry of the Environment [in Russian], Atomizdat, Moscow (1969).
2. N. A. Vartanov and P. S. Samoilov, Applied Scintillation Spectrometry [in Russian], Atomizdat, Moscow (1969).
3. V. O. Vyazemskii et al., Scintillation Methods in Radiometry [in Russian], Gosatomizdat, Moscow (1961).
4. P. P. Khitev and A. A. Fedorov, in: Problems in Mining Geophysics [in Russian], No. 7, Nedra, Leningrad (1966), p. 82.
5. G. F. Novikov, A. Ya. Sinitsyn, and Yu. O. Kozynda, Zap. Leningradsk. Gorn. In-ta, 56, No. 2, 98 (1969).

USE OF n – i – p SEMICONDUCTOR DETECTORS FOR MULTICOMPONENT X-RAY ANALYSIS

A. L. Yakubovich, S. M. Przhiyalgovskii, and G. N. Tsameryan

UDC 539.1.074.55

In performing x-ray analysis, scintillation or proportional counters having low energy resolution in the x-ray region of the spectrum are used as detectors of characteristic radiation from excited atoms of the elements being analyzed for. Because of this, it is necessary to use differential filters when performing x-ray analysis of elements with neighboring atomic numbers in order to separate their analytic lines. Furthermore, in the case of multicomponent analysis, it is necessary to carry out a number of successive measurements of radiation intensities in different portions of the spectrum, which leads to considerable increase in analysis time. In addition, the subsequent analysis of the results is rather complex because the difference effect in the measurement with each filter pair is proportional, but not equal, to the intensity of a given analytic line.

A change to n–i–p semiconductor detectors for characteristic radiation [1-3] brings about an improvement in the metric parameters of x-ray analyzing equipment.

In our studies, we used an XS 253/26 Si(Li) detector made by the SAIP company having an area of 25 mm and a sensitive layer depth of 3 mm. The detector and first stage of the preamplifier were cooled to liquid nitrogen temperature, which provided maximum resolution. One can get some idea of the energy resolution and the relative detection efficiency for radiations of various energies from the Am^{241} spectrum shown in Fig. 1. The resolution for the 13.96 keV line is 300 eV; the detection efficiencies at the energies 13.96, 26.4, and 59.6 keV are approximately in the ratio 100 : 52 : 8.

TABLE 1. Line Contrast and Sensitivity Threshold of Certain Elements for Various Sources of Exciting Radiation

Source of exciting radiation and activity	Element determined	Analytic line	Line contrast	Statistical root-mean-square error, %	Threshold sensitivity, $\%\cdot 10^{-3}$
Fe^{55}, 2 Ci	S	K_α	0,53	0,041	39
	Ca	K_α	12,4	0,0016	1,5
	Ti	K_α	21,2	0,001	0,9
Sn^{119m}, 5 mCi	Fe	K_α	1,6	0,027	12
	Zn	K_α	4,3	0,011	4,8
	Mo	K_α	40	0,0008	0,4
	Zr	K_α	36	0,0012	0,5
	Pb	L_β	4,9	0,0085	3,7
	W	L_β	1,8	0,018	8
Am^{241}, 15 mCi	Fe	K_α	3,2	0,0077	4,8
	Zn	K_α	9,4	0,0028	1,7
	Pb	L_α	8,9	0,0037	1,6
Pu^{238}, 20 mCi	Fe	K_α	9,1	0,0066	4
	Zn	K_α	13,5	0,0036	2,2
	Pb	L_α	7,4	0,0067	4,1

Table 1 presents experimental data characterizing the contrast of analytic lines and the statistical error for x-ray analysis of various elements using a Si(Li) detector and excitation of characteristic radiation by various radioisotopic sources. Contrast of analytic lines is defined as the signal-to-background ratio in the portion of the spectrum corresponding to a half-width at the maximum of the pulse height distribution for counts in an analytic line from a sample containing 1% of a given element. The statistical root-mean-square error was calculated for 10 min measurements of the radiation intensity from a sample under study. Sensitivity threshold is defined as three times the value of the statistical root-mean-square error for an integral counting rate of 10^4 counts/sec.

The capability of separate determination of analytic line intensities for characteristic radiation from elements of neighboring atomic number is illustrated in Fig. 2 by a

Translated from Atomnaya Énergiya, Vol. 32, No. 3, pp 241-243, March, 1972. Original article submitted April 13, 1972.

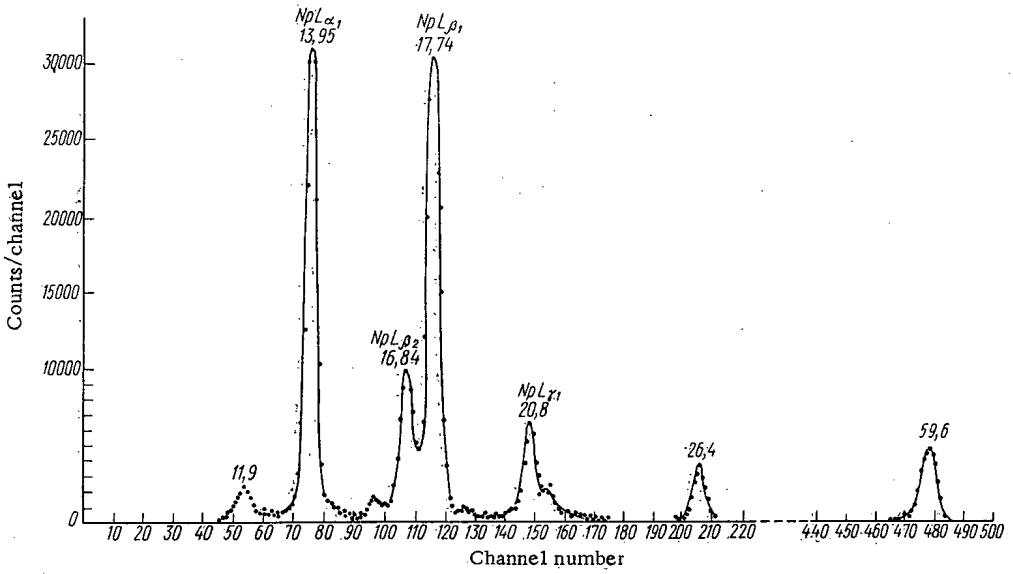

Fig. 1. Am^{241} spectrum.

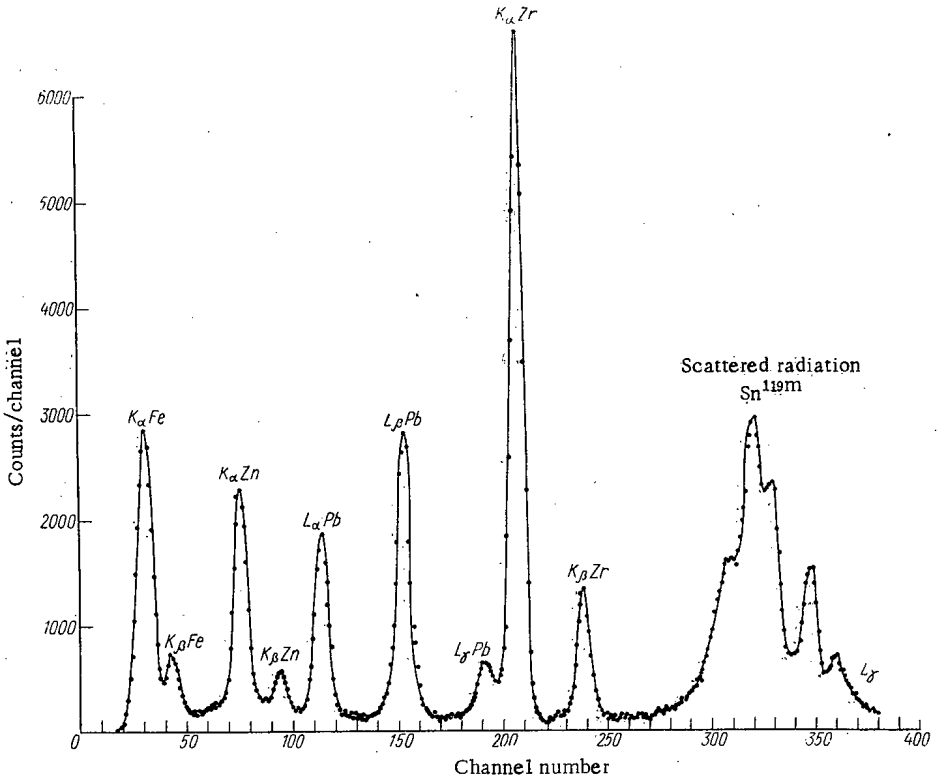

Fig. 2. Spectrum of radiation from a sample containing 10% iron, 3% zinc, 3% lead, and 1% zirconium. Source of exciting radiation was Sn^{119m} (5 mCi); counting time was 10 min.

spectrum of characteristic radiation from a sample containing iron, zinc, lead, and zirconium obtained by irradiation of the sample by a Sn^{119m} source.

The experimental results obtained from testing a Si(Li) detector indicate great promise for its use in x-ray analysis of elements with characteristic radiation energies in the range 2.5-30 keV. The significant degradation in sensitivity for analysis of light elements (with $Z < 15$) results from the strong absorption of soft x-rays by the beryllium of the cryostat window. Analysis by means of the K-series x-rays in heavy elements (with $Z > 55$) is limited by the low detection efficiency for radiation with energies above 30-40 keV.

The use of Ge detectors, which are characterized by better detection efficiency for hard x radiation [4], is more promising for the analysis of heavy elements by means of K-series x-rays.

Because of the clear separation of characteristic radiation lines of elements which are close in energy when a semiconductor detector is used, one can perform multicomponent x-ray analysis without using differential filters. Simultaneous determination of the intensities of several analytic lines in the characteristic radiation from elements in a sample makes possible not only an increase in the speed of measurement, but also an easier development of general methods for considering the mutual effects of elements on the results of x-ray analysis. Recording the complete spectrum of characteristic radiation from all the basic elements in a sample under study, with subsequent analysis of the spectrum on a computer, permits an accurate accounting and elimination of matrix effects on analytical results, which is an important step in the development of x-ray analytic methods.

LITERATURE CITED

1. N. Bowman, Science, 151, No. 3710, 562 (1966).
2. S. A. Baldin et al., Trudy SNIIP, No. 4, Atomizdat, Moscow (1967), p. 12.
3. S. A. Baldin et al., Prib. i Tekh. Éksperim., No. 5, 198 (1970).
4. D. A. Goganov et al., Abstracts of Reports at IXth Conference on X-Ray Spectroscopy [in Russian], Ivanovo-Frankovsk (1971).

EXPERIMENTAL INVESTIGATION OF INFLUENCE OF ELECTRON DYNAMICS ON POLARIZATION PROPERTIES OF SYNCHROTRON RADIATION

V. G. Bagrov and M. M. Nikitin

UDC 621.384.612

At the present time there is pressing need for a detailed investigation of the various characteristics of the synchrotron radiation of relativistic electrons in view of the increasing use to which this radiation is being put in spectroscopy [1, 2]. There is also considerable interest in astrophysical aspects of synchrotron radiation [3]. While the theory of the polarization properties of synchrotron radiation has received a fair amount of attention [4], it must be said that there is a dearth of experimental papers on this subject [5, 6]. The experimental results on the linear polarization of synchrotron radiation given in these papers are somewhat at variance with theory, mainly as regards the inequality of the maxima in the angular distribution of the π-polarization component intensity and the associated asymmetry of the angular distribution of the σ-component intensity. It would appear that such distortions can be ascribed to the dynamics of the motion of the electrons and of the cluster as a whole.

Using the 1.5 GeV electron synchrotron of the Tomsk Polytechnic Institute we have investigated in the vertical plane the angular distribution of the π-component intensity of the radiation from electrons performing vertical betatron oscillations of specific amplitude. In the experiment the light radiation producing the image of the electron beam was selected by means of a diaphragm with a point aperture and the diaphragm moved over the cross section of the image. The mean-square cross-sectional dimensions of the image for a beam energy of 800 MeV were: 60 mm radially, 30 mm vertically. The diaphragm aperture was 2×2 mm. The plane of the light image of the electron beam was found to within ± 30 mm. A polarizer selected the π-component of the radiation. The angular distribution of this component was measured directly on an oscilloscope by means of a mechanical scanning technique with photoelectric conversion. The observations were carried out at 5460 Å and at various energies of the accelerated electrons up to 1 GeV. The variation of the illumination at different points across the image due to the Gaussian distribution of the amplitudes of the vertical oscillations of the electrons was corrected for by means of neutral filters. The results of the experiments reduce to the following.

It was found that when the optical axis of the recording system coincided with the axis of the radiation cone, then the maxima in the angular distribution of the π-component intensity are equal. However, as soon as the axis of the radiation cone deviates from the optical axis of the recording system by some angle less than the spread of the radiation cone, a difference in the sizes of the maxima becomes discernable. The sign of the difference depends on the sign of the angle of incidence of the radiation cone.

Figure 1 shows oscillograms of the angular distribution of the π-component intensity in the vertical plane for a beam energy of 800 MeV; b corresponds to radiation from electrons at the center of the beam and *a*, c to radiation from electrons at the top and bottom edges of the beam (at equal distances from the center). The beam electrons are symmetrically distributed in the vertical plane. The angle θ is measured in the opposite direction from the oscilloscope time sweep (0.2 msec/cm) and is reckoned from the direction of the synchrotron magnetic field. The maximum intensity corresponding to $\theta > \pi/2$ (above the orbit plane) we denote by π'; the maximum intensity corresponding to $\theta < \pi/2$ (below the orbit plane) we denote by π''.

In the orbit plane $\pi' = \pi''$ (see Fig. 1b), whereas above the orbit plane $\pi' > \pi''$ (Fig. 1a) and below the orbit plane $\pi' < \pi''$ (Fig. 1c). The relative difference between the maxima varies in the manner shown in Fig. 2. The z axis here is antiparallel to the synchrotron magnetic field.

Translated from Atomnaya Énergiya, Vol. 32, No. 3, pp. 243-244, March, 1972. Original article submitted April 9, 1971.

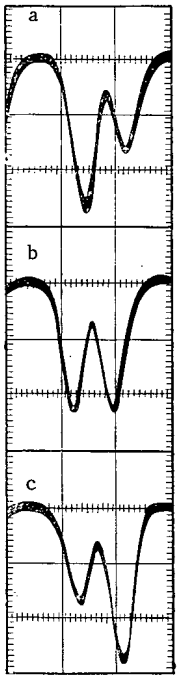

Fig. 1

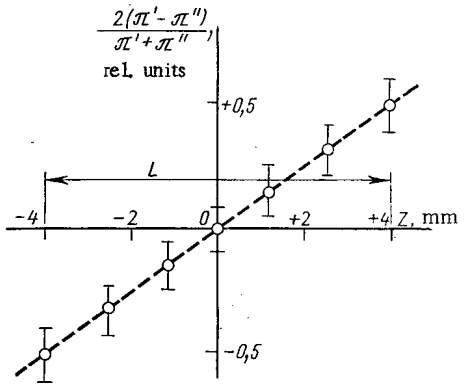

Fig. 2

Fig. 1. Oscillograms of vertical angular distributions of π-component of synchrotron radiation from electrons at different positions in the beam in the vertical plane.

Fig. 2. Relative variation vertically across the beam of the difference between the maxima of the π-component distribution (L is the mean-square vertical dimension of the beam).

The intensity at the minimum of the π-component distribution does not fall to zero over the cross section of the beam as a result of the significant amplitude of the vertical betatron oscillations of the electrons. No distortion of the π-component intensity distribution was observed when the point diaphragm was moved across the image of the beam in the radial direction ($\pi' = \pi''$).

Our experimental results thus completely confirm the theoretical position [4].

The assistance of A. A. Vorob'ev, A. N. Didenko, and A. V. Kozhevnikov is gratefully acknowledged.

LITERATURE CITED

1. R. Haensel and C. Kunz, Z. Angew. Phys., 23, 276 (1967).
2. R. Godvin, Usp. Fiz. Nauk, 101, 493, 697 (1970).
3. I. S. Shpol'skii, Dokl. Akad. Nauk SSSR, 90, 983 (1953).
4. A. A. Sokolov and I. M. Ternov (editors), Synchrotron Radiation [in Russian], Izd. Nauka, Moscow (1966).
5. F. A. Korolev, O. F. Kulikov, and A. S. Yarov, Zh. Éksperim. Teor. Fiz., 43, 1953 (1962).
6. A. A. Vorob'ev, M. M. Nikitin, and A. V. Kozhevnikov, At. Énerg., 29, 389 (1970).

FORMATION OF BEAMS OF POSITIVE PARTICLES WITH 25-70 GeV/c MOMENTUM FROM INTERNAL TARGETS OF IFVÉ ACCELERATOR

N. I. Golovnya, M. I. Grachev,
K. I. Gubrienko, E. V. Eremenko,
V. N. Zapol'skii, V. I. Kotov,
Yu. D. Prokoshkin, V. S. Seleznev,
and Yu. S. Khodyrev

UDC 539.1.074

Physical investigations on the accelerator of the IFVÉ (Institute of High-Energy Physics) have been so far conducted on beams of negative particles extracted from the accelerator at small angles [1]. Important results have been obtained from the experiments on these beams: it is found that the total cross sections for negative mesons are constant at high energies, anti-helium 3 has been detected, etc. However, in order to have a wider program of investigations, in particular, for the study of interaction of particles and antiparticles at high energies, it is necessary to conduct experiments also on beams of positive particles.

The extraction of positive particles from the accelerator, formed at small angles θ, is difficult due to the opposite action of the scattered field of the accelerator, especially if we attempt to form beams of particles traveling in the same direction in a wide momentum range [2, 3]. Below we describe the extraction of positive particles from the inner targets of the accelerator of the IFVÉ, carried out at the end of

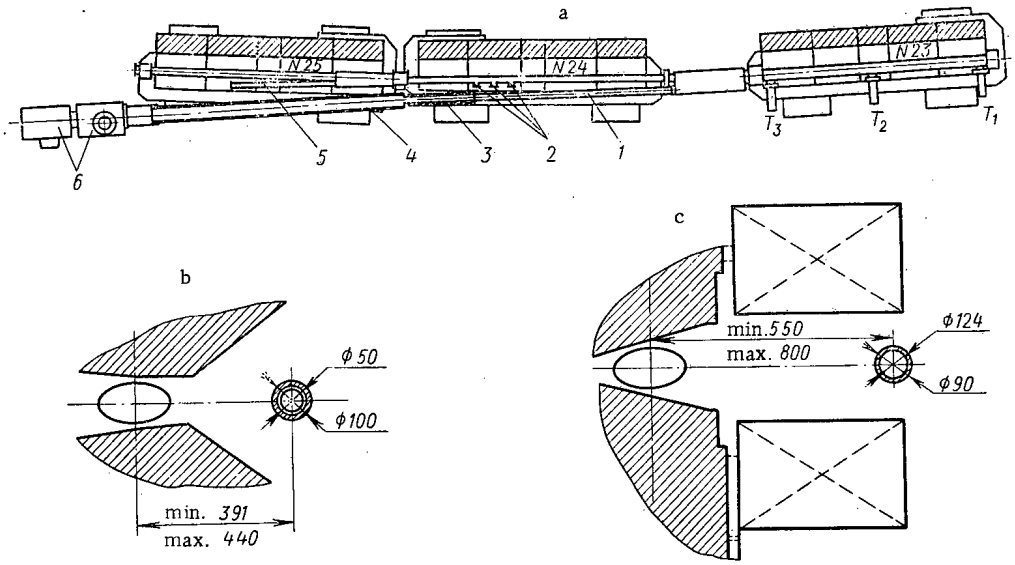

Fig. 1. Schematic diagram of the arrangement of the targets and the extraction segment of the channel of secondary positive particles (a) and sketches of the arrangement of magnetic screens 3 and 4 (b and c respectively): T_1-T_3) targets; 1) ion duct; 2) position of the targets; 5) extraction segment of the channel for negative particles; 6) aperture collimators.

Translated from Atomnaya Énergiya, Vol. 32, No. 3, pp. 244-247, March, 1972. Original article submitted July 22, 1971.

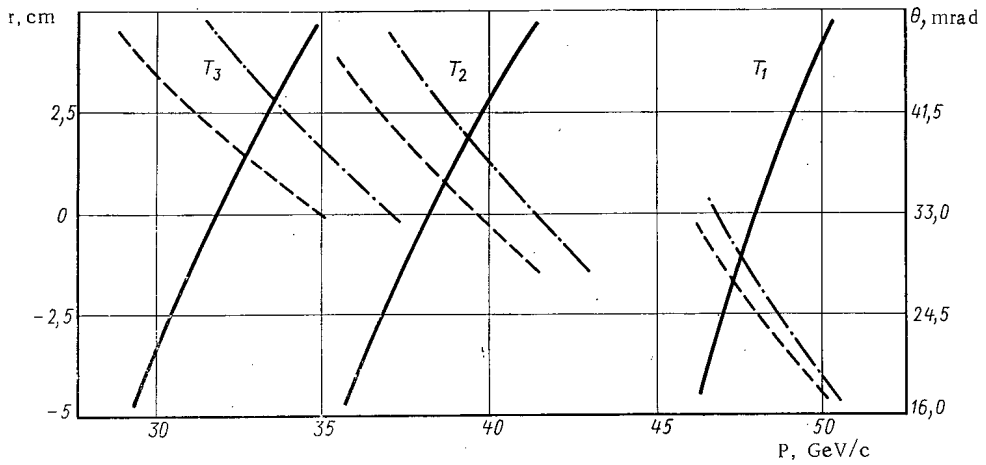

Fig. 2. Dependence of the radial position r of the targets T_1-T_3 (continuous curves) and angles of formation of positive particles θ on the momentum P with magnetic screens (– – –) and without them (– · – · –).

TABLE 1. Computational Characteristics of Beams of Positive Particles

Target	P, GeV/c	r, mm	θ, mrad	Δω, μsr	X_0, mm
T_1	70	+50	5,8	0,5	−58,30
	60	+50	10,4	2,0	−31,6
	55	+50	13,2	3,3	−17,1
	50	+50	16,4	3,4	1,5
	50*	+41,6	17,5	3,5	0
	45	−30	30,7	3,4	8,0
T_2	45	+50	25,6	4,7	−11,3
	40	+50	28,7	4,8	5,7
	40*	+27,8	31,4	5,5	0
T_3	40	+50	30,5	5,8	−17,3
	35	+50	32,5	9,4	0,21
	30	+50	34,9	10,0	23,4
	30*	−32,5	44,0	11,5	0
	25	−40	48,4	9,0	24,6

Note: X_0 is the displacement of imaginary sources from the axis of the channel in the horizontal plane.

1970. Due to the use of magnetic screens and a system of three targets it was possible to form in a single magneto-optical channel beams of positive particles (protons, π^+-mesons, K^+-mesons, and deutrons) in a wide range of momentums P = 25-70 GeV/c at a fixed energy of the accelerated protons E_0 = 70 GeV.

The extraction was done at an angle θ chosen such that the transverse momentum of the particles of the beam $P_\perp = P\theta$ does not exceed a value ~1 GeV/c. The intensity of the beam, which is proportional to $\exp(-aP_\perp^2)$ [4], where $a \approx 5$ $(\text{GeV/c})^{-2}$, even though it decreases by 1-2 orders of magnitude in comparison with the extraction at angles $\theta \approx 0$, remains sufficiently large ($\gtrsim 10^5$ particles/cycle) for conducting physical experiments.

The segment of extraction and the arrangement of the targets and magnetic screens are shown in Fig. 1 schematically. The mutual position of the screens in reference to the equilibrium orbits and their transverse sections are shown there. The screens were made of St. 3 and attenuate the magnetic field of the accelerator by factors of 50 (screen 3) and 5 (screen 4). The geometry of the arrangement of the screens was so chosen that, on one hand, the magnetic field of the accelerator is not perturbed noticeably in the vicinity of the equilibrium orbit and, on the other, a direction of extraction of positive particles close to the direction 5 of the beam of negative particles with momentum up to 65 GeV/c is ensured [1, 5]. It was found possible to use the corresponding channel [15] with small displacement (within 25 cm) of only the aperture collimators 6 and the first objective of the quadrupole lenses for the formation of beams of positive particles.

For the above-mentioned conditions of extraction the angles of formation of positive particles θ are minimum if the targets are placed in the magnetic block 23 (see Fig. 1). Due to the screening of the scattered field the angles of formation of the particles are noticeably reduced, especially for particles with small momentum.

The dependence of the radial position of the targets r and the angles of formation of positive particles θ on the momentum is shown in Fig. 2 for three targets placed in block 23 with and without magnetic screens. It is evident from this figure that the angles of formation of particles with momentum 40 GeV/c decrease by 7 mrad on introducing the screens. This change in the angle θ results in a decrease of $P_\perp^2$ by 0.5 (GeV/c) and correspondingly to an increase of the intensity of the beam of secondary particles by an order of

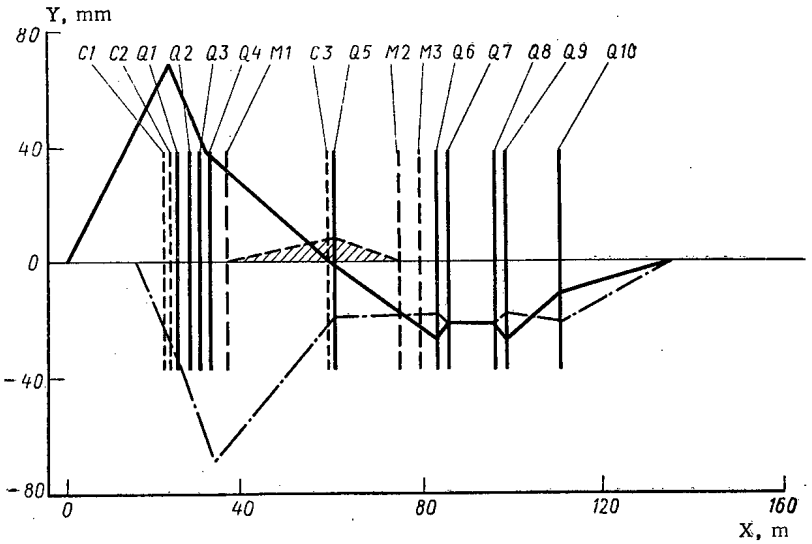

Fig. 3. Optical scheme of the channel of secondary positive particles: C) collimators; M) deflecting magnets; Q) quadrupole lenses. The edge trajectories are shown in the horizontal (– – –), and vertical (– · – · –) planes; the behavior of dispersion is given for $\Delta P/P_0 = +1\%$ (shaded). X) Coordinate along the axis of the beam; Y) coordinate in the plane perpendicular to the beam axis.

TABLE 2. Basic Characteristics of Beams of Secondary Positive Particles (E_0 = 70 GeV)

P, GeV /c	Intensity of beam, 10^5 particles /cycle*	Relative content of particles in the beam (referred to the target), %			
		p	π^+	K^+	d
25	0,5	64	28	8	—
40	1	87	10	3	0,05
50	3	96	3	1	0,03
70	1	100	< 0,01	< 0,01	< 0,001

*For $\Delta P/P = \pm 1\%$ and intensity of accelerated proton beam equal to 10^{12} protons/cycle.

magnitude. The use of magnetic screens permits the extension of the momentum range of the extracted particles toward smaller momentums and to obtain in this range beams of positive particles with intensities sufficient for setting up physical experiments.

The range of momentum of the extracted particles, indicated in Fig. 2, can be enlarged further forming "oblique" beams, whose direction of extraction coincides with the optical axis of the channel. In this case by a variation of the currents in the deflecting magnets the displacement of the beam axis can be eliminated at the location of the experimental equipment. The main computational characteristics of oblique beams formed in the channel are given in Table 1. The parameters of "straight" beams with momentums 30, 40, and 50 GeV/c (indicated by asterisks) are also given there for comparison. It follows from Table 1 and Fig. 2, in operation with oblique beams the momentum range of the extracted particles is appreciably extended toward higher momentums.

The optical scheme of the channel, forming the beam of positive particles extracted from the accelerator, is shown in Fig. 3. The computed solid angles $\Delta\Omega$ of capture of particles in the channel are given in Table 1 for the entire momentum range 25-70 GeV/c. These angles vary in the range 0.5-11 μsr. The dispersion of the beam in the momentum collimator S3 with the dispersion in the magnetic field of the accelerator taken into consideration is 8.2 mm for $\Delta P/P = 1\%$, where ΔP is the momentum spread of the particles with reference to the central momentum P. Considering the linear increase coefficient along the horizontal in the magnetic field of the accelerator (0.16-0.26) and the first objective of the lenses (2.14), we find that the above value of the dispersion ensures reliable extraction of the momentum range $\Delta P/P \gtrsim 1\%$ required for experiments.

The angular divergence of the beam of particles in the parallel segment between the doublets Q6, Q7 and Q8, Q9 does not exceed ±0.5 mrad. This permits an effective use of Cherenkov counters with high resolution [6] for the separation of protons, π^+-mesons, K^+-mesons, and deutrons in the beam. The dimensions of the beams, focussed at the target of the experimental equipment, comprise 1.5 and 1.2 cm^2 in the horizontal and vertical planes respectively.

The relative yields of positive particles, measured with Chernekov counters [7], and the intensities of the beams are shown in Table 2. A characteristic feature of the realized regime of extraction of beams of positive particles is the high relative content of K^+-mesons compared to the extraction at angles $\theta \approx 0°$. For P = 70 GeV/c and E_0 = 70 GeV a pure beam of elastically scattered protons is extracted, in which the impurity of extraneous particles does not exceed 10^{-4}.

The production of beams of positive particles of high energy has enlarged the possibilities of conducting experimental investigations on the accelerator of the IFVÉ significantly. After the initiation measurements of the total cross sections of interaction of protons, π^+-mesons, and K^+-mesons with protons and nuclei have been made on this accelerator and the yields of positive particles have been investigated [7].

In conclusion we take this opportunity to thank S. P. Denisov for helpful discussions and help in tuning the channel, V. S. Kuznetsov for carrying out the magnetic measurements of the fields in the screens, and K. P. Myznikov, V. G. Rogozinskii, N. M. Tarakanov, and B. N. Teterkinfor help in the development and construction of the extraction segment.

LITERATURE CITED

1. K. I. Gubrienko et al., International Conference on High Energy Accelerators [in Russian], Vol. 1, Izd. AN ArmSSR, Erevan (1970), p. 471.
2. Yu. M. Sapunov and A. M. Frolov, Preprint, IFVÉ, 68-69, Serpukhov (1969).
3. K. P. Myznikov et al., Preprint IFVÉ, 68-56-K, Serpukhov (1968).
4. Yu. M. Antipov et al., Preprint, IFVÉ, 70-38, Serpukhov (1970); Yadernaya Fizika, 13, 135 (1971).
5. I. A. Aleksandrov et al., Atomnaya Énergiya, 29, 29 (1970).
6. Yu. P. Gorin et al., Preprint, IFVÉ, 70-48, Serpukhov (1970).
7. Yu. P. Gorin et al., Preprint, IFVÉ, 71-30, Serpukhov (1971).

INFORMATION

EXHIBITIONS

N. Longinova

SOVIET EXHIBITION AT IVTH GENEVA CONFERENCE ON PEACEFUL USE OF ATOMIC ENERGY

The Soviet section of the exhibition occupied an area of 1850 m^2. The exhibits served as a vivid illustration of the standard materials of the IVth Geneva conference and reflected the achievements of the Soviet scientists and engineers in the development of atomic science and engineering. In cinema halls at 70 places 14 new scientific–technical films were shown Books on the atomic theme, published in the Soviet Union in recent years, were also exhibited.

The exhibits and the very appearance of the exhibition were in complete conformity with the motto of the conference, "Atom in the service of progress."

A large section of the exhibition was devoted to the development of nuclear power in the Soviet Union. Models of reactors and atomic power plants constructed and operated in the Soviet Union were shown. Frame type reactors were represented by the model of the reactor and the diphrame Kol'sk atomic power plant (electrical power of one block 440 MW). The model of the reactor of the Beloyarsk atomic power plant with the "see-through" model of the station gave an idea of construction of the channel reactors with nuclear superheating of steam. The model of the reactor and the see-through model of the Leningrad APP showed channel reactors with 1000 MW (elec.) and higher power. Fast reactors were represented by the models of BOR-60 reactors with thermal power of 60 MW and APP with reactor BN-350 (in Shevchenko) with equivalent power of 350 MW (elec.), operating in a block with distilling equipment.

Natural heat-releasing assemblies of research and power reactors were also shown at the exhibition; in particular, the evaporative and steam superheater channels of the second block of Beloyarsk APP, heat releasing assembly of Leningrad APP, the cassette of the second block of Novo-Voronezhsk APP, and also several cassettes of fast reactors were shown.

In the section on the technology of the processing of nuclear fuel an operating industrial pneumatic pulsator and a laboratory multichamber extractor of the type of mixing–settling tank were exhibited; an operating pulsation pump was also demonstrated.

The achievements of the Soviet Union in the field of thermonuclear research were represented along three main directions of the thermonuclear program: 1) closed magnetic traps of the type of "Tokamak" and "Stellarator"; 2) open magnetic traps of the PR type, "Orga" and LIN; 3) devices of the type of "Plasma focus." The first direction was represented by the model of the newest in the series "Tokamak-6." This equipment differs from the previous ones in the absence of the diaphragm restricting the diameter of the plasma filament, and the arrangement of the stabilizing copper sheath. Investigations for the verification of theoretical conclusions are carried out on "Tokamak-6."

The model of the LIN-5 installation acquainted the visitors with the design and the principle of operation of the open traps. LIN-5 differs from "Orga" or PR-6 in the presence of superconducting windings. The filling of the magnetic trap by plasma is accomplished by the injection of a beam of neutral atoms with an equivalent current of 0.5 A.

The third direction was represented by the operating experimental equipment "Belka." In this equipment the plasma is produced by the discharge of a condensor battery between two electrodes of especial

Translated from Atomnaya Énergiya, Vol. 32, No. 3, pp. 249-251, March, 1972.

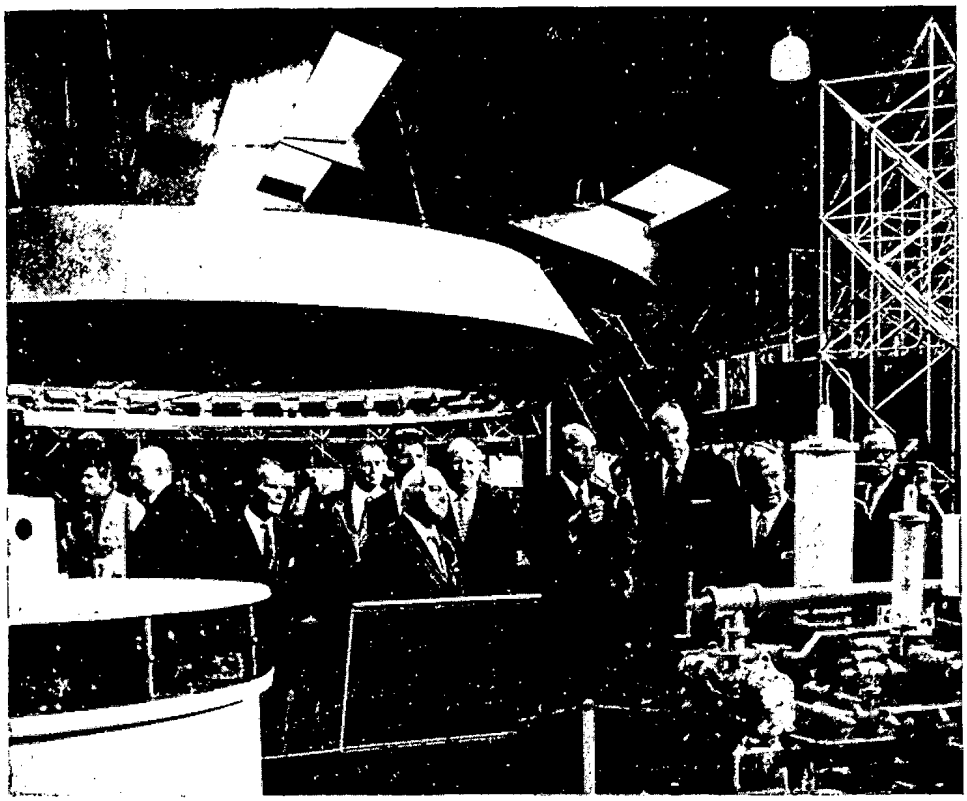

Fig. 1

form in deuterium gas. The discharge proceeds in such a way that the plasma is constricted to a small volume of 0.1 cm^3 (plasma focus). The density and the temperature of the plasma attain very high values in the plasma, which leads to thermonuclear reactions and the formation of neutrons. In "Belka" the plasma could be observed through special windows.

Significant advances in the field of high-current pulse technology and in the technology of high-intensity pulsed magnetic fields have been made in the Soviet Union. An operating pulsed-magnetic equipment MIS-5 was shown in the exhibition; this equipment is intended for hermetic sealing of the casings of fuel elements. To obtain the hermetic sealing the end of the casing is introduced into a single-turn solenoid, in which a strong pulsed magnetic field is excited. A radial compression of the end of the tube occurs under the action of the magnetic pressure, which leads to the formation of a monolithic bar. This process proceeds without melting of the metal and there is no welding seam. This ensures a 100% guarantee of hermetic sealing of the fuel element.

The radiation technology was represented at the exhibition by five main directions: 1) radioisotope power; 2) high-power radiation equipment; 3) apparatus for elementary analysis of the composition of matter; 4) fault detection; 5) therapeutic apparatus. Generators of type "Beta-C" and "Pinguine," operating with Sr^{90}, and also generators of thermal energy operating with Po^{210} installed in the automatic lunar laboratory "Lunokhod-1," were also shown at the exhibition.

Among the radiation processes, leading to the refinement of the existing technology, are the radiation sulfochlorination of paraffin hydrocarbons, accomplished in the USSR on industrial scale since 1966. A model of sulfochlorinator of type ZRS-10, shown at the exhibition, is free from the disadvantages inherent to existing photochemical sulfochlorinators. The output of the radiation sulfochlorinator ZRS-10 is about 20 times higher than that of the photochemical sulfochlorinator.

Models of different irradiating equipment of research and industrial types ("Researcher," UGU-200, and others), a model of the laboratory of activation analysis based on the pulsed homogeneous reactor of IIN, and a compact neutron generator NG-150I with a capacity of $2 \cdot 10^{11}$ neutrons/sec were also exhibited.

Methods of optimization of irradiation processes are widely used in ray therapy. A model of the apparatus "Agat-V," intended for the irradiation of malignant growths and localized and natural cavities in the human body, was also shown.

Different instruments for dosimetry, determination of content of substances, and spectrometry were demonstrated in the section of nuclear instrument manufacture. Along with the instruments ensuring detection (scintillation and semiconductor), intensification, formation and recording of nuclear particles, a spectrometer of x- and γ-rays "Langur" was exhibited; this spectrometer is intended for operation in the energy range from a few kiloelectron-volts to a few megaelectron-volts; momentum analyzers of type AIMA-10^6-M and AM-256-6 were also shown. The million-channel AIMA-10^6-M analyzer facilitates measurement of energy distribution represented in the form of pulse amplitudes, time integrals, and sensor coordinates. Furthermore, with the use of the analyzer it is possible to carry out preliminary analysis of the obtained data, which may be observed visually or routed to external equipment.

Models of accelerators, intended for scientific research and use in national economy [for example, the model of the 70 GeV proton synchrotron of the Institute of High Energy Physics (Serpukhov) and the model of collective accelerator of charged particles] were exhibited. Models of the linear electron accelerator LUÉ-15-10, intended for accomplishing radiation-chemical processes with the use of a beam of accelerated electrons, and linear electron oscillators LUÉ-8-5, used for the sterilization of medical equipment and blood transfusion systems on the assembly line of industrial undertakings, were demonstrated.

Along with the papers of the Soviet scientists, presented at the conference, the exhibition reflected the achievement of the Soviet Union in the field of peaceful use of atomic energy.

SOVIET SECTION IN THE INTERNATIONAL EXHIBITION "ELECTRO-72"

An specialized international exhibition "Electro-72" will be held in Moscow, July, 1972.

Many firms and societies from GDR, Czechoslovakia, Hungary, France, USA, Italy, Sweden, Great Britain, Austria, Denmark, Holland, Belgium, Japan, FGR, and other countries will exhibit modern electrotechnical equipment and apparatus for the production, transmission, and use of electrical power.

The aim of the exhibition is a demonstration of the latest achievements in the field of electrical power engineering, an exchange of scientific-technical experience in utilizing the achievements in construction, production, and operation of modern means of electrical power, and also the collaboration of the representatives of Soviet and foreign business circles in establishing contacts and enlarging mutual trade relations.

The Soviet Union will present the largest and the most diverse exposition. Here one will be able to see unique power blocks for power plants, powerful power transformers, reliable electrical traction equipment, progressive transformer technology, low-volt apparatus, minaturized batteries, and diverse electrical devices and machines of everyday use, and also complexes of equipment for thermal, hydraulic, and atomic power plants, including turbogenerators of 300, 500, 800 thousand kW, the pilot plant of a unique turbogenerator of original construction with 1200 MW power, and complex generator equipment. Simple and highly economical capsule-type hydroelectric generators, supply sources of all classes and denominations, and equipment for control and safety of atomic power plants will be shown at the exhibition

In the Soviet section of the exhibition 212 enterprises, 38 scientific-research institutes, over 12 ministries, and departments from 14 union republics will present their exhibits. In all about five thousand exhibits will be shown.

The visitors and the guests at the exhibition "Electro-72" will get a complete idea of the achievements of native and world electrical power industries.

CONFERENCES AND MEETINGS

A. N. Novikov, Ya. D. Zel'venskii,
S. G. Katal'nikov, V. P. Dmitrievskii,
V. P. Sarantsev, A. V. Trofimov,
G. Saksaganskii, and V. I. Vikhrov

MEETING OF IAEA ON PHYSICAL PROBLEMS OF FUEL DEPLETION IN NUCLEAR REACTORS

A meeting of IAEA experts was held in Vienna from July 12-16, 1971 to discuss physical problems of fuel depletion in nuclear reactors. Its main objective was to discuss the changes in the technique of investigations of depletion since the last meeting (April, 1967) and to make recommendations to the IAEA on the directions of future developments of such investigations. In the meeting attention was mainly devoted to the following problems: nuclear data necessary for investigations; methods of computation of local depletion; homogeneous and heterogeneous methods of overall computation of reactors; effect of contamination and depletion on physical characteristics of reactors; experimental investigations.

Thirty-six representatives from 16 countries and three international organizations participated in the meeting. R. L. Crouter (USA) conducted the meeting; H. Gonzales-Montes and B. Kolbasov were the scientific secretaries. Twenty-four papers were presented.

A comprehensive review of improved nuclear data for the computation of thermal neutron reactors was given by H. D. Lemmel of IAEA. The review contained information on the thermal cross sections of uranium and plutonium isotopes, resonance integrals of plutonium isotopes, characteristics of delayed neutrons formed during the fission of plutonium, and thermal cross sections and resonance integrals of the main fission products.

Currently used methods of computation of the depletion of fuel element and the accuracy of the obtained results were discussed in a communication by J. Tairer (Great Britain) taking the use of WIMS program as an example. Along with the usual method of separation of problems into computation of local depletion and of the computation of the reactor as a whole, the so-called "global" method is being used extensively; in this method the change of the isotope composition of the fuel of each fuel element is taken into consideration in the computation of the reactor as a whole. According to the communication by R. L. Crouter few-group microscopic cross sections of the isotopes, needed for this method of computation, are determined from the results of many-group transport computations done parametrically.

The use of modern computer technology has led to a noticeable progress in detailization of the computations, especially in space–energy description of the spectra of neutrons and preparation of effective cross sections. This improves the possibility of developing universal sets of computational programs suitable for the analysis of depletion in reactors of different types. An example of the studies on the development of such programs was presented in the communication by B. Michelson (Denmark).

In problems of local depletion in a majority of cases neutron spectra are computed from detailed models using the technique of collision probabilities. Some possibilities of speeding-up and refining the computation of spectra were mentioned in the communication by I. Pop-Iordanov (Yugoslavia).

Few-group (up to seven groups) diffusion finite difference approximations ("homogeneous" technique of computation) are mainly used for the computation of a reactor. The two- and three-dimensional programs

Translated from Atomnaya Énergiya, Vol. 32, No. 3, pp. 251-259, March, 1972.

used in this case permit consideration of up to 100,000 units. In using two-dimensional programs the third measurement is taken into consideration by the synthesis method.

The heterogeneous technique of Fainberg–Galinin is used for the computation of heavy-water and graphite–gas reactors. An example of the use of this technique for the solution of the three-dimensional problem of computation of a heavy-water reactor was given in the communication by R. Solanill (Argentina).

In the analysis of transitional processes it is advisable to use high-operational programs with relatively widely spaced grids. It follows from the communication by H. Mërkl (FRG) that for widely spaced grids the technique of collision probabilities can be used effectively in place of the finite-difference models. Ways of solving the problem of optimization of rearrangement of the fuel and the displacement of the control units in boiling-water reactors were discussed in the report by R. L. Crouter.

Several communications were devoted to the procedure of computation of specific types of reactors. The depletion of fuel in water–water power reactors was discussed in three reports; in one of them the depletion characteristics of VVÉR-3 reactor of the second block of Novo-Voronezhskii atomic power plant were given. Problems in the physical computation of heavy-water reactors were discussed in three papers. The results of three-dimensional computations of a reactor with spherical fuel elements were given in the report by E. Tushe (FRG). An interesting communication on the physics of fuel depletion in the high-temperature reactor "Dragon" was presented by S. Hunt, the representative of the European Atomic Energy Agency.

The results of experimental investigations of isotope composition of irradiated fuel were presented in several reports (J. Griffiths (Canada), B. Laponche (France), etc.). J. Griffiths and B. Laponshe demonstrated the possibility of using the results of these investigations for corrections used in the computation of cross sections.

An interesting description of the experimental studies on fuel depletion of heavy-water reactor "Agest" was given by E. Johanson (Sweden). Contemporary methods of experimental investigations of depletion and isotope composition of irradiated fuel were discussed in the communication by A. Fudge (Great Britain). The peculiarities of experimental investigations of fuel depletion in fast neutron reactors were discussed in the report by M. Robin (France).

It was noted during the discussions that it would be advisable to improve nuclear data required for computations: energy evolved in fission of different isotopes, yield and cross sections of characteristic fission products, and also cross sections of Pu^{242}, Am^{241}, Am^{243}, Cm^{242}, Cm^{244}, Pu^{238}, etc. The meeting recommended that IAEA acquire some grams of plutonium standards required for isotope dilution.

The advisability of formulation of a model problem of depletion for comparison and refinement of the programs and cross sections used in computations was also noted. The meeting recommended that this problem be formulated in 1972, so that the results of its solution could be discussed in the next meeting.

TECHNOLOGY AND ECONOMICS OF HEAVY-WATER PRODUCTION*

The Italian National Committee on Nuclear Energy has published a collection of the reports presented at the Symposium on the Technology and Economics of Heavy-Water Production (Turin, September 30-October 1, 1970).

The subjects of greatest interest at the Symposium were the two-temperature method of concentrating deuterium by using water–hydrogen sulfide and ammonia–hydrogen systems (nine reports out of 15), the rectification of liquid hydrogen (two reports), and the rectification of water (one report).

Heavy water is produced today chiefly by two-temperature isotope exchange between water and hydrogen sulfide, one of the originators and theoreticians of which is J. Spevak. At the Symposium he presented a report devoted to the development of this method of separation, from the days of the Manhattan Project to our own time, when enormous installations are being built in Canada. At the conclusion of the report there was a discussion of the problems of calculating and optimizing the process by means of electronic computers, and an analysis was given on the basis of these calculations and the experience of operation at the Savannah River plant (United States).

*Tecnica ed Economia della Produzione di Acqua Pesante. Seric Simposi. Comitato Nazionale Energia Nucleare, Viale Regia Margherita 125, Roma, 1971.

A report by P. H. S. Spray (Canada) was devoted to the experience acquired in the design and construction of heavy-water production plants at Bruce and Port Hawkesbury. The speaker gave a general description of the plants, which are designed to produce 800 tons and 400 tons of D_2O per year. The first stage of concentration uses columns with sieve trays 8.54 m in diameter, with the cold and hot columns constructed one above the other, so that the total height of the combined column is 85 m. The requirements for the choice of materials and for the design, manufacture, and quality control of the equipment were discussed, due regard being given to the extraordinary dimensions of the equipment.

A number of reports were devoted to two-temperature isotope exchange using the ammonia–hydrogen system. Notable among these was the report by P. Brassiforti et al. (Italy), entitled "Problems involved in the construction of a heavy-water production plant." The deuterium source proposed in this report is synthesis gas produced at an ammonia-synthesizing plant. The report included graphs showing the physicochemical properties of pure and ammonia-saturated synthesis gas (enthalpy, specific heat, density) and the ammonia content of the compressed synthesis gas; it also included data on the kinetics of the isotope exchange as a function of temperature and discussed the different variants in which two-temperature schemes may be constructed. The report also gave a detailed description of the two-temperature scheme with an exhaust system, which had been adopted at the Ravenna plant.

A very detailed treatment of the results of a pilot-plant trial of two-temperature exchange between ammonia and synthesis gas was given in a report by S. Walter and E. Nitschke (FGR). They described an experimental plant with a column 400 mm in diameter and an output of 10,000-12,000 Nm^3/h (operating pressure 300 atm). Tests were conducted on modified sieve trays, which provided a very high rate of mass transfer. The authors recommend the construction of three-phase cascades with an exhaust, and the combination of such cascades with ammonium synthesis plants if the concentration of deuterium in the synthesis gas is not too low. In this case they emphasized the possibility of utilizing much of the equipment operating at ammonium synthesis plants. Taking account of the properties of potassium amide, which is used as a catalyst, they proposed a three-stage scheme for purifying the synthesis gas. For a plant with a productivity of 65 tons of D_2O per year, operating with an ammonia plant producing 100 tons of NH_3 per day, the calculated costs of production of 1 kg of D_2O is not more than $47.40.

The experimental data obtained in the trial of the above-mentioned plant were presented in a report by U. Schindewolf and G. Lang (FGR) on the optimization of a production plant. In the calculations it was assumed that the pressure was 300 atm, the flow rate of process gas was 187,000 Nm^3/h with a deuterium concentration of 0.0125%. The following temperature regime is recommended as the optimum: -23 to $-33°C$ for the cold column and 60-80°C for the hot column, with a ratio of hydrogen flow to ammonia flow equal to 5.4 ± 0.5. It was recommended that cascades having no more than two or three stages be built in the region of initial concentration. It was shown that a two-temperature cascade with exhaust can produce heavy water at a cost of about $43 per kg, while a cascade with an extraction column and exhaust produces it at a cost of as little as $42 per kg . A plant which has the same productivity but whose deuterium source is water with a deuterium concentration of 0.015% in equilibrium with hydrogen in the presence of NaOH as a catalyst can produce D_2O at a cost of about $45 per kg.

A. R. Bancroft and H. K. Rae (Canada) discussed the results of an investigation of two-temperature isotope exchange between amines and hydrogen for the purpose of concentrating deuterium. The calculations showed that the low rate of isotope exchange between ammonia and hydrogen in the cold column and the high elasticity of ammonia vapor in the hot column have a considerable influence on the cost of D_2O production by two-temperature isotope exchange using an ammonia–hydrogen system. Both the data in the literature and the results of the authors' investigations indicate that the exchange between hydrogen and aliphatic amines takes place much faster than ammonia–hydrogen exchange; the solubility of hydrogen in monoamines is higher, but the solubility of potassium methylamide in aminomethane is lower than the solubility of potassium amide in ammonia. The net result of this combination of factors is an increase in the rate of mass exchange.

Laboratory calculations indicate that the separation factor α in the hydrogen–aminomethane system is close to the separation factor for the ammonia–hydrogen system. At the same time, the elasticity of the amine vapors is much less than that of the ammonia. In view of these properties, it is possible to reduce the investment costs, on the basis of a preliminary estimate, to 10-30% less than the investment costs for a two-temperature ammonia plant. The report included a table comparing the operating conditions and the most important expenditure factors of various two-temperature processes: the hydrogen sulfide process, the ammonia process, and the process using amines.

An interesting report was given by B. Lefrancois about the Mazingarbe (France) plant, where single-temperature exchange between ammonia and hydrogen is being carried on, with a reversal of the current at each end of the isotope-exchange column. The report includes a description of the plant and a summary of the operating experience of the world's first industrial installation (20 tons of D_2O per year) using an ammonia–hydrogen exchange system.

A report by K. Bimbhata (India) described the operating experience of a low-temperature liquid-hydrogen rectification plant at Nangala. The plant was fed with electrolytic hydrogen, and the main operating difficulties resulted from the clogging of individual parts of the equipment with solid nitrogen. The report emphasized the possibility of using hydrogen with ammonia plants having an output capacity of up to 1000 tons of NH_3 per day, as well as the possibility of combining D_2O with the production of helium and liquid parahydrogen on a cooperative basis, which could reduce the costs of D_2O production. A report by G. Gutowski (FGR) was also devoted to the rectification of liquid hydrogen for the purpose of concentrating deuterium. On the basis of the operating experience of a plant with an output of four tons of D_2O per year, a design was prepared for an installation producing 105 tons of D_2O per year, using as raw material the hydrogen from synthesis was obtained from an ammonia-synthesizing plant with an output of 1500 tons of NH_3 per day. The initial nitrogen–hydrogen mixture is scrubbed free of CO_2 at a pressure of 25 atm by means of MEA scrubbing, and as the gas is cooled to 66°K, other impurities are removed in solid or liquid form (to approximately 2% N_2). After this the gas is heated to 90°K and expanded in a gas-expansion machine to 8 atm. At a temperature of 65°K the gas enters the regenerators and is cooled to 30°K, as a result of which the residual nitrogen precipitates out in solid form. The hydrogen is heated and throttled from 8 to 4.5 atm. The report includes a general schematic of the plant, which can produce 105 tons of D_2O per year at a cost of $21 per pound.

A report by A. Selecki (Poland) discussed the possibility of enriching natural water by the rectification method to a D_2O content of 10% by using a special packing called "Polpak," which, in the author's opinion, can make the process competitive.

A report by S. H. Russel (Canada), devoted to the economics of the utilization of heavy water in nuclear reactors, discussed ways of using heavy water in nuclear reactors as a moderator and a coolant, taking its relatively high cost into account. The report also discussed measures for avoiding losses of heavy water and for extracting and enriching it. It was shown that with a D_2O cost of $50 per kg, the contribution of this cost to the unit investment of atomic power stations is less than $45 per kW of the electrical power generated at the stations of CANDU-PHW. The contribution of the cost of D_2O to the cost of the electrical energy produced is $5 \cdot 10^{-5}$ dollars per kWh.

The authors of the report entitled "Some considerations on a dual-purpose two-temperature process for producing D_2O" (Z. Marchetti and R. Simone (Italy)), starting from the fact that the temperature cycle of a two-temperature D_2O-producing plant is identical with the temperature cycle of closed-cycle electrical power stations using gaseous fuel, arrived at the conclusion that it is possible to generate electrical energy through the operation of a two-temperature D_2O production plant using exchange between hydrogen and water. The authors consider a cascade consisting of unit exchange stages and increasing the deuterium content of the water by a factor of 100. According to their calculations, in such a cascade it is possible to generate in the form of electrical energy almost 40% of the total amount of heat energy supplied to the plant. They estimate that with a D_2O cost of the order of $40 per kg, the cost of the electrical energy thus generated may be about 0.001 dollars per kWh.

The material contained in the collection reflects the present state of heavy-water technology outside the Soviet Union and will be of interest to specialists.

VIIIth INTERNATIONAL CONFERENCE ON HIGH ENERGY ACCELERATORS

In the conference, which was held at Geneva on September 20-24, 1971, the results of recent investigations related to the development and improvement of accelerator equipment and complexes for obtaining counter beams of particles were discussed. The results of these investigations were presented in 120 papers, out of which 31 were from research centers in the USSR.

All the presented projects of both proton and electron accelerators are based on rigid-focusing structures of the magnetic field (as a rule, with separated functions of rotation and focusing) using ordinary or superconducting magnets. Most of the designs of accelerator and storage systems for secondary beams are also made on the same basis (see Table 1).

TABLE 1. Basic Parameters of Ring Accelerators at High Energies ($E \geq 25$ GeV)

Institute, country	Particles	Terminal energy, GeV	Number of particles per pulse	Frequency of rotation	Started in	Cost estimate	Remarks*
CERN, Switzerland	p	300	$2 \cdot 10^{12}$	0,23	1976	1150 mil. Swiss francs	Increase of energy up to 1000 GeV
USA	p	200	$5 \cdot 10^{13}$	0,25	1972	250 mil. dollars	Increase of up to 500 GeV
IFVE, USSR	p	76	$2 \cdot 10^{12}$	0,18	1967	120 mil. rubles	Increase of intensity up to $5 \cdot 10^{13}$ particles/pulse
USA	p	33	$2 \cdot 10^{12}$	0,5	1960	31 mil. dollars	Increase of intensity up to 10^{13} particles/pulse
CERN, Switzerland	p	28	$2 \cdot 10^{12}$	0,5	1959	200 mil. Swiss francs	

*The data presented in the table are for the first phase of installation; results which are proposed to be obtained in the second phase are shown in remarks.

Investigational work on superconducting pulsed magnets with fields of 4-6 T is being intensively carried out in the laboratories. The main direction of these investigations is the reduction of low temperature losses per running meter of the magnet. In order to reduce the losses for pulsed magnets special superconducting cables with thickness of the superconducting filament up to 4-10 μ have been developed. The limiting inductance is also governed by the intensity of the losses, which grow faster than the square of the inductance. Connected with the problem of the intensity of the losses is the choice of the duration of the accelerator cycle (rate of increase of inductance). It is found that on decreasing the cycle duration from 40 to 10 sec the low-temperature losses in different constructions (iron inside or outside the cooled volume) increase 5-20 times. The losses for the 40 sec cycle comprise 5-8 W/m.

Among the projects of high energy linear accelerators the project of doubling the energy of the electron beam of the 20 GeV standord linear accelerator (USA) with simultaneous decrease of the macrospacing of the beam by a factor of two merits attention. The project includes a storage system 6.8 km in length, arranged along the linear accelerator with two loops at the ends. In order to compensate for the power losses in the loops due to radiation two superconducting resonators are provided for.

A large number of papers were presented at the conference that dealt with the investigations on superconducting resonators intended for use with charged particle accelerators. However, in spite of the large volume of scientific-research work in this direction there are a number of difficulties which complicate the exploitation of such results and the production of electric field intensities characteristic of them. Among these difficulties are the aging of the material (nonreproducibility) of the results of measurements after contact of the resonator surfaces with the atmospheric pressure), a pronounced dependence of the quality factor on the peak value of the electric field intensity, and radiational "deformation" of the surfaces.

In the case of niobium resonators these effects lead to a reduction of the Q by an order of magnitude on changing the intensity from 4 to 30 MV/m or on irradiation by neutron flux of 10^{15} cm^{-2}. In the range of intensities higher than 30 MV/m electron emission appears, which leads to a disruption of the superconducting characteristics of the resonator.

Three projects should be noted concerning storage rings for counter beams of high energy particles. The project of two-ring proton storage, commissioned at CERN, where at present counter beams with 4-7 A intensity in vacuum in a 10^{-10} torr chamber are being obtained. According to the computations the losses of the beam at 4 A current comprise ~1% in 1 h. A significant increase in the losses is observed for currents larger than 6 A; the reason for this increase is not yet understood. In view of this the designed radiant emittance, which is $4 \cdot 10^{30}$ cm$^{-2} \cdot$ sec^{-1} is not attained. The experiments are conducted at radiant emittance of 10^{28}-10^{29} cm$^{-2} \cdot$ sec^{-1}.

The second large project is a 25 GeV proton–antiproton ring now in the phase of construction (Novosibirsk). This project is expected to be completed in 1972-1973.

As a longrange perspective of the development of this direction Brookhaven National Laboratory is proposing a project of storage rings for 200 GeV protons. The problem of financing this project is being discussed in the USA.

At the conference considerable attention was devoted to the method of collective acceleration. Better experimental results with this method have been obtained at OIYaI, where work in this direction was first started. At OIYaI acceleration of α-particles up to energies of 29 ± 6 MeV has been obtained with an energy gradient of ~32 MeV/m. The number of α-particles, which could be contained in each electron ring during acceleration is 10^9 for a number of electrons equal to $\sim 5 \cdot 10^{12}$.

The laboratories in Berkley (USA) and Munich (FGR) continued their work on the development of electron rings with maximum number of electrons. The better result obtained by the Munich group on the storage of electrons is $2 \cdot 10^{12}$ elec. in each ring. The research group in Berkley continued the investigation of the instabilities of the electron ring, that appear in their compressor at $5 \cdot 10^{12}$ elec. in each ring. The reasons for the appearance of these instabilities are not definitely understood.

From the work on the construction of the compressor at Carlsburg (FGR) it is shown that there exists a theoretical possibility of attaining frequency of packaging the rings into the accelerator equal to 1000 Hz.

Theoretical investigations of the collective method of acceleration were presented by several institutes. The study of the theory of oscillations of a proton ring inside an electron bunch, carried out at ITEF (Inst of Theoret. and Exper. Phys.) (USSR), generated the largest interest.

The linear theory of these oscillations leads to resonance restrictions on the limiting energy of the accelerated particles in the range of several GeV. These results were discussed in a special session on the theory of collective methods of acceleration and were not refuted at the conference. Effective methods of coping with resonance effects are not as yet indicated.

The method of acceleration of multinucleon particles in synchrotrons with soft focusing has been developed further. This method was first used on OIYaI synchrotron, where deuterons were accelerated up to an energy of 10 GeV.

Scientists of Princeton university reported the acceleration of nitrogen ions (N^{5+}, N^{6+}) in a cynchrotron up to 4 and 7 GeV respectively. A significant dependence of the intensity of the accelerator on the vacuum conditions in the accelerator chamber was confirmed during the acceleration of these multiply charged ions. Thus the change in the vacuum conditions from 10^{-7}-$2 \cdot 10^{-7}$ mm Hg led to a decrease in the intensity by an order of magnitude. It is shown that for the Princeton synchrotron an improvement of the vacuum in the chamber to 10^{-6} mm Hg is needed for the acceleration of multiply charged ions at a pulse repetition frequency of 18-20 Hz. Similar studies have also been made on a bevatron at Berkley, where N^{7+} ions were accelerated to 36 GeV. In the opinion of the authors the main objective of these improvements is to open up possibilities in the field of space physics.

Some theoretical investigations and computations in the area of further development of "Linatron" type accelerators (Institute of Physics, Torina, Italy) were presented at the conference; one of the variants of this accelerator was proposed at FIAN (USSR). Investigations on the extension of the cyclotron method of acceleration to the range of relativistic energy for protons and electrons were also presented (Laboratory of nuclear problems of OIYaI).

Investigations on the automatic control of the beam in the synchrotron with the aid of computers are being carried out successfully. The control program developed for IBM-1800 computer permitted a threefold decrease of the amplitude of deflection of the closed orbit in the synchrotron at CERN at 28 GeV. Windings of two resonance harmonics in the structure of the magnetic field (sixth and seventh) were used as the control elements.

ON CERTAIN PROSPECTS OF DEVELOPMENT OF HIGH ENERGY PHYSICS

The traditional international seminar on the prospects of future developments of high-energy physics was held at Morg (a small town near Geneva) on September 17-18, 1971. This seminar, to which scientists of different countries are invited, is sponsored by the Joint Institute of Nuclear Research and the CERN. The main objective of the seminar is to discuss the prospects of development in the field of high-energy physics. The state and the immediate plans for the largest accelerators, and also the prognosis of the development of the existing equipment and the construction of new accelerators in the next 10 years were discussed at the last seminar. In view of the fact that the future accelerators are gigantic installations requiring large capital investments, the possibility of cooperation of countries for the construction of new equipment was also discussed.

The communications by A. D. Solov'ev (Serpukhov) and R. Wilson (Batavia, USA) on the state of large accelerators and the physical programs planned on them generated great interest. The work on 76 GeV proton synchrotron of the IFVÉ and the programs of experiments conducted on this accelerator were highly appraised.

It was mentioned that large essential difficulties are not foreseen in launching the 200 GeV (USA) accelerator. The system of injection has been completely installed and test triggering of the accelerator has been achieved. Protons with intensity of the order of 1 μA have been accelerated. This is a high intensity, even though it is smaller than the project intensity by a factor of 20, primarily due to poor vacuum which was caused by certain defects in the construction of the vacuum chamber. An acceleration up to the full energy is at present impossible due to insufficient electrical strength of the insulation of the electromagnet windings. In order to eliminate these defects apparently several months will be required. The physical program is being prepared on a wide front. The first batch of experimental instrumentation will be ready for operation at the accelerator at the end of 1971.

The participants of the meeting listened to the communication on the state of the work on the proton storage rings of CERN with great interest. Experiments on counter beams are being conducted at present in five segments of intersection of the beams. About 10 experiments are conducted simultaneously. The construction of a large accelerator at CERN has started. Contracts for the construction of the main units of the accelerator have already been signed and it is proposed that its first unit (200 GeV) will be finished in 1976.

As regards more distant prospects of the development of accelerators, the tendency to use counter electron–proton machines for physical investigations quite clearly is being considered. Thus, at the Stanford linear electron accelerator it is proposed to build electron storage rings with energy up to 25 GeV. The program also provides for the construction of a 75 GeV proton accelerator and the production of counter electron–proton beams. The development of such experimental equipment is considered also in the programs of Brookhaven and CERN.

From the point of view of the construction of future accelerators two possibilities were discussed: the use of superconductivity in traditional magnetic systems and the method of collective acceleration.

The present state of superconducting pulsed magnets offers the basis for counting on obtaining magnetic fields of 40 kG. Cost estimates for a 1000 GeV accelerator show that the use of superconducting magnets in the accelerator gives a two-three times gain in comparison with the system of ordinary magnets. However, there is some basis for the expectation that toward the end of seventies commercial superconductors will be available ensuring a transition to 200 kG fields.

The discussion on the preliminary projects of collective accelerators showed that it will take another two-three years for checking separate variants of the accelerating systems, after which the final choice of the system of future accelerators will be made.

CONFERENCE ON GAS DISCHARGE DEVICES WITH HOLLOW CATHODE

The conference was held at the university in Orsay (a suburb of Paris) on September 20-23, 1971. About 100 persons from 12 countries participated in it.

In recent years investigations of hollow cathodes have shown significant advantages of these over ordinary cathodes. This made it possible to construct new physical electronic devices and modernize the old ones. This conference was the first devoted to hollow cathodes and generated great interest in scientific workers and engineer-designers of electronic instruments.

Reports on the following sections were presented at the conference: 1) glow discharge (six papers); 2) arc discharges (five); 3) high-volt discharges (one); 4) plasma sources (seven); 5) light sources (four); 6) sources of electrons, ions, and metastables (three).

The largest interest was generated by the reports on the use of hollow cathodes in laser and ion plasma accelerators (two reports on ion plasma accelerators were presented outside the program), and also on the analysis of physical processes in hollow cathodes.

A major part of the papers was devoted to experimental and theoretical investigations in discharges with hollow cathode: the mechanism of generation of metastable atoms, the processes of radiation and

measurements of temperatures of different parts of the cathode, the effect of magnetic fields, etc. Several papers were devoted to experimental investigation of oscillations in plasma. The investigation of arc discharge was given considerable attention. This is due to the possibilities of their extensive use in different physical and technical devices.

Theoretical investigations were presented only in one article (A. I. Morozov and A. V. Trofimov, USSR), in which a more general theory of positive column was given in comparison with the theoretical investigations of Shottky.

Many articles were presented on the construction of lasers with gas and metallic (vapors of metals) fillings, in which a hollow cathode is used. Two papers (H. Koul, England; Tzeifang, FGR) on Hall type plasma accelerators (discharge in crossed electric and magnetic fields) generated large interest. The American delegate R. Paulik communicated the development of an ion accelerator for space objects with 1-2 kW power. In this communication attention was mainly given to the investigation and construction of highly economical cathodes with lasting resource. The interesting article by S. Williams et al. (England) should also be mentioned.

Two reports on the development of new devices were presented: Thyratrons with hydrogen filling (B. Baker, England) and Rectifier elements (A. I. Nastyukha et al., USSR). Interesting results on the use of plasma guns with hollow cathode were presented in the paper by R. Dugdale et al. (England). K. Chang and K. Hang (USA) presented an interesting paper on the use of discharge with hollow cathode for obtaining stationary collisionless nonthermalized plasma (Q-machine). A number of instabilities existing in hot plasma and also some astrophysical processes can be modelled on this equipment.

The program of the conference was so arranged that there was much time available for free discussions. Excursions to the laboratories of the university and the polytechnique institute, and also to the nuclear centers at Saclay and Fontaine-aux-Roses were arranged during the conference. Two items of equipment shown at Orsay: one for the study of pulverization of the cathode material and the other for making a gas laser with a hollow cathode.

THE THIRD ALL-UNION CONFERENCE ON HIGH-VACUUM PHYSICS AND TECHNOLOGY

The Third All-Union Conference on High-Vacuum Physics and Technology was held in Leningrad on October 5-7, 1971; it was organized by the Central Office and the Leningrad Regional Office of the Scientific and Technical Society for the Instrument-Making Industry, the Scientific Council for Accelerators of the USSR Academy of Sciences, and the Committee for the Manufacture of High-Vacuum Equipment and Instruments. A total of 174 plenary and sectional reports were presented, dealing with the following main subjects: the physics and physical chemistry of surface and exchange processes under conditions of extremely low pressure; the dynamics of rarefied gases; the phenomena of condensation and cryosorption of extremely rarefied gases; ultrahigh vacuum systems and equipment (calculation and theoretical studies, experimental investigations, and operational and construction work); vacuum technology in nuclear physics and scientific instrument manufacture; physics and scientific problems of vacuum technology in electrical-vacuum and thin-film instrument manufacture; instruments, equipment, and questions of scientific methodology involved in vacuum measurements; the present status and future prospects of the unification and standardization of vacuum equipment.

The Conference included exhibits of the latest types of apparatus in vacuum measurements and mass spectrometry.

A number of reports were devoted to theory and the analytic generalization of experimental results obtained by studying the interactions of nuclear particles and electromagnetic radiation emitted from the surface of a solid in a vacuum. M. D. Malev's report proposed an absorption–diffusion model for such interaction, which covered a wide range of conditions, including stimulated desorption under the influence of electron, ion, and photon bombardment, the thermal desorption of hydrogen from metals, and the isobaric sorption of gases by active metals. The mathematical foundation for the model consists in the solution of the diffusion equation for a gas–metal system, using the equations of gas balance on the metal –vacuum boundary as a boundary condition. The resulting solutions were in good agreement with experimental data and may be effectively used in the design of vacuum systems for thermonuclear and nuclear installations.

A study by L. B. Begrambekov et al., dealt with the processes of diffusion and thermal desorption of embedded particles from nickel and molybdenum after they had been bombarded with 10-40 keV He^+ ions. The critical desorption curves were found to have two maxima, which the authors identified with the desorption of the particles included in the near-surface layer (the first maxima) and with the diffusion and subsequent desorption of atoms embedded in the interior of the target (the second maximum). It was noted that the time interval between these maxima for a continuous rise in temperature is independent of the density of the embedded ions up to a certain critical value ($4 \cdot 10^{16}$ cm^{-2} for ions with an energy of 30 keV), but drops sharply after this value has been exceeded. The value obtained for the activation energy for diffusion is considerably higher than the value corresponding to the usual migration of atoms through the interstices. The authors concluded that the reverse diffusion of the embedded atoms is slowed down when the metal is irradiated with a stream of fast ions; this conclusion is very important for the manufacture of plasma installations for various purposes.

An experimental study by R. B. Tagirov et al. yielded interesting data on the application of high-temperature light sources for the photodesorption degassing of unheated surfaces. For a radiant-energy density of 0.3 J/cm^2, a single pulse leads to the complete photodesorption of a monomolecular layer of adsorbate; when large hydrocarbon molecules are present, this photodesorption is accompanied by the photodissociation of these molecules and the formation of molecular fragments easily removable with an exhaust pump.

The reports of A. T. Aleksandrova et al. and L. M. Ammosova et al. dealt with measurements of the constants of diffusion of structural steels and alloys with respect to hydrogen and helium. It was shown, in particular, that the hardening heat treatment of steels of the ferrite–martensite and austenite classes causes a considerable increase in the penetrability of the steel to hydrogen. The vacuum tightness of the hermetically sealed envelopes and chambers of electronic vacuum instruments, electrophysical apparatus, and nuclear installations made of high-quality steels with a dense macrostructure is determined essentially by the concentration of nonmetallic inclusions.

Among the numerous studies on the physics and physical chemistry of sorption phenomena, including those in the cryogenic sector, we should mention the report of V. B. Yuferov on sorption–condensation exhaust pumping, which appears to be very promising for the construction of large thermonuclear installations. The author generalized a large amount of available experimental material on the use of layers of readily condensable gases (carbon dioxide, water vapor, inert gases) for pumping out considerable quantities of hydrogen and helium; he presented a wide range of information on sorption isotherms, the sticking probabilities of various gases, and other parameters of cryosorption exhaust pumping.

A number of reports were devoted to methods for calculating the vacuum parameters of various structures, including systems with sorbing walls. L. S. Gurevich et al. described a universal method for calculating the parameters of complex high-vacuum structures with sorbing walls, based on the utilization of the well-developed algebra of radiant fluxes. The method of statistical simulation, widely used in vacuum technology for calculating the permeability of complicated elements, was further developed in a study by L. N. Rozanov, V. M. Lebedev, and V. V. Shchenev. The authors derived a number of graphical interrelations between the dimensionless diameters of the elements for which calculations were made; these and the use of similarity methods considerably simplify the numerical calculation of real systems.

Graphical–analytical methods of analysis and technical–economic optimization of the periodic vacuum systems and structural-periodic vacuum chambers characteristics of accelerator design were developed by G. L. Saksaganskii. A detailed analysis of the parameters of molecular flow in vacuum systems with sorbing walls, using the Monte Carlo method, was made in a study by L. I. Kalashnik and É. M. Livshits. These results are of considerable significance for the further development of methods for designing the vacuum systems of charged-particle accelerators and experimental thermonuclear installations of various types.

Among the materials devoted to the investigations of parameters and new developments in high-vacuum pumps, those of greatest interest for the design of radiation-physics apparatus are the combined titanium getter-ion pumps designed by A. S. Nazarov et al., the cryogenic and cryosorption pumps described in the reports of A. S. Gribov et al. and S. F. Grishin et al., and the investigations on the exhaust pumping of hydrogen by means of magnetic-discharge pumps in various modifications, designed by A. D. Artemov et al., by V. G. Rogozinskii, V. V. Ryabov, and V. L. Ushkov, and by A. Kh. Rodionov et al. In particular, it was shown to be possible to increase the efficiency of diode-type pumps by changing to rectangular anode cells, and it was also shown that there may be effects resulting from the saturation of cooled pumps after relatively brief exhaust pumping of hydrogen in the $5 \cdot 10^{-5}$ torr pressure range.

The design characteristics and the operating and technological characteristics of a novel type of extremely-high-vacuum system of electron–positron accumulators with energies of 700 and 3500 MeV were described by V. V. Anashin et al. The authors constructed a set of built-in magnetic-discharge pumps distributed along the length of the chamber and operating on the magnetic fields of the accumulators, with effective exhausting of the small-aperture chambers of the accumulators to a pressure of $(1\text{-}2)\cdot 10^{-9}$ torr. In order to reduce the desorption beam emitted from the walls of the chamber as a result of synchrotron radiation, the cooled radiation vessel is covered with a thin layer of gold (10-15 μ), which is applied galvanically.

Yu. A. Balovnev proposed a novel method for admitting pure hydrogen at rates up to 10^{18} sec^{-1} into a vacuum system. Atomic hydrogen formed by the electrolysis of water in a chamber with a palladium cathode membrane connected to a vacuum system will diffuse intensively through the membrane at low temperatures. The method can be used for manufacturing ion sources.

The reports on vacuum-measurement and gas-analysis technology, which is of great importance for the manufacture of control devices and the automation of the vacuum systems of accelerator and thermonuclear installations, included material on increasing the accuracy of measurements and on vacuum metrology. In particular, G. G. Zhmakin obtained experimentally a set of corrected calibration characteristics for extremely-high-vacuum manometer converters and showed that at pressures of less than 10^{-8} torr the characteristics differ substantially from those previously assumed.

A study by G. A. Nichiporovich and I. F. Khanina showed that one of the principal reasons for such discrepancies is the existence of ion desorption currents. When the anode is contaminated, these currents are greater by two orders of magnitude than the x-ray background. The authors believe that the optimum regime for thermal degassing of the anode is electron bombardment at a current of ~40 mA and a voltage of ~200 V. In this regime the anode temperature does not exceed 100°C, so that there is no diffusion of impurity atoms onto the surface of the anode, and consequently the increase in ion desorption currents that is associated with this diffusion does not take place. V. T. Grinchenko and V. V. Pichugin described an ionization-type vacuum gage with modulation of the electron current of the cathode as the pressure of the neutral component of the gas varied over a range of 10^{-9}–10^{-3} torr in the presence of various kinds of interference (corpuscular beams and electromagnetic radiation) whose intensity was 10^3 times that of the useful signal. B. P. Kozyrev designed a novel type of thermal vacuum gage with a shielded thermoelement; the gage was capable of measuring pressures down to 10^{-6} torr, which means a sensitivity greater by two orders of magnitude than that of series instruments.

A. A. Birshert and L. P. Khavkin proposed a new method for the quantitative analysis of gaseous mixtures which consists in measuring the kinetic variations in pressure along a linear system into which the mixture to be analyzed is fed. The system consists of a number of containers separated by filters made of porous glass, with pores 1000 Å in diameter. The experimental results obtained are in good agreement with the calculated results.

The reports of M. I. Men'shikov and A. M. Grigor'ev discussed the technological features of vacuum-metrology and gas-analysis instruments for automated devices and systems controlled by electronic computers. They considered questions involving, in particular, the need for a logarithmic output signal.

A. M. Grigor'ev gave reasons for the desirability of replacing the torr, the traditional unit of vacuum measurement, with a quantity proportional to the logarithm of the ratio of the residual-gas pressure to some constant pressure, such as atmospheric pressure. The introduction of this unit (the boyle) considerably simplifies the construction of automated circuits for the control of vacuum installations.

In general, the work of the Conference gave evidence of the substantial development and better understanding of many important problems of high-vacuum physics and technology. The results achieved will obviously have considerable influence on the design of the vacuum systems of large radiation-physics installations constructed today and of apparatus used in nuclear physics and instrument-making.

The most interesting material of the Conference is scheduled to be published in 1973-1974 in the form of collections entitled: "Extremely High Vacuum in the Design of Radiation-Physics Apparatus" and "High-Vacuum Pumps, Instrumentation, and Equipment."

THE FIRST ALL-UNION CONFERENCE ON NEUTRON RADIATION METROLOGY

The developing atomic technology of today creates certain requirements for metrological methods to provide the necessary neutron measurements.

The First All-Union Conference on Neutron Radiation Metrology (measurements on reactors and accelerators) was held in Moscow from October 18 through October 22; it was organized by the State Committee on Standards, SMSSSR, the USSR State Committee on the Use of Atomic Energy, and the All-Union Scientific-Research Institute for Physicotechnical and Radiotechnical Measurements (VNIIFTRI).

The participants in the Conference heard 112 reports. The reports were divided into sections according to subject: problems of neutron-radiation metrology; nuclear data for neutron measurements; continuous-operation detectors and specimens of substances usable for the recording of neutrons; questions of calibration and certification; measurements of the characteristics of neutron fields in reactors by means of various specimens of substances and individual continuous-operation detectors; measurements of the characteristics of neutron fields in accelerators; and questions relating to the estimating of the reliability of measurement results, to the planning of experiments, and to the comparison of measurements and instruments.

A survey report by R. D. Vasil'ev (VNIIFTRI) was devoted to the problem of neutron-radiation metrology; he gave an analysis of the present state of the art and foreseeable trends in the metrology of physical quantities which characterize neutron fields in nuclear-physics installations (reactors, critical assemblies, and accelerators). The report discussed the traditional metrological questions involved in direct measurements of individual physical quantities which require the use of standards. However, as the number of measurements required in practice increases, an increasingly important role is played by indirect measurements that can be used in the absence of direct measurements, to find with excellent accuracy quantities expressed in units for which no standard specimen is available. Where indirect measurements are made, great care must be taken to make periodic comparisons between measuring devices and methods. The report listed the results of the most important international and national comparisons and analyzed the sources of discrepancies between them.

The activities of the Center for Nuclear Data were described in a report by V. I. Popov (Physical and Electrical Institute – FÉI). It included a brief survey of the present status of the most important primary reference cross sections for neutrons. It was noted that the cross sections have errors of as little as 10%, but this is not always satisfactory for practical needs.

The wide use of the neutron-activation method of measurement made it necessary to set up both a centralized system for supplying standard specimens and a methodology for processing the results. A report presented by a group of authors from the VNIIFTRI discussed the program of standardizing neutron-activation measurements that is being carried on by this Institute in collaboration with the I. V. Kurchatov Institute of Atomic Energy, the Moscow Engineering Physics Institute, and other organizations. Neutron-activation detectors may be divided into groups in several different ways according to their applicability to the recording of neutrons of various energy groups ("thermal" detectors up to 0.5 eV, resonance detectors for 0.5-3000 eV, and threshold detectors for 0.5-15 MeV), according to the purpose for which they are used (detectors for measuring the neutron spectrum and detectors for tracking), and according to their temperature stability. The activation detectors and calibration sources are certified at the facilities of the VNIIFTRI. The report also raises the question of working out standard methods for the processing of measurement results. This question is part of the problem of using metrology to ensure consistency between the results of neutron-activation measurements. It must be noted that in the development of methods for neutron-activation detectors, not enough attention is devoted to spectrum calculations.

Many reports were devoted to the measurement of the characteristics of neutron fields in reactors by means of specimens of different substances. Of considerable interest among these was the report by A. M. Aglitskii et al. on measurements of fast-neutron fluxes and spectra in the reactor of the Novo-Voronezh Atomic Power Station by the method of threshold reactions. The fast-neutron spectra were reconstructed from experimental data by methods using exponential approximation.

A report presented by the Institute of Atomic Physics described the problems involved in the determination of high-energy fast-neutron spectra and fluxes encountered when materials are irradiated on research reactors.

Direct-charge detectors (DCD) are being used more and more widely for the monitoring of neutron fields in reactors. N. D. Rozenblyum et al. gave an interesting account of the DCD studies being conducted at the All-Union Scientific-Research Institute of VNIITe. It discussed the present stage of development of DCDs. It was noted that this method was metrologically equivalent to the method of radioactive indicators.

The use of filters and of a method involving two DCDs makes it possible to measure fluxes of epithermal, thermal, and resonance neutrons, as well as their cadmium ratio.

The development of DCDs has now progressed to the point where it is possible to issue certified detectors capable of measuring absolute fluxes of neutrons with an error of ±5%.

Although the Conference was described as a coordinating meeting, it was more in the nature of a scientific and technical symposium. It adopted a resolution determining the further development of work along the lines of neutron-radiation metrology. The materials of the meeting will be published in a separate collection.

A. V. Abrosimov, V. M. Korolev,
V. F. Likholap, E. P. Petryaev,
I. I. Kreindlin, Yu. A. Skoblo,
A. N. Maiorov, V. M. Iryushkin,
V. B. Timofeev, O. A. Korneichuk,
and V. A. Vasil'ev

EXPERIMENTAL EQUIPMENT FOR INVESTIGATION OF RADIOLYSIS OF ORGANIC SUBSTANCES

A loop-type experimental equipment for the study of the processes of radiolysis of individual organic compounds and their mixtures in liquid and vapor phases has been developed and is operating at the Institute of Nuclear Power of the Academy of Sciences of the Belorussian SSR on an IRT-2000 reactor. The construction of the equipment permits the irradiation of the products both in flowing and circulating conditions. The pressure in the reaction zone can be varied from 1 to 70 atm and the temperature from 50 to 350°C.

A schematic diagram of the equipment is shown in Fig. 1.

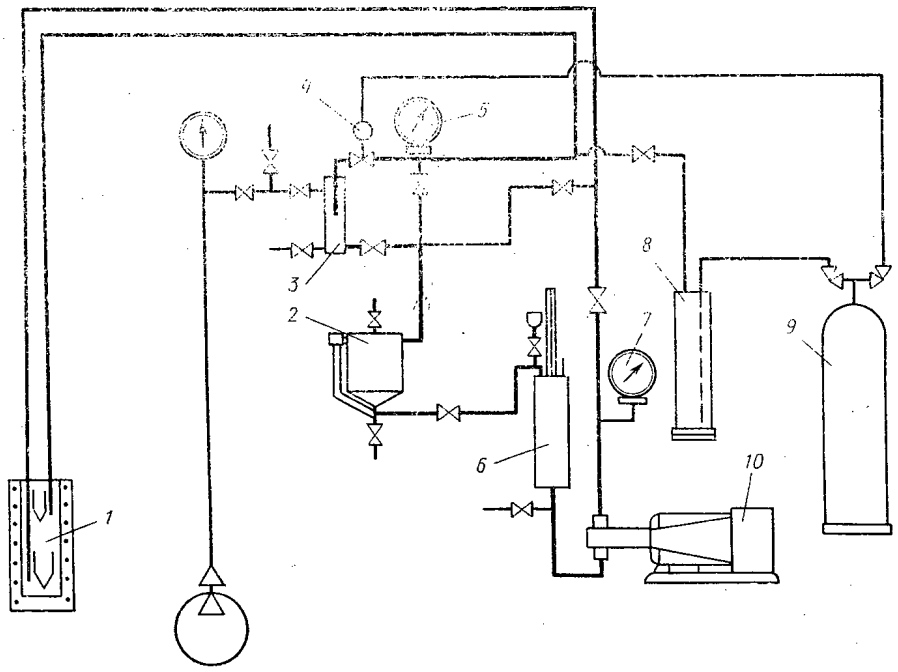

Fig. 1. Schematic diagram of the equipment: 1) reaction tank; 2) receiving capacity; 3) gas separator; 4) pressure regulator; 5) electrocontact manometer; 6) space for raw material; 7) standard manometer; 8) drier; 9) cylinder with compressed nitrogen; 10) fluid-flow pump.

Translated from Atomnaya Énergiya, Vol. 32, No. 3, pp. 259-262, March, 1972.

The radiolysis of the compounds occurs under the action of n- and γ-radiations of the reactor in the reaction tank with 100 ml volume, which is placed in the vertical channel of the IRT-2000 reactor. The temperature of the medium subjected to irradiation is measured by two Chromel–Alumel thermocouples and is recorded by a secondary instrument ÉPP-09. The reaction zone is heated by a 1.0 kW electric heater and is remote-controlled from the equipment desk.

The solution from the container of the raw material is subjected to irradiation by a high-pressure fluid flow pump. The pump is furnished with regulating screws which facilitate changing its output within the range 35-700 ml/h; this makes it possible to change correspondingly the absorbed dose for constant reactor power. The change of the rate of flow of the liquid being irradiated is accomplished by the use of a special device mounted in the container of the raw material.

The pressure necessary for the experiment is provided by a pneumatic regulator. At the input line the pressure is controlled by a standard manometer. The electrocontact manometer, installed at the exit line, automatically holds the system at a given pressure.

The irradiated product enters the gas-separator, from where the radiolytic gases are led off to special ventilation; a part of these gases is removed for analysis. The rate of separation of the radiolytic gases is also controlled at the exit of the gas-separator. The liquid phase is led out through a valve for the measurement of the flow rate and for sampling of the liquid specimens in the analysis or it is collected in the receiving space. In the case, where it is necessary to operate in the circulating regime, the irradiated mixture can be again returned to the raw material space and directed to the zone of irradiation.

A scavenging of the reaction tank by nitrogen is provided for in the equipment in order to remove air before the irradiation of the solutions; an evacuation of the line in sampling the gas specimens is also provided for.

All the technological lines, units, and accessories of the equipment are made of Kh18N10T stainless steel.

The equipment allows one to carry out investigations on radiolysis of different compounds quite rapidly and with an adequate degree of accuracy.

THE GID-2 RADIOISOTOPE RELAY INSTRUMENT

Gamma-defectoscopes are widely used in industry today for monitoring the quality of various materials and products. In the monitoring process it is necessary to guarantee the safety of the operators working with the γ-defectoscopes, the precise orientation of the γ-ray beam with respect to the object being monitored, and the reliability of signals indicating the location of the source. For this purpose, and also in order to automate the monitoring process and make it more productive, the GID-2 radioisotope relay instrument for interlocking and for signaling the position of radiation sources in γ-defectoscopes has been developed at the All-Union Scientific-Research Institute of Radiation Technology (VNIIRT).

The instrument is made up of a scintillation-type detection unit (GDS-1nm), a detection unit using gas-discharge counters (GDG-1n), and a radio-electronics unit (BR-N) (see Fig. 1).

The high time and temperature stability of the principal parameters and the availability of a check on the operation of the instrument are made possible by appropriate design of its electronic circuitry, which is similar to that of the RTR-1 instrument.* However, the GID-2 has certain features not present in the RTR-1: two detection units can be connected at the same time and switched on alternately (by hand or automatically); the instrument can operate on a 24-V dc source or on a 220 V, 50 Hz ac source; the design of the GID-2 makes it usable either in the laboratory or under field conditions; and the radio-electronics unit (BR-N) can be mounted on the control panels of γ-defectoscopes.

The use of a scintillation-type detection unit means that the radiation source can be accurately oriented in place with respect to the object being monitored, with a γ-ray exposure dose rate of 1-2 MR/h.

The accuracy of orientation of the radiation source in relation to the object being monitored is ±3% for pipes 0.7-1.2 m in diameter, ±2% for pipes 1.2-5 m in diameter, and ±1% for pipes 5-10 m in diameter, depending on the distance of the film from the source, for a source moving at rates up to 6 m/min.

*Kreindlin et al., Atomnaya Énergiya, 28, 4 (1970).

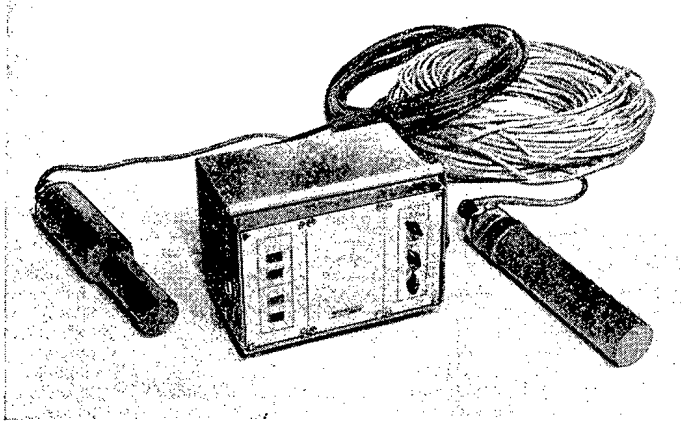

Fig. 1. The GID-2 radioisotope relay instrument.

When the radiation source is in the irradiation position, the GDS-1nm detection unit is disconnected in order to protect it from overloading by the irradiation, and the GDG-1n, which has a sensitivity only 1/40 as high, is connected.

When the γ-ray exposure doses exceed the limits of irradiation overload of the detectors, the detectors will be used with additional shielding in each specific case.

The GID-2 instrument can be used in interlock circuits, for position monitoring of the level of separation of two media in rooms where there is no danger of explosion, and also for solving other problems of this kind. The connecting of two scintillation-type detection units extends the range in which this instrument can be used for position monitoring.

The instrument is triggered by a radiation exposure dose rate of not more than 0.025 MR/h in the sensitive zone of the detector. The time constant of the instrument can be adjusted over a range of 0.1-10 sec. The instrument can be used in either positive or negative operation. The hysteresis is adjustable over a range of 0.4-0.9. The switchable power is 500 VA of alternating current at a voltage of 380 V and a current value of up to 5 A It can operate at temperatures from −40 to +50°C and at relative humidity levels up to 98%. The thermal stability of the triggering and releasing thresholds is no worse than ±0.3%/deg.

The use of the GID-2 instrument can reduce technological costs considerably. Thus, for example, in the "Trassa" γ-defectoscope an average of 2500 rubles is saved annually by the use of this instrument. The GID-2 instrument is now being mass-produced.

LIQUID-HYDROGEN BUBBLE CHAMBER "LYUDMILA"

The official opening ceremony of liquid-hydrogen bubble chamber "Lyudmila" was held in the Institute of High Energy Physics on January 14, 1972. This unique physics equipment was constructed in OIYaI (Joint Institute of Nuclear Research) and is installed in one of the beams of the 70 GeV proton synchrotron in accordance with the agreement on scientific–technical collaboration between the State Committee on the use of atomic energy in the USSR and the OIYaI.

The 2 m bubble chamber of the OIYaI is a thick-walled metal tank of almost cylindrical shape; a neck for the expansion mechanism is welded to one of its end faces. The cylindrical frame of the chamber is slit along the directrix; a flange for holding the glass, i.e., illuminator, and suspensions of the chamber is welded at the location of the slit. The dimensions of the operating volume of the chamber are 200 × 60 × 51 cm.

The expansion mechanism is of piston type. A piston 400 mm in diameter is set into motion forcibly. The chamber can operate twice in each cycle of operation of the accelerator with an interval of ~0.3 sec. The cycle expansion and compression of the operating volume lasts ~50 μsec. The cooled chamber is filled with ~900 liter of liquid hydrogen at −247°C. The thermal insulation of the chamber is of Dewar flask type, but unlike the ordinary flask in this case there is a multilayer superposition of metalized thin synthetic films which reflect infrared rays efficiently. Due to this the operation of the chamber is quite

safe. A special liquifying equipment, developed by the cryogenic section of the OIYaI, ensures the supply of liquid hydrogen to the chamber. The system of illumination into the chamber is of self-collimation type. A mirror, coated with thin dark bands, is placed at the bottom of the chamber. The thickness of the mirror, the distance between the bands, and their widths are computed in such a way that the objectives gather only the light scattered by chains of gas bubbles forming along the tracks of the charged particles. Pulsed sources of light are placed at the center of a square with 460 mm side. Four photographic cameras with special objectives with focal length of 143 mm are placed at the corners of the square. The optical axes of the objectives are parallel to each other and are directed along the magnetic lines of force in the chamber. The optical system of the chamber is so constructed that it does not introduce distortions. A large glass covering the operating volume of the chamber from above has fine intersecting reference lines on it, which provide a coordinate system for subsequent reconstruction of stereographic pictures of the events, recorded by the cameras, with the use of a computer. The operating volume of the chamber is photographed on four separate 50 mm nonperforated films. The average scale of the picture is 1:15. The dimensions of the frame of the film are 143 × 44 mm. Additional characteristics of the frame are printed in between the frames.

The chamber is mounted between the poles of a special electromagnet which produces a constant field of 26 thousand Oe in the operating volume. With the specific geometry of the gap taken into consideration this is the maximum magnetic field that can be produced without using superconductivity. Such a strong field, which is yet another distinguishing feature of "Lyudmila" permits attainment of a relatively high accuracy in the determination of the momentum and sign of the charge of the investigated particles.

This elaborate complex includes a special system for the supply of liquid hydrogen and a compressed gas to the chamber for the expansion system, electronic equipment for the control of the chamber, synchronization of its operation with the accelerator and for maintaining a given regime of operation of all the units of the chamber, a power supply system, and a system for transporting the beam of charged particles, produced by the accelerator, to the chamber. A special building has been constructed to house the chamber and all necessary conditions for the safe operation with a large quantity of liquid hydrogen are ensured.

Besides the specialists of the OIYaI and IFVÉ (Institute of High Energy Physics) a number of Soviet design, construction, erection, and industrial organizations and enterprises participated in the construction of this complex. Specialists from the participating countries of OIYaI, in particular from Czechoslovakia, made a large contribution by developing and constructing the elaborate screened optical system of the reflecting mirror.

The official opening of the bubble chamber "Lyudmila" occurred after four months of the start of its operation. It was put into operation during the period September 26 to October 4, 1971. During this period ~6 thousand photographs were obtained in proton beams with momentum up to 35 GeV/c. The analysis of these photographs showed a high quality of the pictures and a good agreement of the operating characteristics with the computed values. Simultaneously prelimiary physical results on the multiplicity of generation of secondary charged particles in the interaction between the protons with the indicated limiting momentum and protons of the target were obtained.

The bubble chamber "Lyudmila" offers the scientists of the OIYaI new possibilities for conducting investigations on the largest proton accelerator. The chamber is installed in the channel, along which pure beams of different particles, protons and antiprotons, K^+- and K^--mesons, π^+- and π^--mesons, and also quasimonochromatic beams of γ-quanta with momentum up to 35 GeV / c could be transported into it.

A collaboration of laboratories and scientific groups, which are ready or are getting ready to participate in the processing of the film information, obtained with the use of "Lyudmila," will undoubtedly make in the near future a significant contribution to the progress in high energy physics.

A NEW PHYSICS JOURNAL

In 1970 the Joint Institute of Nuclear Research issued through Atomizdat two collections of review articles under the title "Problems of Physics of Elementary Particles and Atomic Nucleus."

In 1971 the publication of the reviews continued in the form of a periodic collection-journal entitled "Physics of Elementary Particles and Atomic Nucleus" (abbreviated ÉChAYa). The journal is published quarterly. The chief editor of the journal is Academician N. N. Bogolyubov. The editorial board of the journal consists of well-known experimental and theoretical physicists. The first issues of the journal contain theoretical and experimental reviews on a wide range of problems of physics. Among these, for example, is the article by a group of Dubna physicists headed by V. P. Sarantsev "Collective acceleration of ions" (Vol. 1, No. 2, 1970). This interesting and apparently very promising method of acceleration has been proposed and developed in our country by the authors of the article. The reviews are of interest to our readers, desirous to know the recent advances in this field, as well as to foreign physicists who are showing increasing interest in the collective method of acceleration.

The first issue of 1972 contains theoretical articles devoted to the analysis of asymptotic properties of cross sections at large energies (A. A. Logunov et al.), and quark model (P. N. Bogolyubov, A. I. Akhnever, and M. P. Reklo). In view of the experiments at Serpukh, which showed disagreement between the obtained cross sections and those predicted by Pomeranchuk's theory, the theoretical analysis of asymptotic cross sections has generated increasing interest. A rigorous mathematical approach to the analysis of asymptotic cross sections is described in the article by A. A. Logunov et al. The theory of coupled states of quarks is analyzed in the article by P. N. Bogolyubov. A method of eliminating the difficulties of the three-quark model (magnetic moments and Pauli principle) is proposed. As a result a nine-quark model is obtained, in which it is possible to assign quarks with unit charges instead of one third. A quark model of photoformation of neutral vector mesons is discussed in the article by A. I. Akhnever and M. P. Rekalo.

The same issue contains a review by V. V. Glagolev and K. D. Tolstov, in which experimental data on elastic and inelastic collisions of π-mesons with nucleons at large energies are presented. Although the topic of the review is quite restricted, the amount of collected material is so large that only specialists connected with this field of physics can locate them in the original literature and even they would waste much time in doing that. This has undoubtedly been done by the authors and to much good. Their review will be read with great interest by specialists working in this field and by a wider circle of physicists wanting to acquaint themselves with the contemporary state of elementary particle research.

In the future it is proposed to devote odd issues of the journal to the physics of elementary particles and the even issues to the physics of the atomic nucleus.

A cursory acquaintance with a part of the material from ÉChAYa gives the impression that the most interesting problems of that branch of physics, which was earlier called nuclear physics, are discussed in this publication at a very high level. At present nuclear physics has been divided into branches, among which the interconnection is becoming increasingly weak. It may be hoped that ÉChAYa will help in enhancing and sustaining the interaction.

Translated from Atomnaya Energiya, Vol. 32, No. 3, p. 263, March, 1972.

J. Spanier and E. Gelbard

MONTE CARLO METHOD AND PROBLEMS OF NEUTRON TRANSPORT*

Reviewed by V. Z. Yuzgin

The results of the investigations in the field of application of the Monte Carlo method to the problems of neutron transport have been unified in the monograph by Span'e and Gelbard. The authors are well known as prominent specialists having made large contributions to the development of the theory of the Monte Carlo method and standard American programs for the computation of reactors.

The first three chapters of the book acquaint the reader with the general theory of the Monte Carlo method. The presence of random sampling is essentially the only distinguishing feature of this method; therefore the authors devote the first chapter to the exposition of the elements of theory of random sampling, in which basic definitions and necessary information from the probability theory are given, and also the most commonly used methods of sampling (methods of inversion and exclusion, their generalization to the case of many measurements and other special methods) are described. The chapter ends with a discussion of the fundamental problem of sampling of uniformly distributed numbers on a computer.

Specific problems directly related to the Monte Carlo method are given in the second chapter. Different modifications of this method are considered taking the example of solution of linear algebraic equations. The departure from the tradition of starting a manual on the Monte Carlo method from the discussion of evaluation of integrals is not accidental. The approach taken by the authors permits relatively easily a gradual transition from the solution of matrix equations to the solution of simple integral equations, and then to the transport equation. Furthermore, in the discussion of many-group equations of neutron transport in the thermal region methods of solution of matrix as well as integral equations are used. This is related to the discrete representation of the energy variable in conjunction with continuous representation of the space variables.

Standard methods of reducing variance are described in the third chapter, wherein it is emphasized that the reduction in the variance should not lead to an extreme increase in the computer time. The choice of the so-called standard of the methods is subjective. Spanier and Gelbard give preference to those methods which they have used in practice most often and successfully. They have omitted, for example, the conventional Monte Carlo method, the common method of evaluation of definite integrals with the use of orthogonal polynomials, apparently proposed for the first time by S. M. Ermakov and V. G. Zolotukhin, and also the exponential transform. In the same way as Hemmersly and Hendscomb do, the authors of the present monograph define the efficiency of a method as a quantity inversely proportional to the product of the variance and the time consumption of the estimate.

In the next three chapters original methods applied to specific problems of neutron transport are described: computation of flux of thermal neutrons and computation of the probability of escaping resonance capture. The method of superposition is discussed in the fourth chapter; in the following chapters the authors take recourse to this method in order to pass on from a problem, which is difficult to solve by the Monte Carlo method, to a more convenient problem. The so-called method of surface source occupies a significant place in this chapter. The chapter ends with a comparison of the characteristic features of the conjugate method and the method of superposition in the solution of specific problems.

*Atomizdat, Moscow (1972), 270 pp.

Translated from Atomnaya Énergiya, Vol. 32, No. 3, pp. 263-264, March, 1972.

The fifth chapter discusses particularly a practical problem of reactor physics: many-group computation of the thermal flux of neutrons. A special attention is devoted to methods used in the MARC program developed by the authors. The usual procedures of the Monte Carlo method, which are used in the computation of fluxes, are also described in this chapter. The authors point out problems which are difficult to solve using these procedures.

In the last chapter it is shown convincingly that with the use of principle of superposition it is possible to solve problems of resonance absorption, which cannot be solved by simpler methods. The point is that in problems of resonance absorption one has to consider a delayer consisting of different materials with variable density (in particular, in this problem the conjugate method becomes ineffective due to the impossibility of eliminating fluctuations of neutron weights by a simple procedure). On the other hand the problems of resonance absorption have some characteristic features which permit an effective use of the method of superposition. Ways of reducing the volume of stored information are suggested in the chapter.

Taking current problems of reactor physics the authors have shown that the Monte Carlo method is a fine and flexible tool; its potentialities, far from being exhausted, become increasingly greater with the development of computer technology.

The new book of Span'e and Gelbard will undoubtedly generate great interest in specialists engaged in computations of nuclear reactors and radiation protection.

V. K. Knyazev

RADIATION STABILITY OF VARNISH COATINGS*

Reviewed by S. É. Vaisberg

The monograph is devoted to the current problem of use of varnish coatings under the conditions, where penetrating radiations are incident, mainly in the field of atomic engineering. Unlike manuals and monographs published earlier ("Protective Coatings in Atomic Engineering," S. M. Gorodinskii and B. V. Tikhomirova (editors), Gosatomizdat, Moscow, 1963; B. V. Tikhomirov, "Polymer Coatings in Atomic Engineering," Atomizdat, Moscow, 1965) in the present monograph narrower aspects of the problem are elucidated: of all polymer coatings only varnish coatings are considered and, furthermore, of different aspects of its use attention is mainly devoted to its radiation stability.

The monograph is designed mainly for engineering-technical workers in the field of operation and construction of atomic units with the use of varnish coatings. It can be useful also for scientific workers in the field of radiational study of materials.

The book describes the intended use, composition, properties, and methods of study of varnish coatings. It then gives information on their radiation stability, encompassing problems of radiolysis, changes in electrical, mechanical, and sorption–desorption properties, and also data on chemical stability. Technical characteristics pertaining to direct application of the coatings in conditions of penetrating radiations are given. The existing technical material is collected in the Appendix in the form of tables.

This publication is very useful; only the fact that data collected up to 1967 are presented in it, lowers its value somewhat.

*Atomizdat, Moscow (1971).

JOURNAL OF LOW TEMPERATURE PHYSICS

As part of its program to provide scientists with complete up-to-date information on advances in the important field of low temperature research and technology, Plenum Press will publish the JOURNAL OF LOW TEMPERATURE PHYSICS beginning February 1969. Edited by Professor John Daunt of the Cryogenics Center, Stevens Institute of Technology, and an editorial board numbering many of the major contributors to current progress in low temperature physics, the JOURNAL will publish bimonthly original papers and occasional review articles on fundamental theoretical and experimental data basic to developments in all areas of cryogenics. Prospective contributors may submit articles to: Dr. John G. Daunt, Cryogenics Center, Stevens Institute of Technology, Hoboken, New Jersey 07030.

DEVELOPMENTS IN APPLIED SPECTROSCOPY*
Volume 7-B

The Seventh National Meeting
Society of Applied Spectroscopy
held in Chicago, May 13-17, 1968

Edited by **E. L. Grove**
Illinois Institute of Technology
Research Laboratories, Chicago, Illinois

Alfred J. Perkins
University of Illinois College of Pharmacy
Chicago, Illinois

Concentrating on the physical-organic aspects of spectroscopy, this volume continues to present the latest and most significant developments in the field. Reports describe spectroscopic and infrared analyses of various polymeric materials and carbonate apatites, as well as current applications of internal reflection and NMR spectroscopy. Also included is a special section on spectrochemical applications to textiles and fibers.

CONTENTS: Spectral properties of carbonate in carbonate-containing apatites, **Racquel Z. LeGeros, John P. LeGeros, Otto R. Trautz,** and **Edward Klein** • Polarized infrared reflectance of single crystals of apatites, **Edward Klein, J. P. LeGeros,** and **R. Z. LeGeros** • Analytical infrared spectra of particulate alpha-aluminas, **Conrad M. Phillippi** • Analysis of acrylonitrile-butadiene-styrene (abs) plastics by infrared spectroscopy, **D. B. Gesner** • Design and application of a high temperature infrared cell for the study of polymeric materials, **W. R. Feairheller** and **W. J. Crawford** • Spectroscopic studies of hydrogen bonding, **C. N. R. Rao** and **A. S. N. Murthy** • Vibrational and electronic raman effect, **J. A. Koningstein** • Raman spectroscopy of polymeric materials, Part I — selected commercial polymers, **Dorothy S. Cain and Albert B. Harvey** • **Internal Reflection Spectroscopy:** Internal reflection spectroscopy of non-aqueous solvent systems: halides in liquid sulfur dioxide, **D. F. Burow** • Application of ATR to low temperature studies, **J. W. Cassels** and **P. A. Wilks, Jr.** • Characterization of commercial formulations by combining several chromatographic techniques with multiple internal reflection and mass spectrometry, **T. S. Hermann, R. L. Levy, L. J. Leng,** and **A. A. Post** • **NMR Spectroscopy:** A comparative NMR study, **P. D. Klimstra** and **R. H. Bible, Jr.** • An NMR study of acrylic polymers, **Daniel A. Netzel** • The use of digital computers for NMR calculations, **Milton I. Levenberg** • The analysis of ABX spectra, **George Slomp** • **Spectrochemical Applications to Textiles and Fibers:** Spectrochemical elemental analyses of textiles and textile fibers, **Robert T. O'Connor** • The applications of infrared spectroscopy in the investigations of cotton, **Elizabeth R. McCall** • Spectroscopy and computer dyeing, **Braham Norwick** • The application of internal reflection spectroscopy to the quantitative analysis of mixed fibers, **P. A. Wilks, Jr.** and **J. W. Cassels.**

Approx. 260 pages PP $12.50

*Place your continuation order today for books in this series. It will ensure the delivery of new volumes **immediately** upon publication; you will be billed later. This arrangement is solely for your convenience and may be cancelled by you at any time.

PLENUM PUBLISHING CORPORATION
New York and London
Consultants Bureau • Plenum Press • IFI/Plenum Data Corporation
227 WEST 17th STREET, NEW YORK, N. Y. 10011
In United Kingdom: Donington House, 30 Norfolk Street, London, W.C. 2